Dissertation
submitted to the
Combined Faculties for the Natural Sciences and for Mathematics
of the Ruperto-Carola University of Heidelberg, Germany
for the degree of
Doctor of Natural Sciences

The focal adhesion protein zyxin mediates wall tension-induced signalling in vascular cells

Presented by
Diplom – Biotechnologist Agnieszka Wójtowicz
born in: Wrocław, Poland
Oral-examination:

Heidelberg 2008

……
……
……

Referees: Prof. Dr. F. Wieland
Prof. Dr. M. Hecker

CONTENTS

ABBREVIATIONS

ANOVA	analysis of variance
ANP	atrial natriuretic peptide
AT-1	angiotensin II type 1 receptor
BNP	brain natiuretic peptide
BSA	bovine serum albumin
CNP	c-type natriuretic peptide
cGMP	cyclic guanosine monophosphate
CXCL1	chemokine (C-X-C motif) ligand 1
CXC3L1	chemokine (C-X3-C motif) ligand 1
DMEM	Dulbecco's modification of eagle's medium
DNA	deoxyribonucleic acid
DTT	dithtiotreitol
EC	endothelial cells
ECM	extracellular matrix
EDTA	ethylene diamine tetraacetic acid
EGTA	ethylene glycol tetraacetic acid
ELISA	enzyme-linked immunosorbent assay
ET-1	endothelin-1
FA	focal adhesion
FAK	focal adhesion kinase
FBS	fetal bovine serum
FCS	functional class scoring
FN	fibronectin
GAPDH	glyceraldehyde-3-phosphate dehydrogenase
GSEA	gene set enrichment analysis
HUVEC	human umbilical vein endothelial cells
HRP	horseradish peroxidase
HSP	heat shock protein
ICAM-1	intercellular adhesion molecule-1

IEF	isoelectric focusing
IL-8	interleukin 8
KEGG	Kyoto encyclopedia of genes and genomes
MATra	magnet assisted transfection
MCP-1	monocyte chemoattractant protein-1
N	nucleus
NES	nuclear export signal
NO	nitric oxide
NOS-3	type 3 (endothelial) nitric oxide synthase
NP-R A/B/C	natriuretic peptide receptor type A/B/C
ORA	over-representation approach
PBS	phosphate buffered saline
PCR	polymerase chain reaction
PKG	protein kinase G
PP1	protein phosphatase 1
PVDF	polyvinylidenefluorid
RAAS	renin-angiotensin-aldosterone system
RNA	ribonucleic acid
Rp8pGPT-cGMPS	guanosine, 3´,5´-cyclic monophosphorothioate, 8--(4-chlorophenylthio)-, Rp-isomer
RPM	revolutions per minute
RT	reverse transcriptase
RT-PCR	reverse transcription-polymerase chain reaction
SEM	standard error of the mean
SDS	sodium dodecylsulfate
SDS-PAGE	sodium dodecylsulfate-polyacrylamide gel electrophoresis
siRNA	short interfering RNA
SMC	smooth muscle cell
SF	stress fibres
WT	wild type
VASP	vasodilator-stimulated phosphoprotein
VCAM-1	vascular cell adhesion molecule-1

VCAN	versican
VEGF	vascular endothelial growth factor

1. Introduction

1.1 Wall tension

Among the multiple accomplishments of the French mathematician Pierre-Simon Marquis de Laplace, the quantitative description of wall tension in 1806 generally is not the first coming into ones mind. However, the wal tension Laplace is law of fundamental importance for the cardiovascular system and especially the pathophysiology of blood pressure-induced remodelling processes in the vessel wall (Lehoux 2006; Haga 2007). Hemodynamic forces, which include transmural blood pressure, cyclic strain and fluid shear stress (Figure 1.1), constitute a special category of biophysical stimuli that elicit important biological effects in affected cells (Gimbrone 1995; Resnick 1995).

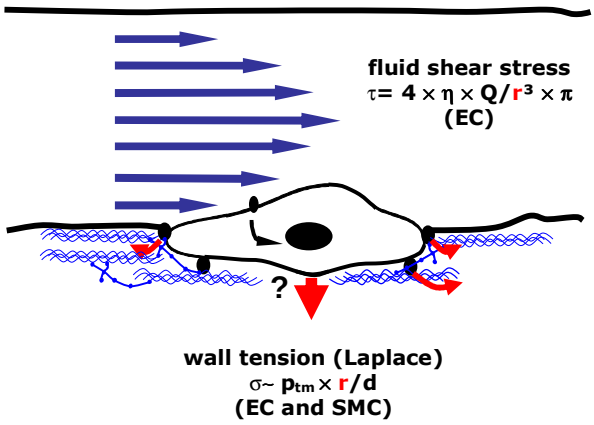

Figure 1.1: Main mechanic forces in the arterial system. Whereas fluid shear stress (FSS) mainly affects EC, wall tension is also sensed by SMC

Laplace's law describes the relation between the transmural pressure difference, radius, and thickness of the vessel wall as a tensional force. Thus, the wall tension (σ) depends on transmural pressure (P_{tm}), radius (r) and wall thickness (d) in tubular vessels (Glagov 1992) as follows:

$$\sigma = P_{tm} * r/d$$

Regarding this definition of wall tension it becomes evident that chronic mechanical overload has several important implications for the vascular system. Faced with hypertension, Laplace's law provides an elegant loophole to evade supra-physiological wall tension, i.e. wall thickening.

Indeed, as will be discussed in some detail below, compensatory accommodation to high pressure conditions occurs via this mechanism – hypertrophic (conduit arteries) or hyperplastic (resistance size arteries) wall thickening ultimately restores basal levels of tensile stress (Lehoux 2006) at the costs of an increased total pheriperal resistance. Depending on time course and pressure level, vessels respond in two principal ways. Besides short term responses to increased perfusion pressures, termed pressure-induced myogenic constriction (Meininger 1992), the long-term response is recognized as compensatory vascular remodelling accompanying prolonged hypertension (Collins 1990; MacMahon 1990; Previtt 2002). Increases of intravascular pressure in hypertension lead to cytoskeletal reorganization within smooth muscle cells (SMC) and remodelling of the vessel wall, resulting in a thickened medial layer with high content of extracellular matrix proteins as well as smooth muscle hyperplasia and hypertrophy (Heagerty 1993; Mulvany 1992; Osol 1995; Lehoux 1998; Previtt 2002). In the course of this process, SMC undergo a change from a quiescent and contractile to a synthetic phenotype. This is accompanied by migration of SMC into the subendothelial space, where these cells organize extracellular matrix components resulting in the formation of a neointimal cell layer. Endothelial cells (EC) respond to increases in circumferential wall tension with a marked change in the secretion of autacoids leading to adaptation of vascular function and structure. Physiologically active relaxing and contracting factors, e.g. angiotensin II, endothelin-1, bradykinin, acetylcholine and ANP with a variety of additional activietes, e.g. as growth factors, (Sumpio 1990; Suga 1993; Day 1995; Harrison 1995; Schiffrin 1999) are synthesized, secreted and metabolized by the endothelium and crucially contribute to the development of pressure-induced vascular remodelling.

Although relieving the high levels of wall tension, this process is highly problematic in terms of the mechanical properties of the vascular system. Whereas adaptive

remodelling in specialized vascular beds, e.g. in leg veins, is clearly physiological, pressure-induced remodelling in hypertension finally not only results in a fixed high resistance to flow which problematic for cardiac function, but also participates in the phenotypical modulation of endothelial and vascular smooth muscle cells, promoting vascular damage due to endothelial dysfunction, and, ultimately, atherosclerosis (Folkow 1973). This is also reflected by the fact that pressure induced vascular remodelling already at initial steps seems to include some pro-inflammatory components. For example, expression of pro-inflammatory gene products by EC and SMC is observed already in early phases of remodelling (see 1.4).

At the clinical level, manifest hypertension, i.e., hypertrophy and/or hyperplasia of the vessel wall are known to be the most important contributors to the development of stroke as well as heart and kidney failure. Moreover, thay play a major role in the development of coronary artery disease and consequently myocardial infraction (Collins 1990; MacMahon 1990; Perry 1995; Pasterkamp 2000).

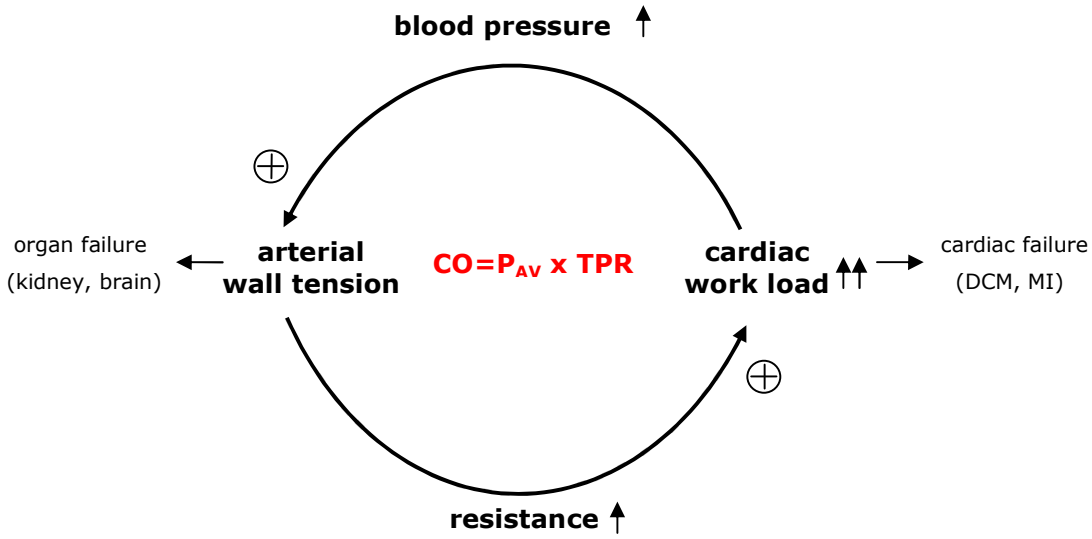

Figure 1.2: The vicious cycle of pressure/resistance–induced hypertrophic remodelling in the cardiovascular system. In order to stabilize cardiac output (CO), the arteriovenous pressure gradient (P_{AV}) must be increased in case of high total peripherial flow resistance (TPR). If chronic, this relation results in compensatory and mutual cardiac and arterial remodelling finally leading to organ failure (see text). The situation of wall tension increases occurring repeatedly in the development of manifest hypertension.

Although the end points, i.e., pressure-induced vascular remodelling and atherosclerosis, have been well characterized, the onset of the remodelling process is still not well understood. How do alterations in wall tension change the phenotype of vascular cells? How can a simple mechanic stimulus re-program the whole transcriptome of affected cells?

1.2 Vascular mechanotransduction

The term “mechanotransduction” refers to the many pathways by which cells convert mechanical stimuli into chemical activity (Ingber 2006). Mechanical load increases protein synthesis and induces the expression of specific genes (Komuro 1993) as well as being a potent stimulus for the secretion of several factors in vascular cells. In accordance with this principle, most agents exert their actions by interfering with certain molecules of known signal transduction cascades.

Keeping in mind the several consequences of manifest hypertension, understanding the initial and specific signalling events leading to the phenotype changes of vascular cells necessary for the onset of remodelling is of high scientific and clinical interest.

What is known? Focal adhesions are a key factor for detecting and responding to mechanical stresses (Davies 2001; Shyy 2002). While the cytoskeleton has an obvious role in structural cell integrity and motility, it has become clear in recent years that cytoskeletal proteins also transmit and modulate the tension between extracellular matrix, focal adhesion sites, and intracellular compartments, thus regulating many cellular and biochemical processes as, e.g., signalling to the nucleus. One class of receptors that modulates both cell-substratum adhesion and signalling are integrins (Burridge 1988; Ingber 1991; Ingber 2002; Ingber 2006). In cultured cells, integrins concentrate at focal contacts where they build a transmembrane linkage between elements of the extracellular matrix and the cytoskeleton (Burridge 1988; Ingber 2002; Ingber 2006). Since the integrins do not possess intrinsic signalling activity, it is thought that signalling occurs via the ability of these proteins to regulate activities of associated signalling partners (Nix 1997). The initial circumferential stretch, driven by a step increase in pressure, also activates stretch-sensitive cation channels. Their activation leads to increased levels of intracellular calcium and thus, e.g., to SMC

contraction (Davis 1999). Those plasma membrane channels have been suggested to be primary stretch sensors in mechanotransduction (Lansman 1987; Morris 1990). However, conclusive evidence for their involvement in mechanotransduction is still lacking. From that point, different mechanotransduction cascades can be initiated according to the nature of the mechanical stimulus perceived.

During the stimulation of vascular cells by wall tension several kinases are activated: focal adhesion kinase (FAK), rho-kinase (ROCK) and MAP kinase pathways (Lehoux 1998; Tsuda Y. 2002; Li 2003; Li 2003; Lehoux 2006), finally resulting in the activation of stress-inducible transcription factors such as AP-1, C/EBP (Lauth 2000; Wagner 2000; Cattaruzza 2001; Cattaruzza 2002), CREB, NFκB (Li 2003; Lehoux 2006) as well as Sp-1 and Egr-1 (Wilson 1998; Morawietz 1999).

Although all these pathways and transcription factors participate in the cellular stress response to mechanical overload, the activation of factors such as AP-1 or C/EBP, also part of other stress processes, e.g. inflammation, is not sufficient to explain the highly specific and particular gene expression pattern in EC and SMC in response to high levels of wall tension. Recently, we could characterize zyxin, a cytoskeletal protein normally associated with focal adhesion contacts to be crucially involved in wall tension-induced vascular smooth muscle cell signalling (Cattaruzza 2004).

1.3 Zyxin in vascular mechanotransduction

Zyxin is a cytoskeletal phosphoprotein widely expressed in human tissue. It is present at sites of cell adhesion contacts, where together with its binding partners: α-actinin and vasodilator-stimulated phosphoprotein (VASP), it is responsible for the integrity and dynamics of the actin fibre formation (Crawford 1991; Crawford 1992; Reinhard 1995; Hoffman 2006). When cells are exposed to mechanical stress, zyxin relocates to actin stress fibres and helps to reinforce the cytoskeleton (Yoshigi 2005). Additional to its architectural function, zyxin has been already proposed to potentially be capable of participating in intracellular signalling (Sadler 1992; Beckerle 1997). However, the generation of zyxin-deficient mice (Hoffman 2003) did not reveal any functional phenotype. Affected mice are viable, although they seem to be smaller than wild type

mice. Thus, the function of zyxin still is not fully analyzed and might only be revealed in pathological models.

What makes zyxin so remarkable in terms of mechanotransduction? Sequence analysis revealed that zyxin has a specific modular organization, consisting of functional actA- and LIM-domains as well as a nuclear export signal (NES) (Sadler 1992; Schmeichel 1994; Nix 1997). These domains have been shown to be involved in direct association with VASP or α-actinin (Reinhard 1995; Gertler 1996) and otherspecific protein-protein or protein-nucleic acid interactions (Schmeichel 1994) as well as being functional in nuclear export (Nix 1997). Although the structure is reminiscent to signalling molecules (Figure 1.3), the function of zyxin in cellular signalling is not well understood. However, isolated domains overexpressed in cell culture shuttle between focal adhesions and the nucleus (Nix 1997). Moreover, zyxin can be activated by ANP in cardiomyocytes and leave focal adhesions (Smolenski 2000; Kato 2005). Finally, we were able to show for the first time in vascular SMC that in response to mechanical stress zyxin indeed relocates to the nucleus of those cells, where it may alter transcriptional patterns (Cattaruzza 2004).

Thus, zyxin is a protein that may specifically transduce mechanical stimuli between cellular compartments and the nucleus, not only being part of the sensing machinery but also orchestrating the transcription of vascular cells exposed to mechanical stress.

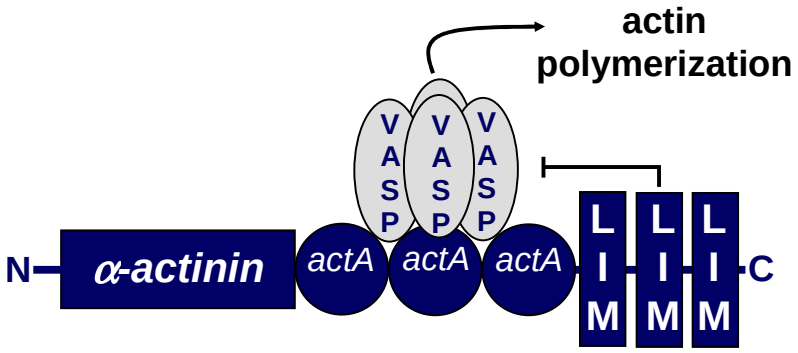

Figure 1.3: Domain structure of zyxin.

1.4 Wall tension-induced gene expression

Levels of circumferential strain exerted on vascular cells are a result of arterial wall expansion due to pressure-induced wall tension and contraction. To compensate supra-physiological levels of this tensile force, several signalling pathways (see above) are activated in vascular cells resulting in altered gene expression (Lehoux 1998; Lehoux 2006). However, up to now, only a limited number of stretch-responsive genes have been characterized and no valid systematic analysis of the endothelial and smooth muscle cell transcriptome in response to increases in wall tension has been published. Many of the already known stretch-induced gene products encode proteins involved in the environmental adaptation of the affected cells. Therefore, identification of all differentially expressed genes under conditions of high wall tension would be of high interest in order to gain a first functional insight into the initial signalling mechanisms and phenotypic changes of vascular cells during vascular remodelling.

In EC, an increase in cyclic stretch has been proposed to induce the expression of several pro-angiogenic and pro-inflammatory gene products such as vascular endothelial growth factors (VEGF), cell adhesion molecules (ICAM-1, VCAM-1) and chemokines (MCP-1), which in turn lead to subsequent changes in the structure of the vessel wall (Resnick 1995; Obuwole 1997). At least some of these gene products as well as a number of heat shock proteins (Frye 2005) are, however, regulated by wall tension-induced oxidative stress. Oxidative stress, brought about by the activity of NAD(P)H oxidase, is also found in inflammation (Griendling 2000; Schiffrin 2003) and other cellular stresses. Although this enzyme promotes remodelling, it is thus not specific for mechanotransduction. In SMC, VEGF was the first gene identified as mechanically inducible (Feng 1999). Further, in human and rat SMC also genes such as cyclooxygenase-1, plasminogen activator inhibitor-1, the B-type endothelin receptor, matrix metalloproteases and matrix proteins, e.g. fibronectin and tenascin-C, have been classified to be mechano sensitive (Feng 1999; Cattaruzza 2004).

1.5 The role of natriuretic peptides in cardiac and vascular remodelling

Although zyxin seems to be the long sought-after mechanotransducing protein, one important question remains to be answered: How does wall tension activate zyxin and induce its nuclear translocation?

Blood vessels possess a variety of autocrine and paracrine mechanisms enabling them to immediately react to local modifications of hemodynamic forces including wall tension changes. As pointed out before, cardiac and vascular cells sense such forces and secrete various vasoactive substances to regulate vascular tone and maintain homeostasis (Lüscher 1986; Lüscher 1986; Moncada 1991; Cohen 1995; Kojda 1999; McIntyre 1999). Thus, besides systemic parameters such as sympathetic activity, local mechanisms participate in a truly autonomic way to maintain of vascular function and structure.

Interestingly, an apparently unrelated systemic control circuit regulating total body fluid and osmolarity employs the sensing of wall tension in cardiac atria in order to determine total blood volume (Kramer 1986, Zisfein 1986, Dietz 1989). Besides the main “savers” of salt and water, the renin-angiotensin-aldosteron system (RAAS) and the anti-diuretic hormone vasopressin, the system is composed of salt and fluid “eliminators”, namely three natriuretic peptides (NP): ANP, BNP and CNP together with three functionally distinct receptors (NP-R) of the A, B and C-type (Koller 1992).

The release of ANP, BNP and CNP from the atria is triggered by increases in atrial filling and, consequently, wall tension. Those molecules then promote sodium and water excretion by increasing the rate of glomerular filtration and inhibiting sodium reabsorption by the kidney (Laragh 1985). Moreover, ANP-mediated actions are also characterized to cause prominent increases in endothelial permeability (Brenner 1990; Wijeyaratne 1993). Therefore, increased ANP levels are detected in individuals suffering form congestive heart failure, chronic renal failure and in severe essential hypertension (Koller 1992; Ruskohao 1992; Yandle 1994) presumably to stabilize renal function and relieve the cardiovascular system of increased (blood) volume.

Most intriguing in the context of vascular mechanotransduction is the mode as to how the first NP characterized, atrial natriuretic peptide, is released from atrial myocytes into the blood (Ruskoaho 1886; Lang 1985; Kinnunen 1993; Dietz 2005). According to these authors, the main physiological stimulus for increased ANP release is a supra-physiological distension of the atria, caused by increased filling pressures (see Laplace's law), which always occurs when blood volume is elevated.

Several lines of evidence show that indeed endothelial cells are indeed the atrial sensor for increases in wall tension responding with the release of the vasoconstricting peptide endothelin-1. Consecutively specialized atrial myocytes are induced to release ANP into the blood (Mäntymaa 1990; van Wamel 2001) via activation of the A-type ET-1 receptor. In the isolated perfused rat heart ET-1 increases both basal and wall stretch-induced atrial ANP secretion (Mäntymaa 1990; Shirakami 1993).

ANP exerts its physiological responses through binding to a specific membrane-bound receptor with intrinsic guanylyl cyclase activity (de Bold 1981; Goetz 1988; Maack 1992), also referred to as natriuretic peptide receptor type A (NPR-A) (Garbers 1991; Garbers 1994). NPR-A-derived cGMP in turn activates the downstream cGMP-dependent effector-kinase PKG. Many studies demonstrate that NPR-A is the specific and only receptor mediating the hypotensive and diuretic/natriuretic actions of ANP (Lopez 1997). ANP however has a low affinity for the B-type natriuretic peptide receptor (NPR-B) which appears to be activated preferentially by CNP (Garbers 1994). The C-type natruretic receptor (NPR-C), also called clearance receptor, does not seem to be involved in important biological effects of natriuretic peptides, and is thought to serve as a "scavenger" receptor for eliminating excess ANP by internalizing it (Maack 1987; Maack 1992). All NP receptors and signalling pathways are summarized in Figure 1.4.

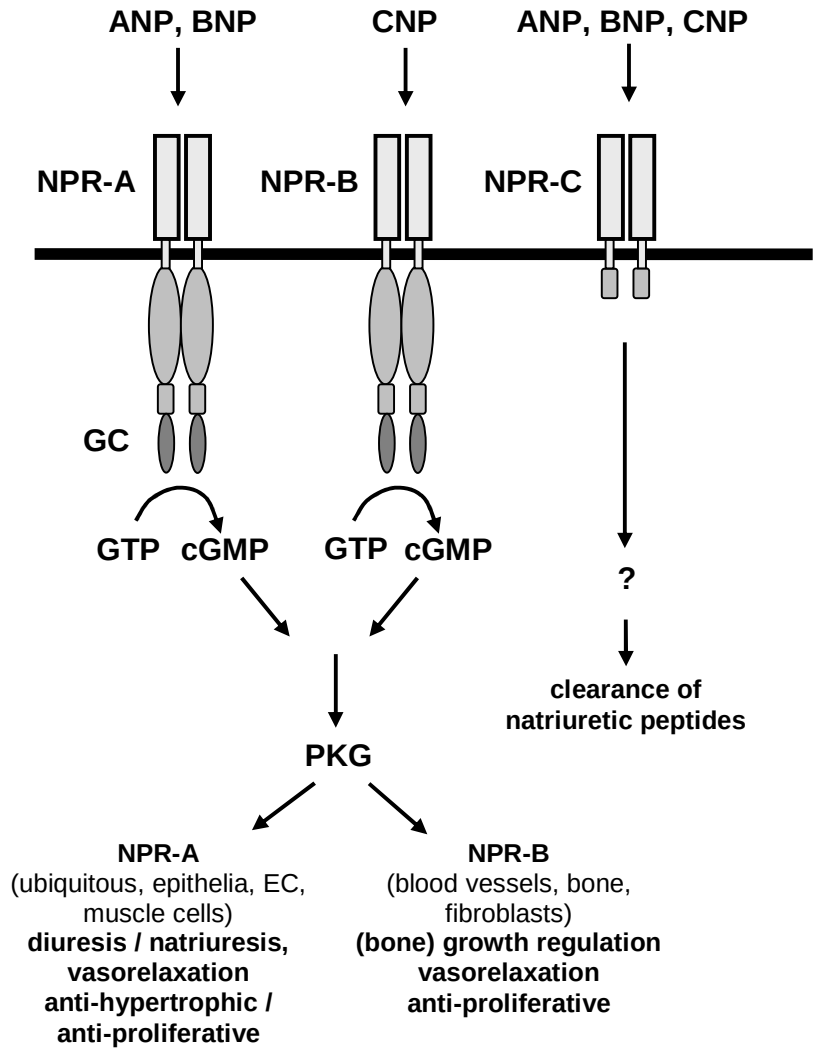

Figure 1.4: Schematic representation of the natriuretic peptides, their receptors and their intracellular signalling pathways.

Since several components of this complex multi-cellular cardiac mechanosensing machinery are expressed in the vasculature, especially in EC, we have analysed if these proteins also mediate the onset of wall tension-induced signalling in human cultured primary endothelial cells.

1.6 Aims of the study

As described, the cytoskeletal protein zyxin is an integral part of (pathophysiologic) mechanotransduction in vascular cells. In rat aortic smooth muscle cells zyxin is activated upon mechanical overload, then translocates to the nucleus and is involved in the first steps of vascular remodelling – stretch induced gene expression (Cattaruzza 2004). Although an association of wall tension and zyxin in mediating intracellular signalling in vascular cells has been defined, molecular mechanisms of this process remain fully unexplored. It is not yet clear whether zyxin is a mechanosensor itself or is an early protein in the specific response pathway.

In order to understand the role of zyxin in vascular mechanotransduction, this work will address three main issues:

First, how is zyxin activated in response to increased levels of wall tension in endothelial cells?

Secondly, what are the principal changes in gene expression in endothelial and smooth muscle cells in response to wall tension? Moreover, what role does zyxin play in wall tension-induced gene expression? To answer these questions, we will use human cultured primary EC and an siRNA-mediated zyxin knock down approach as well as aortic SMC derived from wild type and zyxin-deficient mice. These cells will be exposed to cyclic stretch (equivalent to an increase in vessel radius, see Laplace's law) and characterized by systematic genome-wide micro-array analyses.

Thirdly, the role of zyxin in vascular function will be explored using a perfusion chamber and femoral arteries freshly isolated form wild type and zyxin-deficient mice.

2. MATERIALS

2.1 Synthetic oligonucleotide primers for PCR

The oligonucleotide primer sequences for all gene products used in real time PCR gene expression analysis are listed in table 1. Oligonucleotides were synthesized by IBA (Göttingen, Germany) and dissolved in water to a final concentration of 1 nmol/µl.

Table 1: PCR DNA primers

Gene product	Primer sequence (forward/reverse)	Annealing temperature (°C)
Mouse MCP-1 (Demicheva)	5´ -TTC CTC CAC CAC CAT GCA G- 3´ 5´ -CCA GCC GGC AAC TGT- 3´	60
Mouse AT-1 (own)	5´ -TGT TCC TGC TCA CGT GTC TC- 3´ 5´ -CAT CAG CCA GAT GAT GAT GC- 3´	60
Mouse ET_A-R (own)	5´ -CTA AGC AGC CAC ATG GAA GA- 3´ 5´ -CCA TTG CTA GGC AGG GCC AA- 3´	60
Mouse ET-1 (own)	5´-GCG TCG TAC CGT ATG G- 3´ 5´-TGG TGA GCG CAC TGA C- 3´	58
Human IL-8 (own)	5´ -TAG CCA GGA TCC ACA AGT CC- 3´ 5´ -GCT TCC ACA TGT CCT CAC AA- 3´	60
Human CXC3L1 (own)	5´-TCT GAA GGC TGG GTT CTG AT- 3´ 5´ -TGT CAG GGG GAC AGG TAT TC- 3´	58
Human IL-8 receptor (CXCL1) (own)	5´ -TCC TGC ATC CCC CAT AGT TA- 3´ 5´ -CTT CAG GAA CAG CCA CCA GT- 3´	58
Human VCAN (own)	5´ -CAA GCA TCC TGT CTC ACG AA- 3´ 5´ -TGG TTG GGT CTC CAA TTC TC- 3´	60
Human VCAM-1 (own)	5´ -CAT GGA ATT CGA ACC CAA ACA- 3´ 5´ -GAC CAA GAC GGT TGT ATC TCT GG- 3´	60
Human ICAM-1 (own)	5´ -TGA TGG GCA GTC AAC AGC TA- 3´ 5´ -GGG TAA GGT TCT TGC CCA CT- 3´	60
Human GAPDH (Wagner et al)	5´ -GAC CAC AGT CCA TGC CAT CAC TGC- 3´ 5´ -ATG ACC TTG CCC ACA GCC TTG G- 3´	60
Human NPR-A (own)	5´ -AAC GCA TTG AGC TGA CAC G- 3´ 5´ -GTC CAG GGT GAT GCT CTC AT - 3´	58
Human NPR-C (own)	5´ -AGT GAG ATG GCT ATG GAG G- 3´ 5´ -TCC TCC ATA TTG AGC CCT TG- 3´	58
Human ANP (Wagner)	5´ - GAT AAC AGC CAG GGA GGA CA - 3´ 5´ - ATC ACA ACT CCA TGG CAA CA - 3´	60
Human BNP (Wagner)	5´ - TTA CAG GAG CAG CGC AAC C - 3´ 5 – GGA CTT CCA GAC ACC TGT GG - 3´	58
Human CNP (Wagner)	5´ - TCG CCT TCT GCA AGA GCA C - 3´ 5´ - GAT TCG GTC CAG CTT GAG G - 3´	60

Mice WT zyxin (genotyping)	5′-TAC AAG GGC GAA GTC AGG GCG AGT G-3’ 5′-TGG ACG AAG TTT CCG TGT GTT G-3′	58
Mice NEO zyxin (genotyping)	5′-GAC CGC TTC CTC GTG CTT TAC-3′ 5′-TGG ACG AAG TTT CCG TGT GTT G-3′	58

2.2 Bacterial strains and plasmids

Table 2: Plasmids

Vector	Characteristic	Source
pCR 2.1-TOPO 3.9	pUC origin, lacZα reporter fragment; T7 promoter/priming site, f1 origin; ampiciline resistance ORF; kanamycin resistance ORF	Invitrogen (Karlsruhe, Germany)

Table 3: Chemically competent E. *coli* cells

Bacterial cells	Genotype	Source
One Shot TOP10F´	*mcr*A Δ(*mrr-hsd*RMS-*mcr*BC) Φ80*lac*ZΔM15 Δ*lac*X74 *rec*A1 *ara*D139 Δ(*ara-leu*)7697 *gal*U *gal*K *rps*L *end*A1 *nup*G	Invitrogen
E. cloni 10G	F´*mcr*A Δ(*mrr-hsd*RMS-*mcr*BC) *end*A1 *rec*A1 Φ 80d*lac*ZΔM15 Δ*lac*X74 *ara*D139 Δ(*ara,leu*)7697 *gal*U *ga*lK *rps*L *nup*Gλ *ton*A	Lucigen Corporation (Middleton, USA)

2.3 Small interfering RNAs

Table 4: siRNA target sequences constructed by Qiagen

siRNA	Target sequence	Source
Hs_ZYX_1_HP Validated	AAG GTG AGC AGT ATT GAT TTG	Qiagen (Hilden, Germany)
AllStars Negative Control	N/A	Qiagen

2.4 Antibodies

Table 5: Regularly used secondary antibodies

Secondary antibody and specification	Source
Alexa Fluor 488 goat anti-mouse and anti-rabbit IgG	MoBiTec (Göttingen, Germany)
Alexa Fluor 594 goat anti-rabbit IgG	MoBiTec
Goat anti-rabbit IgG peroxidase	Sigma Aldrich (Schnelldorf, Germany)

Table 6: Primary antibodies

Primary antibody and specification	Source
Mouse anti-human eNOS /NOS-3	BD Transduction Laboratories (California, USA)
Rat anti-mouse CD31 clone MEC 13.3, polyclonal	Santa Cruz Biotechnology (Heidelberg, Germany)
Mouse anti - β-actin	Sigma Aldrich
Rabbit anti-human B72 LH-ZyxinPLAG (against peptide CDFPLPPPPLAGDGDDAEGAL, zyxin amino acids 70 to 89)	Mary Beckerle, Huntsman Cancer Research Centre, University of Utah
Rabbit anti-human B71 LH-ZyxinNES (against peptide CSPGAPGPLTKEVEELEQLT, zyxin amino acids 344 to 363)	Mary Beckerle, Huntsman Cancer Research Centre, University of Utah
Mouse anti-human Atrial Natiuretic Peptide, monoclonal	Chemicon Europe (Hampshire, UK)
Rabbit anti-human alpha Atrial Natiuretic Factor (1-28), monoclonal	Penisula Laboratories INC (San Carlos, California, USA)
Rabbit anti-human Atrial Natiuretic Factor (1-28)	AbCam (Cambridge, UK)
anti-mouse eNOS /NOS-3	BD Pharmingen (San Diego, California, USA)
Mouse anti-human Natriuretic Peptide Receptor type C, polyclonal	Abnova (Taipel, Taiwan)

2.5 Cell culture.

Table 7: Cell culture media, buffers, antibiotics and supplements

Name of product	Company
Collagenase	Sigma Aldrich
Dispase	Böhringer (Mannheim, Germany)
D-MEM + GlutaMAX-I	Invitrogen
Endothelial cell growth supplement (ECGS)	Promocell (Karlsruhe, Germany)
FBS	Invitrogen
Gelatine	Sigma Aldrich
Hank's BSS	PAA (Cölbe, Germany)
M199 + GlutaMAX-I	Invitrogen
OPTIMEM I	Promocell
Penicillin	Invitrogen
SMC growth media	Promocell
Supplemental Mix	Promocell
Streptomycin	Invitrogen

2.6 Mouse strains

C57BL/6J mice were initially ordered from Charles River Laboratories, Sulzfeld, Germany, and further bred in the animal facility of the University of Heidelberg.

Zyxin *null* mice (line zyxin-185) were kindly provided by Dr. Laura Hoffman and Dr. Mary Beckerle from the Huntsman Cancer Research Centre, University of Utah, Salt Lake City, USA. Further, the zyxin *null* mouse line was sanitized to be housed at the animal facility at the University of Heidelberg. Animals were studied in compliance with institutional and legislatory regulations.

Table 8: Mouse strains

Strain	Source
C57BL/6J	Charles River Laboratories, Sulzfeld, Germany
C57BL/6J zyxin (-/-) null (line 185)	Huntsman Cancer Research Centre, University of Utah, Salt Lake City /JBF

2.7 Kits

Table 9: Kits

Name	Company
QIAprep Mini Plasmid Kit	Qiagen (Hilden, Germany)
QIAquick Gel Extraction Kit	Qiagen
Rneasy Mini Kit	Qiagen
Sensiscript RT Kit	Qiagen
QuantiTect SYBR Green® Kit	Qiagen
ReadyPrep Protein Extraction Kit (Cytoplasmic/Nuclear)	BioRad (München, Germany)
ReadyPrep 2-D Cleanup Kit	BioRad
TOPO TA cloning Kit	Invitrogen
Human Endothelin-1 ELISA Kit	R&D Systems (Wiesbaden, Germany)
Human CXCL8/IL-8 ELISA Kit	R&D Systems
Human pro-ANP ELISA kit	Biomedica (Graz, Austria)

2.8 Reagents

Table 10: Regularly used reagents and substances

Substance	Company
Acetylcholine chloride, minimum 99% TLC	Sigma Aldrich
Angiotensin II, human	Calbiochem (San Diego, California, USA)
Atrial Natiuretic Factor 1-28, human	Calbiochem
Bio-Lyte 3-10 Ampholyte	BioRad
BQ-788	Sigma Aldrich
DETA/NO	Sigma Aldrich
ECL Plus Western Blotting Detection reagent	Amersham (Little Chalfont Buckinghamshire, UK)
Endothelin 1, human and porcine,	Calbiochem
MATra-si Reagent	IBA (Göttingen, Germany)
®-(-)Phenylephrine hydrochloride	Sigma Aldrich
Phosphatase Inhibitors	Active Motif (Rixensart, Belgium)
Protein phosphatase 1 (PP1)	New England BioLabs (Ipswich, MA, USA)
Proteinase K	Sigma Aldrich
RNAlater RNA stabilization reagent	Qiagen
Rp8pGPT-cGMPS	Calbiochem
Taq Polymerase	Bioron (Ludwigshafen, Germany)

2.9 Solutions and buffers

Phosphate Buffered Saline (10X) pH 7.4:

130.0 mM	NaCl
2.7 mM	KCl
7.0 mM	Na_2HPO_4 x $2H_2O$
4.0 mM	KH_2PO_4

Tris Buffered Saline, pH 7.4:

25.0 mM	Tris-HCl
137.0 mM	NaCl
2.7 mM	KCl

TEN Buffer:

10.0 mM	Tris/HCl (pH 8.0)
1.0 mM	EDTA
100.0 mM	NaCl

2.10 Microbiological media

Luria-Bertani (LB) Medium (pH 7.0)

1.0 % (w/v)	Bacto-tryptone
0.5 % (w/v)	Yeast extracts
1.0 % (w/v)	NaCl

LB-Agar Plates

1.0 % (w/v)	Bacto-tryptone
0.5 % (w/v)	Yeast extracts
1.0 % (w/v)	NaCl
1.5 % (w/v)	Agar

The Luria-Bertani medium was prepared with distilled water, autoclaved and stored at room temperature. LB agar (50° C) was supplemented with 50 µg/ml ampicillin and poured into Petri dishes. The dishes were stored at 4° C.

2.11 Software

Table 11: Frequently used software and programs

Software/Program	Company
KCjunior™ Software	BIO-TEK Instruments (Winooski, Vermont, USA)
LightCycler™ software version 3.5.3	Roche (Mannheim, Germany)
MyoView™ Pressure Myograph software	Danish Myo Technology (Atlanta, USA)
MetaMorph® imaging system version 3.5	Universal Imaging Corporation (Marlow Buckinghamshire, UK)
NanoDrop® software	NanoDrop (Wilmington, USA)
Quantity One® 1-D analysis software	BioRad (USA)
Quantity One® image acquisition software	BioRad
PDQuest™ 2-D Analysis Software	BioRad
InStat statistics program	GraphPad Software, Inc (S. Diego, USA)
BLAST (Basic Local Alignment Search Tool) www.ncbi.nlm.nih.gov	National Center for Biotechnology Information (NCBI)
ExPASy tool www.expasy.ch	SwissProt
P-87 Flaming/Brown Micropipette Puller	Slutter Instrument Company (Novato, USA)
SAS MicroArray Solution version 1.3	SAS Institute Inc. (Carry, NC, USA)
Gene set Enrichment Analysis (GSEA)	Broad Institute of MIT and Harvard (USA).
KEGG database	KUBiC, Kanehisa Laboratory (Kyoto, Japan)

3. Methods

3.1 Cell culture

3.1.1 Isolation and culture of mouse aortic smooth muscle cells (mAoSMC)

Isolated mouse aortae were cut into small rings (1 mm) and washed several times with HBSS/Hank´s buffer until all blood was removed. The tissue was digested overnight at 37° C, 5 % CO_2 in 1.4 ml SMC growth medium containing 5% FBS and 250 µl of a 1 % collagenase solution in 40 mm ø culture dishes. The resulting cell suspension was centrifuged for 5 minutes at 1000 rpm. The pellet was resuspended in 2 ml of SMC growth medium (50% D-MEM + GlutaMAX-I Medium, 50% Smooth Muscle Cell Growth Medium, supplemented with 5% FBS, 50 U/ml penicillin, 50 µg/ml streptomycin and 0.25 µg/ml fungizone antimycotic) and seeded into a 6 cm ø culture dish. The cells were cultured using standard cell culture techniques. After passage 1, SMC growth medium was replaced by SMC culture medium (D-MEM, supplemented with 15% FBS, 50 U/ml penicillin, 50 µg/ml streptomycin and 0.25 µg/ml fungizone antimycotic). Cells were incubated at 37º C, 5% CO_2, in a humidified atmosphere.

Every batch of isolated and cultured mouse aortic smooth muscle cells was tested for expression of specific SMC markers including SMC isoforms of α-actin by immunofluorescence analysis. Typically, cells were 90% positive for α-SM-actin and were essentially negative for the endothelial cell marker vWF.

3.1.2 Isolation and culture of human umbilical vein endothelial cells (HUVEC)

Human umbilical vein endothelial cells (HUVEC) were isolated routinely from fresh human umbilical cords as described in Lienenlüke et al. (Lienenlüke 2000). Briefly, umbilical veins were gently flushed with Hank's buffer solution until they were essentially blood-free, filled with dispase solution until the cord was moderately swollen and incubated for 30 minutes at 37° C. Veins were then again flushed with

Hank's buffer and the suspension containing the isolated cells was collected in a sterile 50-ml tube. The cells were then centrifuged at ambient temperature for 5 minutes at 1000 rpm. The sedimented endothelial cells were then resuspended in HUVEC culture medium consisting of M199 medium supplemented with 120 mM TES-HEPES pH 7.3, 20% fetal bovine serum, 50 U/ml penicillin, 50 µg/ml streptomycin, 0.25 µg/ml Fungizone antimycotic and 4 µl/ml endothelial cell growth supplement (ECGS) containing 22.5 mg/ml heparin. The cells were routinely cultured on standard plastic dishes or collagen type I BioFlex elastomer plates (Flexcell® International Corporation) additionally coated with 2% (w/v) gelatine in 0.1 N HCl. Culture medium was changed at two-day intervals. The purity of HUVEC was >95% as tested by immunofluorescence analysis using vWF as an EC marker. The cells were essentially free of α-SM-actin (< 1%).

3.1.3 Transfection of HUVEC with siRNA

HUVEC were efficiently transfected with short interfering RNA (siRNA; see Table 4) using magnet-assisted transfection (MATra, IBA). Briefly, to transfect one well of a 6-well plate, 3 µg of siRNA (Qiagen) was diluted in OPTIMEM I medium to give a final volume of 200 µl for each well to be transfected (final concentration approximately 30 nM). For the formation of the transfection complex, 3 µl of MATra-si reagent (IBA, Göttingen) was added to the diluted siRNA, carefully mixed and allowed to incubate at ambient temperature for 25 minutes. HUVEC were once washed in OPTIMEM I, the medium was discarded and then fresh OPTIMEM I (2 ml per well) was added to the cells. The siRNA/magnetic beads were then layered dropwise onto the cells (200 µl/well). Cells were incubated with the transfection complex on a custom-made magnetic plate which was specifically designed to fit the wells of the Flexcell plate (Universal Magnet Plate, IBA) for 15 minutes in the cell incubator to allow beads to penetrate the target cells. Thereafter, to induce rapid zyxin turn over, cells were shortly exposed to cyclic stretch (30 minutes, 0.5 Hz, 10% elongation). After this manoeuvre, the medium was changed to prevent cytotoxic effects from the transfection reagent, and the cells were kept further under their normal culture conditions. Gene silencing was optimal 72 hours after transfection.

Therefore, experiments with transfected HUVEC were performed 72 hours post transfection.

3.1.4 Mechanical Strain

The Flexercell® strain unit was used as a model to mimick the effects of vascular wall tension. Endothelial cells (EC) were cultured on flexible membranes of BioFlex® Plates (Flexcell® International Corporation, Hillsborough, USA) which can be stretched in a defined manner. Before starting the experiment, EC were growth-arrested for 2 hours in HUVEC quiescence medium. Depending on the experimental conditions, defined cyclic stretch was applied to the cells using the computer-assisted Flexcell® Tension™ system FX3000T (Flexcell® International Corporation).

All strain protocols were performed at a frequency of 0.5 Hz using stretch profiles up to 10% cyclic elongation for up to 18 hours. Messenger RNA or cellular protein was harvested at specific time points after the initiation of stretch. Alternatively, the cells were fixed with either methanol/acetone or 4% formaldehyde in PBS for further immunofluorescence analysis, or proteins were isolated from the supernatant of the cells.

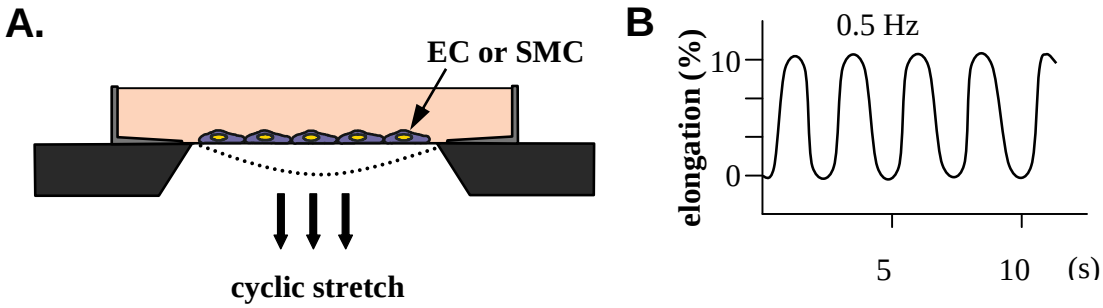

Figure 3.1: Schematic diagram of the FlexCell model (A) and a typical strain profile (B) applied to mouse smooth muscle cells (SMC) or human endothelial cells (EC) in culture.

3.1.5 General experimental procedures with cultured cells

Cells were incubated with or without ANP (1 nM) or ET-1 (10 nM) in the presence or absence of BQ788 (1 µM) or Rp8pGPT-cGMPS (100 µM) respectively. Reagents

were added to the cell culture medium (volume 2 ml). After treatment cells were kept at static conditions or exposed to cyclic stretch for 6 hours. Thereafter cell culture media were collected and frozen at -80°C for further analysis. Cells were either lysed with RLT buffer (Qiagen) for mRNA isolation, fixed as described above for fluorescence analysis or collected by centrifugation (3000 rpm, 4°C) for cell fractionation and Western blot analysis.

3.2 Molecular biology

3.2.1 Isolation of genomic DNA from mouse tails for PCR genotyping.

DNA isolation from the tails was performed according to a standard protocol (Hogan 1993). From 0.7 to 1 cm of the mouse tail was incubated in 150 µl digestion buffer containing proteinase K (1 mg/ml) at 55° C for 6 hours. Every hour the samples were mixed to facilitate tissue degradation. Thereafter, the digestion mixture was incubated at 95°C for 10 – 20 minutes, gently mixed and centrifuged at 13000 rpm for 10 minutes at ambient temperature to collect undigested tail debris. Finally, the DNA containing supernatant was stored at -20° C for further PCR analysis (see 3.2.9.4).

For PCR genotype analysis zyxin mice primers (mice WT zyxin and mice NEO zyxin) were used (Table 1). The program was as follows (Table 12). The PCR products were either wild type *zyxin*, (327 bp) or null mutant (473 bp).

Table 12: Program for genotyping

PCR step	Temperature (in °C)	Time
Denaturation	95° C	60 seconds
Annealing	58° C	30 seconds
Extension	72° C	50 seconds
	95° C	1 minute
Final extension	72° C	3 minutes

Digestion buffer for tail DNA:

670.0 mM	Tris/HCl, pH 8.8
166.0 mM	ammonium sulphate
65.0 mM	$MgCl_2$
1.0 % (v/v)	β-mercaptoethanol
0.5 %	Triton X-100

3.2.2 Isolation of total RNA from tissue samples and cultured cells

To isolate total RNA from cells, the QIAGEN RNeasy kit was used according to the manufacturer's instructions. In order to avoid any RNase activity, RNase-free water and RNase-free reaction tubes were used during the procedure. Briefly, total RNA was extracted by adding 350 µl of lysis buffer containing 1% β-mercaptoethanol per well of a 6-well plate. Thereafter, lysates were scraped from the wells into microcentrifuge tubes and homogenized for 30 seconds. An equal volume of 70% ethanol was added and mixed with the lysates. The mixture was then transferred to the mini spin column, centrifuged for 25 second at 13000 rpm following two washing steps. Finally, the RNA was eluted with 30 µl RNase-free water.

3.2.3 Determination of nucleic acid concentration

The concentration of nucleic acids was determined spectrophotometrically using the NanoDrop ND-1000 spectrophotometer (NanoDrop, Wilmington, USA) by measuring light absorption at 260 nm. Nucleic acid purity was checked by determinating absorption at a wawelenght of 230 and 280 nm, respectively.

3.2.4 Agarose gel electrophoresis of DNA

Agarose gels were used to separate nucleic acid molecules according to their size. Depending on the expected number of base pairs, gels containing 0.8% (w/v, >1000 bp) to 2.5% (w/v, >50 bp) agarose were prepared using 100 ml 0.5x TBE buffer. The suspension was heated until all the agarose was melted and 3 µl of ethidium bromide (10 mg/ml) was added. After cooling to approximately 60° C the gel was poured into the horizontal gel chamber. TBE buffer (0.5x) was used as the

electrophoresis buffer. Before loading the samples, 0.2 volumes of loading buffer were added and the sample was mixed. Electrophoresis was carried out at a steady voltage of 120-140 V. The size of the DNA fragments in the agarose gels was determined using appropriate size standards. DNA fragments were detected and analyzed by the Gel Doc XR gel documentation system (BioRad).

5X TBE buffer

450 mM	Tris base
450 mM	Boric acid
20 mM	EDTA, pH 8.0

6X Glycerol loading buffer

10 mM	Tris/HCl, pH 7.5
10 mM	EDTA, pH 8.0
30.00 %	Glycerol
0.01 %	bromophenol blue
0.01 %	xylene green

3.2.5 Extraction of DNA fragments from agarose gels

This method was used to extract and purify double-stranded DNA molecules of 70 bp to 10 kilo base pairs (kb) from low melting agarose gels. The principle of this method depends on the selective binding of DNA to silicagel membranes on QIAGEN spin columns. The kit was used according to the supplier's instructions.

3.2.6 TOPO cloning

For the construction of specific real-time RT-PCR standards, PCR fragments were ligated into the TOPO cloning vector system (Invitrogen). The kit was used according to the manufacturer's protocol.

3.2.7 Transformation of *E. coli*

Transformation of bacteria was done by gently mixing an aliquot of adequate competent bacterial cells (25-40 µl) with 1-2 µl of plasmid DNA or a ligation reaction. After incubation for 35 minutes on ice, bacteria were heat shocked for

30 seconds at 42° C and then immediately cooled down for 2 minutes on ice. After adding 600 µl of pre-warmed S. O. C. medium, bacteria were incubated at 37° C with shaking for 1 hour to allow recovery from the heat shock. They were then plated on LB-agar plates containing the appropriate antibiotic.

3.2.8 Small-scale isolation of plasmid DNA

Plasmids grown in mini-cultures (7 ml) over night were purified using the Qiagen Plasmid Mini Spin Kit according to the manufacturer's instructions.

3.2.9 Polymerase Chain Reaction (PCR)

The polymerase chain reaction (PCR) is a very sensitive and powerful technique (Mullis. K.B. 1987; Saiki 1988) for the exponential amplification of specific DNA sequences *in vitro* by using sequence-specific synthetic oligonucleotides and a thermo-stable DNA-polymerase. The method was used for the amplification of genomic DNA for genotyping and in combination with reverse transcription of RNA for determination of mRNA expression levels of stretch-inducible gene products.

3.2.9.1 Reverse transcription PCR (RT-PCR)

To generate a representative cDNA pool from RNA templates 1-5 µg of total RNA were mixed with 1 µl of oligo (dT) 18 primer (10 pmol/µl) and RNase free water to a total volume of 14 µl. To facilitate hybrid formation of the oligo dT-primers with polyA-tails of mRNA, the mixture was heated to 70° C for 10 minutes and then quickly chilled on ice. After a brief centrifugation, the following was added to the mixture:

4 µl of 5x First strand buffer

1 µl of 0.1 M reverse transcriptase enzyme (RT)

1 µl of 10 mM dNTPs

The content of the tube was gently mixed and incubated at 42° C for 50 minutes for first strand cDNA synthesis. Then, the reaction was inactivated by incubating the mixture at 70° C for 10 minutes, and 180 µl of RNase-free water was added to dilute the resulting cDNA. These samples were used for the PCR reactions described below.

3.2.9.2 PCR amplification of DNA fragments

Semi-quantitative PCR was performed by normalizing to the relative amount of cDNA of a house-keeping gene. For this purpose, glyceraldehydes-3-phosphate dehydrogenase (GAPDH) was chosen as an internal standard. The PCR reaction was performed in an automatic thermocycler (Biometra) programmed as shown in Table 13.

Table 13: Program for semi-quantitative PCR

PCR step	Temperature (in °C)	Time
Pre-denaturation	95° C	5 minutes
Denaturation	95° C	30 seconds
Annealing	56°- 60° C (depending on the primers used)	40 seconds
Extension	72° C	2 minutes
Final extension	72° C	5 minutes

3.2.9.3 Quantitative real-time PCR

For quantitative analysis of changes in gene expression real-time RT-PCR analysis was used essentially as described in Wagner et al. (Wagner 2002). The plasmid standards for the gene products to be measured were cloned into pre-cut TOPO wectors (3.2.6) and the number of molecules / µl was calculated according to size (bp) and concentration. The number of plasmid templates used as standards varied between 10^2 to 10^8 depending on the expected abundance of the gene product to be determined. As control gene products for the normalization of the cDNA amount added to the reaction, GAPDH and the endothelial cell marker PECAM-1/CD31 were used. Real-time PCR was carried out in a LightCycler instrument (Roche Diagnostics, Penzberg, Germany). The QuantiTect SYBR Green® kit (Qiagen) was used for the amplification reaction according to the manufacturer's instructions.

3.2.10 Microarray analysis

For the microarray analysis human endothelial cells were isolated from umbilical cords equal in length, age and growth characteristics. HUVEC were cultured on flexible membranes and only those that reached 90% confluence within 2 days were used for experiments. HUVEC were subjected to 10% cyclic stretch at a frequency of 0.5 Hz for 6 hours (Chapter 3.1.4). Three independent experiments (static control plus stretched samples) were performed using cells from three unrelated individual umbilical cords. High quality mRNA was isolated as described, tested by real time RT-PCR, aliquoted and stored at -80° C. Similarly, mouse SMC derived from wild type and zyxin-deficient mice were seeded on Flexercell plates and subjected to cyclic stretch as described above. Again, total RNA was isolated, tested for quality and stored at -80° C in aliquots. Fifteen µl (corresponding to 5-10 µg total RNA) of each sample were delivered for microarray analysis.

Further, Affymetrix GeneChip expression measures (Cope 2004) were performed by microarray-team, Mannheim (Prof. Dr. Norbert Gretz, Walter Bosbach, Li Li, Priyanka Shahi, Susanne Böhn; University Clinics of Mannheim). Hybridization and processing of the genome wide array HG-U133A chips (human) and the genome wide array chips, MG-430 2.0 (mouse) were performed according to the standard protocols available from Affymetrix (Santa Clara, CA, USA). Detailed information about the analytical settings and conditions are available on http://www.ma.uni-heidelberg.de/inst/zmf/affymetrix/ablauf_e.html. Raw microarray data from Affymetrix CEL files were normalized using the method of Huber *et al.* (Affymetrix Microarray Suite methods in comparative studies, http://affycomp.biostat.jhsph.edu). Analysis of variance (ANOVA) was performed using the SAS software package MicroArray Solutions version 1.3 (SAS Institute Inc. 2004; http://www.ma.uni-heidelberg.de/inst/zmf/affymetrix/datenanalyse_e.html). Gene annotation was obtained through the Affymetrix NetAffx index (http://www.affymetrix.com/analysis/index.affx). Besides the simple analysis of single differentially expressed gene products, pathways of gene products functionally linked to each other were characterized to facilitate interpretation of the bulk of data. To define significantly affected pathways, two approaches were used; first, an over-

representation (ORA) approach using Fisher's exact test as described by Draghici *et al.* (2003), and second a functional class scoring (FCS) approach using a modified Gene Set Enrichment Analysis (GSEA, http://www.broad.mit.edu/gsea) as described by Subramanian *et al.* (2005) and Mootha and Lindgren *et al.* (2003) was used as implemented in the Bioconductor Package Global Test 3.0.4. A total number of 327 pathways generated from the KEGG database (Kyoto Encyclopedia of Genes and Genomes, http://www.genome.ad.jp/kegg/pathway.html), Gene Ontology (GO) annotations (Consortium 2000), and the module map for cancer compiled by Segal *et al.* (2004), were taken for analysis using the Bioconductor Annotation Package hgu95av2 1.8.4 (Kanehisa 2000, 2008; Manoli 2006). The overall number of significantly/non-significantly differentially expressed genes per chip was cross-tabulated against the number of significantly/non-significantly expressed genes of a pathway (Kenzelmann 2007), with a *P*- value < 0.001 judged to be significant.

3.3 Protein chemistry

3.3.1 Isolation of total cellular protein

Proteins were extracted from freshly harvested or frozen cells by homogenization in hypotonic protein lysis buffer (Table 14). Lysates were incubated on ice for 30 minutes and centrifuged at 3000 rpm for 5 minutes at 4°C. The supernatant, containing cellular membranes, organelles and cytosolic proteins, was collected and stored at –80° C or used immediately for Western blot analysis (3.3.6).

Samples for protein analysis by two-dimensional (2-D) gel electrophoresis were prepared using chaotropic and reducing agents (Link 1999; Rabilloud 1999). For harvesting of the cells, they were collected with a cell scraper (Sarstedt Inc.) in 1 ml of PBS and transferred into a microcentrifuge tube and centrifuged at 3000 rpm for 3 minutes. The pellet was resuspended in 250 µl of the strongly chaotropic 2-D sample buffer (Table 14) and thoroughly mixed several times for 15 minutes to sheer genomic DNA and dissolve all proteins. The lysates were then centrifuged for 3 minutes at room temperature to sediment insoluble components and the supernatants were stored at –80° C until analysis.

Table 14: Components of protein lysis buffer and chaotropic buffer

Protein lysis buffer	Chaotropic 2D sample buffer
10 mM KCl	7 M urea
0.1mM EDTA	2 M thiourea
0.1mM EGTA	4% CHAPS
10 mM Hepes	50 mM DTT
1% Triton X-100	0.2% Bio-Lyte 3/10 ampholyte
2 mM DTT	0.2% phosphatase inhibitors
50 µM Pefablock.	
25µM protease inhibitors	

3.3.2 Protein dephosphorylation

For the dephosphorylation of zyxin, total non-denatured cell lysates were used. The Mn^{2+}-dependent protein phosphatase 1 (PP1) was chosen for its broad substrate spectrum including some activity towards phosphotyrosine residues. The reaction was performed in PP1 buffer (100 mM NaCl, 50 mM Hepes, 0.1 mM EGTA, 2 mM DTT, 0.025% Tween 20, pH 7.5) supplemented with 1 mM $MnCl_2$ with 0.5 units of PP1 at 30°C for 90 minutes in a total volume of 20 µl. After adding 10 volumes of chaotropic lysis buffer (Table 14) and protein solubilisation, PP1-mediated dephosphorylation was further analyzed by standard 2-D gel electrophoresis procedure followed by Western blot as described below.

3.3.3 Enrichment of nuclear protein

For enrichment of the nuclear protein fraction from cultured cells for 2-D gel electrophoresis, the ReadyPrep protein extraction kit (BioRad) was used according to the manufacturer's protocol. The nuclear pellet was then solubilised in sample buffer (Table 14) and used for 2-D gel electrophoresis.

3.3.4 Determination of protein concentration

To determine protein concentration, the colorimetric Bradford protein assay (Bradford 1976) was employed. This is a dye-binding assay based on the differential colour change of Coomassie Brilliant blue G dye in response to various concentrations of protein. As an external standard, the bovine serum albumin (BSA; stock solution of 1 mg/ml) was diluted in order to obtain standard dilutions in the range of 10 - 100 µg/ml. The Bradford reagent was diluted in 1:5 ratios with deionised water. In a 96-well plate, 80 µl of each standard used and the samples (diluted 1:100) were mixed with 200 µl of the diluted Bradford reagent. Optical density of the color reaction was measured at 595 nm in a microplate reader (PowerWave XS universal microplate reader, BIOTEK Instruments) and the standard was used to generate a calibration curve.

3.3.5 Sodium Dodecylsulfate polyacrylamide gel electrophoresis (SDS-PAGE)

For the separation of proteins exclusively on the base of their size, SDS-PAGE was used. For the preparation of the gels the solutions described in Table 15 were freshly prepared. SDS-polyacrylamide gels were made according to the Laemmli method (Laemmli 1977). Gels from 10 – 12% were poured between the glass plates depending on the size of the proteins to be separated and overlaid after polymerization with a 4% stacking gel. Proteins were denatured by the addition of 4x sample loading buffer and heated for 5 minutes at 95° C. Thereafter, proteins were separated by electrophoresis at fixed voltages of 100 V for the stacking gel, and 200 V through the separating gel.

Tris-glycine-SDS running buffer (1X)

25.0 mM	Tris HCl, pH 8.3
192.0 mM	Glycine
0.1%	SDS

Loading Buffer (4X)

150.0 mM	Tris HCl, pH 6.8
300.0 mM	DTT
6.0%	SDS
0.3%	Bromophenol blue
30%	Glycerol

Table 15: Formulations for SDS-PAGE separating and stacking gels

	Separating gel 10%	Separating gel 12%	Stacking gel 4%
Acrylamide stock (30%)	3.3 ml	4.0 ml	0.65 ml
1.5 M Tris HCl, pH 8.8	2.5 ml	2.5 ml	-
0.5 M Tris HCl, pH 6.8	-	-	1.25 ml
dd H_2O	4.1 ml	3.35 ml	3.05 ml
20% SDS	50 µl	50 µl	50 µl
10% APS	50 µl	50 µl	25 µl
TEMED	10 µl	10 µl	10 µl

3.3.6 Western blot analysis

After separation by SDS-PAGE (3.5.4), proteins were transferred onto a pre-hydrated (5 minutes in 100% methanol and 45 minutes in ddH_2O) PVDF membrane at 350 mA for 45 minutes in the transfer buffer**.** The membrane was then dried for 2 hours at 50°C or directly blocked for at least 2 hours with blocking buffer.

The primary antibody (Table 6, diluted 1:1000 to 1:10000 in washing buffer) was added to the membrane and incubated at ambient temperature for 2 hours. Thereafter the membrane was washed 3 times for 10 minutes with washing buffer. The appropriate secondary antibody conjugated to horseradish peroxidase (Table 5; 1:10000) was added and the membrane was further incubated at ambient temperature for 1 hour. After 1 hour, the membrane was washed 3 times for 10 minutes in washing buffer.

The complex of proteins with primary and secondary antibodies was detected by using ECL solution (Amersham Pharmacia Biotech, Freiburg, Germany), according to

the manufacturer's instructions. The light generated by the enzymatic reaction was detected in a ChemiDoc chamber (BioRad)

Transfer buffer

25.0	mM	Tris
19.2	mM	Glycine
20%		Methanol

Washing Buffer

Triton X-100	2.5 g
PBS 1X	1.0 L

Blocking Buffer

Milk powder 2.5 g per 50 ml of washing buffer

3.3.7 Two-dimensional gel electrophoresis

The analysis of complex protein mixtures and protein modifications was performed by using the Protean IEF System (BioRad Laboratories) for the first dimension and the Protean II xi cell system (BioRad Laboratories) for the second dimension protein separations. 2D gel elecrophoresis was established according to the protocol described by O'Farrell (O'Farrell 1975) with minor modifications (see below).

3.3.7.1 Isoelectric focusing (IEF)

During the first dimension proteins are trapped at their respective isoelectric point (pI), the pH at which a given protein has no net charge and hence does not migrate in an electric field. ReadyStrip IPG Strips pH 3-10 (length 17 cm; BioRad) were used following the instructions provided. Each sample was diluted in rehydration buffer (to the total volume of 300 µl and maximal protein concentration of 20 mg/ml) and applied directly into the focusing tray to allow uniform absorption in the course of rehydration of the strip. The loaded strip was then covered with mineral oil to prevent fluid evaporation during the next steps and mounted into the Protean IEF focusing tray (BioRad). Rehydration was run under static conditions for 19 hours at 20°C. Thereafter, isoelectric focusing was performed according to the optimized program

(for detailed conditions see Table 16). IEF was run with a current of 50 µA per strip for about 19 hours at 20°C until no current was measureable.

Table 16: Focusing conditions for 17 cm ReadyStrip, pH 3-10

End voltage	Volt per hours	Ramp
10.000 V	60.000 V x hour	rapid

Table 17: Equalibration and rehydration buffers used for 2-D gel electrophoresis analysis

Rehydration buffer	Equalibration buffer I	Equalibration buffer II
7 M urea	6 M urea	6 M urea
2 M thiourea	0.375 M Tris HCl, pH 8.8	0.375 M Tris HCl, pH 8.8
4% (w/v) CHAPS	2% SDS	2% SDS
50 mM DTT	20% glycerol	20% glycerol
0.2% 100x Bio-Lyte 3/10 ampholyte	2% (w/v) DTT	
0.2% protease inhibitor		

3.3.7.2 Equilibration and SDS-PAGE

Before proceeding with the second dimension, IEF strips were equilibrated in SDS-containing equilibration buffers I and II (Table 17) for 10 minutes each followed by rinsing with 1X Tris-glycine-SDS running buffer.

For SDS-PAGE, 12% separating gels were prepared according to the standard protocol described above (Laemmli 1970). After full polymerization (over night) equilibrated IEF stripes were mounted onto the separating gel and fixed with 1% agarose. SDS-PAGE electrophoresis was run in 1X Tris-glycine-SDS running buffer (3.3.5) at a current of 16 mA per gel for 30 minutes, then at 24 mA per gel for another 5 hours. The Kaleidoscope Precision Plus Protein Standard (BioRad Laboratories) was used to monitor the progress of the run. After electrophoresis, proteins were

transferred onto PVDF membranes. Zyxin was detected by using the B72 antiserum as described (3.3.6).

3.4 Enzyme-linked immunosorbent assay (ELISA)

Pre-coated enzyme-linked immunosorbent assay (ELISA) was used for quantitative determination of interleukin-8 (IL-8), endothelin-1 (ET-1) and atrial natiuretic peptide (ANP) concentrations in cell culture supernatants. All samples were thawed only once at the time of testing and analyzed according to the procedures provided by the manufacturers.

3.5 Immunofluorescence analysis

3.5.1 Cell fixation

Human cells, grown on glass cover slips or BioFlex membranes, were routinely fixed by using one of the fixation techniques described below.

For solvent fixation and study of the localisation of zyxin, cells were fixed with 50% methanol/50% acetone (1 ml was added and incubated further for 20 minutes at −20°C in the dark). The cover slips were allowed to air dry for 2 hours and re-hydrated with PBS. For observation of actin filaments and distribution of ANP in HUVEC, paraformaldehyde fixation was performed. First, after the medium was aspirated and cells were washed with PBS, 1 ml of PBS containing 4% formaldehyde was added into each well and incubated for 10 minutes at 4^{o}C in the dark. Thereafter, cells were quenched with 50 mM ammonium chloride in PBS and membranes were permeabilized by 0.1% Triton X-100 in PBS at room temperature for 10 minutes.

3.5.2 Immunostaining of fixed cells

After fixation the cover slips were placed upside in a 6-well plate, covered with blocking buffer (10% goat serum in 0.1% Triton/PBS, pH 7.4) at ambient temperature for 30 minutes. Cover slips were then placed downside on paraffin plastic toil with the primary antibody diluted in blocking buffer (20 µl) for 2 hours at room temperature, washed in PBS, and finally exposed upside to the fluorescent dye-conjugated

secondary antibody labelled with Alexa 488 or Alexa 594 in blocking buffer (1 hour at room temperature). Following this incubation, 3 washing steps with PBS were performed before post-fixation by using 50 mM acetic acid in ethanol. The coverslip was then mounted onto a large coverslip with 6-20 µl of 50% glycerine in PBS and sealed with nail polish. Mounted slides were then analysed using the image system (Olympus) equipped with the MetaMorph analysis software. Primary and secondary antibodies used are listed in Tables 5 and 6 (Chapter 2.4).

Blocking buffer

10% goat serum (Sigma Aldrich)
0.1% Triton in PBS, pH 7.4

3.6 Immunohistochemistry

3.6.1 Tissue preparation for paraffin embedding

The freshly prepared tissues were fixed in zinc fixative solution for 24 hours to prevent alterations in the cellular structure. The dehydration process was accomplished by passing the tissue through a series of increasing ethanol concentrations. For this purpose, the tissue was placed in 70%, 80% and 96% ethanol for at least 1 hour at ambient temperature. Later, the ethanol was removed from the tissue by incubating it 1 hour in isopropanol. Finally, the tissue was embedded in melted paraffin (Sigma Aldrich) and incubated at 60° C overnight. The day after, paraffin with the tissue was poured into the metal mould to form a block. The block was allowed to cool and was consecutively processed for sectioning or stored at room temperature. The paraffin sections (5 µm thick) were dried at 40° C overnight and then processed further for immunohistological analyses.

Zinc fixative solution

0.1 M Tris HCl, pH 7.4
3.2 mM $Ca(CH_3COO)_2$ X H_2O
22.8 mM $Zn(O_2CCH_3)_2(H_2O)_2$
35.9 mM $ZnCl_2$

3.6.2 Haematoxylin staining of paraffin sections

The stored slides with the paraffin sections were first incubated three times in Xylol for 5 minutes, followed by consecutive incubations in 99%, 85% and 70% ethanol for 5 minutes each. Slides were then washed 5 minutes in ddH_2O and placed for 5 minutes in 0.1X Mayer´s haematoxylin solution (Sigma Aldrich). Staining was terminated by washing in running tap water for 10 minutes. Thereafter slides were incubated in ddH2O for 1 minute followed by 70%, 85% and 96% ethanol and two times in Xylol for 5 minutes each. Finally, the stained tissues were sealed using DePeX mounting medium and analysed by convential light microscopy.

3.7 Perfusion of isolated murine femoral arteries

Freshly isolated femoral arteries isolated from wild type C57BL/6J or C57BL/6J zyxin (-/-) *null* mice were subjected to defined perfusion conditions by using a Pressure Myograph System Model 110P (Danish Myo Technology, Copenhagen, Denmark).

Perfusion buffer (Table 19) was freshly prepared at the day of the experiment by dropwise addition of 25X solution II to 800 ml water plus 40 ml solution I under stirring (for details see Table 18). Thereafter, the buffer was adjusted to one liter with ddH_20 and saturated with carbon dioxide and oxygen (95% O_2, 5% CO_2) for 20 minutes. Partial O_2 pressure was maintained at a value of 160 mmHg, P_{CO2} at a value of 37 mmHg, pH was equilibrated to 7.4 and the solution was completed by adding EDTA (260 µl/l) and D-glucose (2 g/l). Buffer samples (0.5 ml) were taken at various time points for control of pH and P_{O2}/P_{CO2} using a blood gas analyser (Radiometer, Kopenhagen, Denmark).

Table 19: Perfusion buffer pH 7.4 (1X)

Solution I		Solution II	
Chemical	**Concentration (mmol/l)**	**Chemical**	**Concentration (mmol/l)**
NaCl	119.00	$NaHCO_3$	2.10
$CaCl_2$	1.25	KH_2PO_4	1.18
KCl	4.70		
$MgSO_4$ x 7 H_2O	1.17		

Table 18: Perfusion buffer pH 7.4 (25X)

Solution I		Solution II	
Chemical	**Concentration (g/l)**	**Chemical**	**Concentration (g/l)**
NaCl	173.850	$NaHCO_3$	52.10
$CaCl_2$	5.875	KH_2PO_4	4.08
KCl	8.760		
$MgSO_4$ x 7 H_2O	7.390		

For the isolation of the femoral arteries, animals were euthanized in CO_2 chambers. The excised leg was placed in a Petri dish with equilibrated perfusion buffer. The femoral artery was first separated from the accompanying vein and dissected from connective tissue. Segments of the femoral artery (0.5 - 1 cm) were cut from the distal and proximal end to be investigated. Artery segments were mounted on glass capillaries and inserted into the myograph system (Figure 3.2), which was modified for the investigation of smaller vessels (diameter ~120 µm).

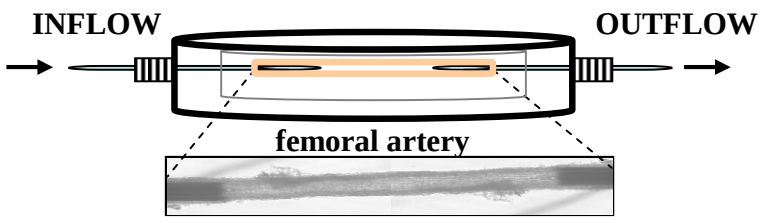

Figure 3.2: The *in situ* perfusion model of the femoral arteries.

The glass capillaries used for perfusion experiments were fabricated using a P-87 Flaming/Brown micropipette puller (Sutter Instrument Company, Novato, USA). To achieve a final tip-diameter of 120 µm, capillaries were pulled from 0.15 mm glass cannulas (GB150-8P, Science products GmbH, Hofheim, Germany) with the program optimized according to an operation manual provided by the manufacturer's of the puller. Thereafter, the capillaries were cut to the appropriate length (approximately 1.5 cm).

Buffer temperature was kept at 37°C. The mounted vessel was gradually pressurized at 10-30 mmHg over a period of about 15 minutes. After that the vessel was equilibrated at an intraluminal pressure of 20 mmHg for 1 hour. The vessel chamber was continuously refilled with pre-heated (37°C) and equilibrated perfusion buffer.

A pressure transducer set in line with the femoral artery together with the MyoView™ interface allowed continuous application and control of temperature and pressure. Analysis of changes in the diameter of the vessel was obtained by using the MyoView™ software, processing the video microscope real time image of the vessel, and was calculated automatically according to the adjusted calibration.

3.7.1 *In situ* studies of endothelium-dependent relaxation

The pressure myograph allows to quantitatatively determine the response of pressurised femoral arteries to vasoactive substances. The response of the arteries cannulated in the system was recorded as changes in luminal diameter. Baseline measurements were obtained at 3 points of the experiment: once freshly after isolation (passive diameter), than after 1 hour pressurising at 60 mmHg, when static conditions with constant flow were achieved (diameter measured under physiological conditions). Thirdly data were obtained from arterial segments pre-constricted with phenylephrine (0,1 µmol/L) with an intraluminal pressure set at 60 mmHg. Artery segments were allowed to equilibrate for one hour before being pre-constricted to 40 - 60% of their resting diameter with 1 µmol/L phenylephrine for subsequent relaxation studies. Pre-constricted vessels were studied for dilator responses by giving cumulative doses of acetylcholine (end concentrations of 10 nmol/L – 10 µmol/L), to the bath. Changes in vessel diameter were monitored as described. Contraction in

response to phenylephrine was measured as change in diameter caused by 0,1 µmol/L phenylephrine. Relaxation in response to acetylocholine was expressed as gradual increase in diameter caused by different agonist concentrations in every vessel. Results were presented as the percentage of relative changes in vessel diameter.

The functional and cellular integrity of the segments was routinely checked by immunohistochemical staining for the endothelial cell marker CD31.

3.8 DOCA-salt model of hypertension and telemetric blood pressure measurement

Before induction DOCA-salt hypertension in mice, they were unilaterally nephrectomized and implanted with the telemetric catheter. After 6 days, a DOCA pellet (50 mg DOCA, 21 days release time, Innovative Research of America) was implanted subcutaneously, and additionally drinking water was supplemented with 1% (w/v) NaCl. In two performed experiments, wild-type and zyxin-/- mice were subjected to the same treatment. Thereafter the blood pressure was monitored using a radiotelemetry system (PA-C10, Data Sciences International) in conscious, unrestrained mice, as described by Mills *et al.* (Mills 2000).

3.9 Statistical analysis

For statistical analysis the InStat software version 3.0 (GraphPad Inc., San Diego, USA) was used. Data are presented as means ±SEM. In all cases, *P-values* < 0.05 were considered as statistically significant. When comparing more than two groups, ANOVA was used, as was appropriate. For statistical procedures concerning the microarray analyses see 3.2.10.

4. Results

4.1 Mechanism of wall tension-induced zyxin activation in human cells

This part of the thesis was conducted at the cellular level with emphasis on human primary cultured endothelial cells. In order to mimic supra-physiological wall tension, cells were exposed to cyclic stretch using a well-characterized *in vitro* model, the Flexercell strain unit (Shrinsky 1989; Cattaruzza 2004; Kakisis 2004; Lacolley 2004).

4.1.1 Effect of cyclic stretch on the cellular localisation of zyxin

HUVEC grown on flexible elastomers respond with a rapid remodelling of their actin cytoskeleton if exposed to cyclic stretch. In order to localize zyxin, immunofluorescence analysis of endothelial cells using the zyxin specific antserum B71 was performed.

The analysis showed that under static conditions zyxin was mostly located in focal adhesion points (Figure 4.1 A).

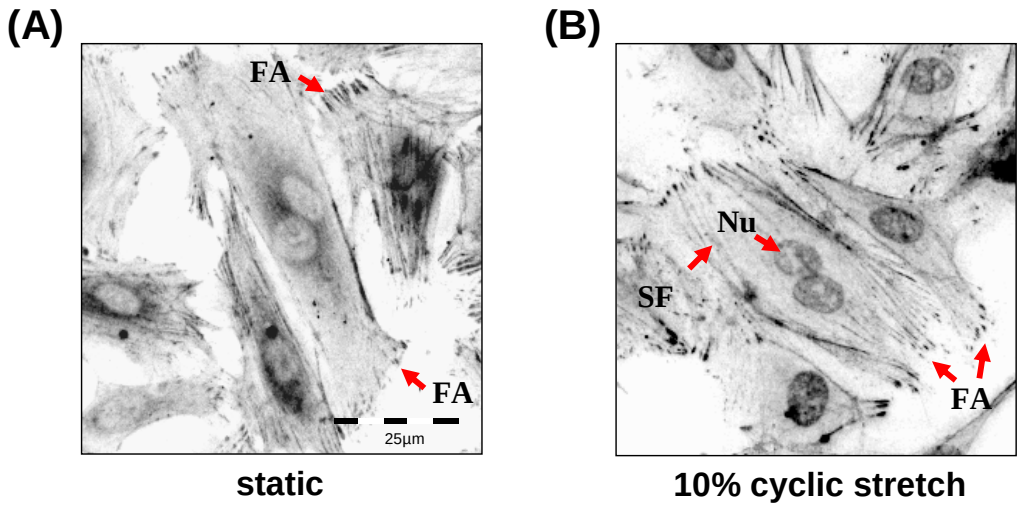

Figure 4.1: Immunofluorescence analysis of zyxin localization in HUVEC. Human umbilical vein endothelial cells grown on collagen-coated BioFlex plates were subjected to cyclic stretch (10% elongation, 0.5 Hz, 6 hours). Zyxin was detected by the specific B71 antiserum. Immunofluorescent staining of zyxin revealed a pediment localisation of zyxin in focal adhesions (FA). Cyclic stretch, however, causes a translocation to stress fibres (SF) and the nucleus (Nu; panel B). Focal adhesions, however, remain intact in this process as analyzed by staining for vinculin, another component of FA (not shown).

Upon exposure to cyclic stretch (10% elongation, 0.5 Hz, 6 hours), zyxin was released from focal adhesions and accumulated in stress fibres and the nucleus, as shown in Figure 4.1 B, right panel.

To evaluate the kinetics of zyxin translocation in more detail, cells were exposed to cyclic stretch as described before (10% elongation, 0.5 Hz) but fixed at different time points (after 30 to 360 minutes). Immunofluorescence analysis revealed that zyxin not only relocates, but shuttles between focal adhesions, stress fibers and the nucleus of endothelial cells until, after 6 hours, the protein is stably located in the nucleus (analyses for up to 18 hours are not shown). Zyxin relocated to stress fibers and the nucleus already in the early phases of mechanical overload, i.e. after 30 to 60 minutes (Figure 4.2).

Within 90 minutes, zyxin accumulated at high density in nuclear compartments of the endothelial cells and then dissociated back to the focal adhesions at around 120 minutes. After this relocation, zyxin was redistributed to the nucleus at about 240 minutes and remained there for up to 18 hours (Figure 4.2).

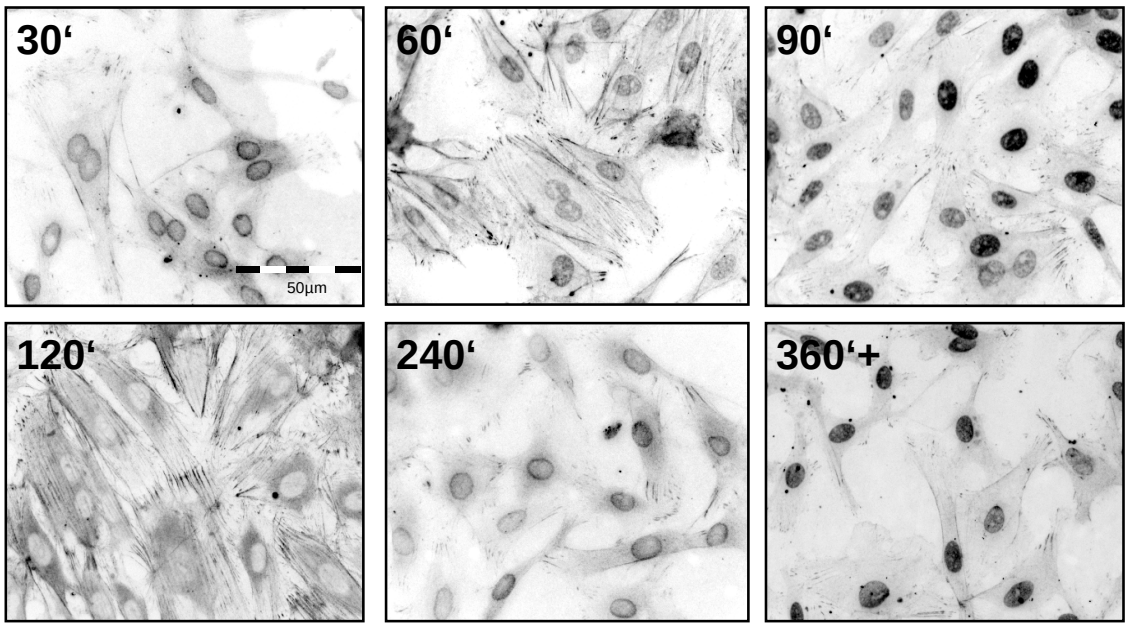

Figure 4.2: Time course of stretch-activated zyxin translocation. One of 6 representative immunofluorescence analyses of zyxin shuttling between focal adhesions, stress fibers and the nucleus in HUVEC exposed up to 6 hours to cyclic stretch (10% elongation, 0.5 Hz). Although the time course of translocation varies in a range of several minutes, the characteristic biphasic kinetics could be observed in all experiments.

4.1.2 Effect of ET-1 and ANP on zyxin activation

To analyse whether - as in atrial myocytes – ET-1 and ANP mediate wall tension-induced signalling also in endothelial cells, we applied ANP (10 and 1 nM) to the cultured HUVEC for 6 hours. ANP (1 nM) in fact stimulated zyxin translocation from focal adhesions to the nucleus (Figure 4.3), suggesting that is a surrogate stimulus for wall tension.

To assess the role of ET-1 in ANP-induced zyxin activation, the cells were exposed to ET-1 (10 nM) with or without the ET_B receptor-selective antagonist BQ788 (1 μM) in the presence or absence of cyclic stretch and/or ANP (1 nM). Immunofluorescence detection of zyxin demonstrated that in cells exposed to cyclic stretch ET_B receptor activity was crucial for zyxin translocation to the nucleus (Figure 4.4, panel A-III). However, in cells additionally exposed to ANP, BQ788 had no effect on zyxin translocation (Figure 4.4, panel A-IV), suggesting that ET-1-induced ET_B-R activation occurs upstream of the ANP-mediated effects.

To further demonstrate that ET-1-induced ET_B-R activation mediates ANP release and consecutively zyxin translocation to the nucleus, static cells were exposed to ET-1 (10 nM) with or without BQ788 (1 μM). Under static conditions, ET-1 alone in fact triggered zyxin translocation further supporting the hypothesis that ET-1 facilitates ANP felease from endothelial cells (Figure 4.4, panel C-II) similar to the situation in the atria of the heart.

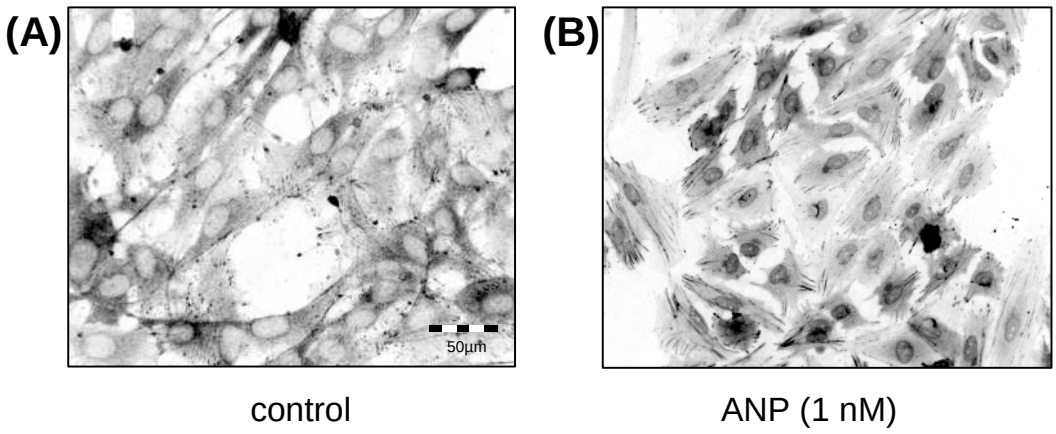

Figure 4.3: Effects of ANP on the cellular localisation of zyxin in cultured HUVEC. Exemplary analysis of zyxin relocation to the nucleus. HUVEC were preincubated as outlined in Materials and Methods (section 3.1.5). ANP (1 nM) activates the nuclear translocation of zyxin also in quiescent cells (B).

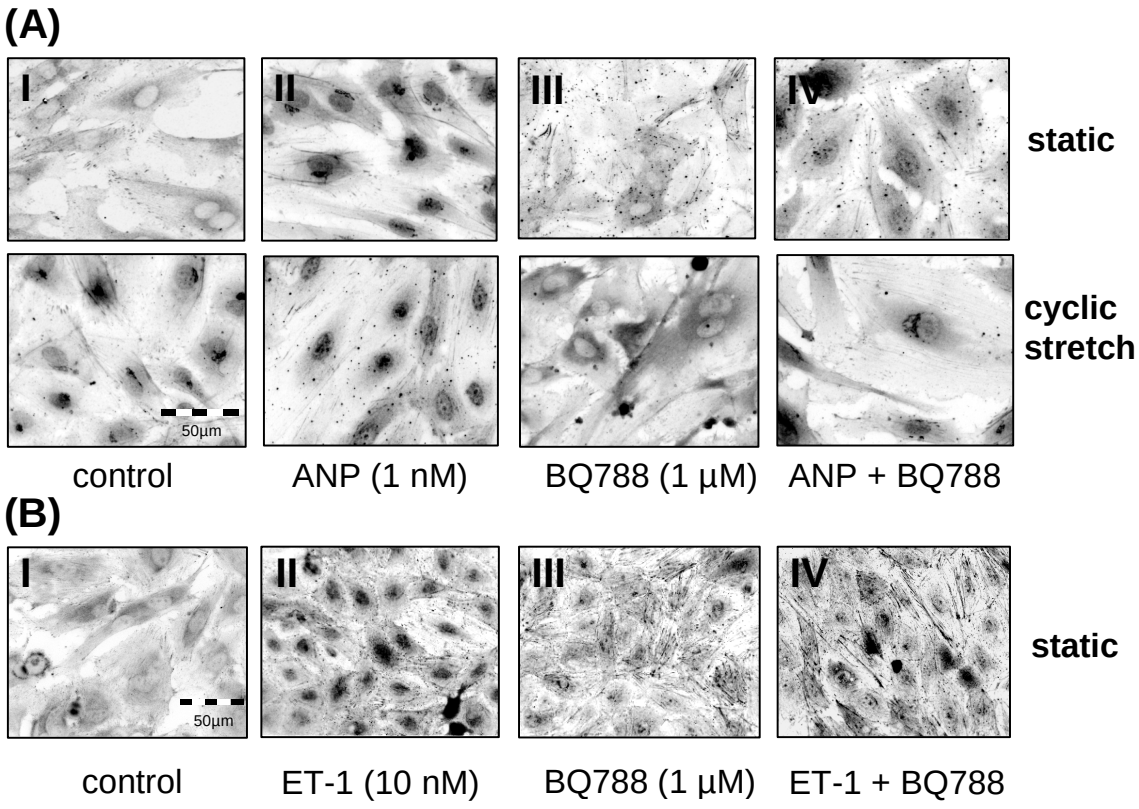

Figure 4.4: Effects of ANP and ET-1 on the cellular localisation of zyxin in cultured HUVEC. HUVEC were preincubated as outlined in Materials and Methods (section 3.1.5). (A) Pretreatment with ANP (1 nM) elicts nuclear translocation of zyxin in quiescent cells (A-II). The ET_B-R-specific antagonist BQ788 inhibits stretch-induced zyxin translocation to the nucleus (A-III). However, BQ788 does not affect ANP-mediated effects in these cells (A-IV). (B) ET-1 alone also stimulates zyxin translocation in quiescent endothelial cells (B-II). This effect is ET_B-R-dependent (B-III).

4.1.3. Effects of cyclic stretch on functional natriuretic peptide gene expression

After it was evident that ANP mediates stretch-induced zyxin translocation to the nucleus of human endothelial cells, the effect of cyclic stretch on the expression of all types of natriuretic peptides, ANP, BNP and CNP, was examined next. In line with previous reports (Cai 1993), human umbilical vein endothelial cells express all natriuretic peptides (Figure 4.5). Interestingly, however, prolonged exposure to cyclic stretch (6 hours, 10% elongation, 0.5 Hz) had diverse consequences on the expression of the three genes. As shown in Figure 4.5, cyclic stretch stimulated both CNP (panel A) and ANP (panel C) gene expression, but had no effect on BNP (panel B).

It has been demonstrated previously that expression of ANP is controled by ET-1 in atrial myocytes. Similarly, the effects of ET-1 and its B-type receptor on ANP gene expression in HUVEC were analyzed. ANP up-regulation was abolished in HUVEC exposed to cyclic stretch, when the ET_B-R was blocked by using the specific inhibitor BQ788 (Figure 4.5, panel C).

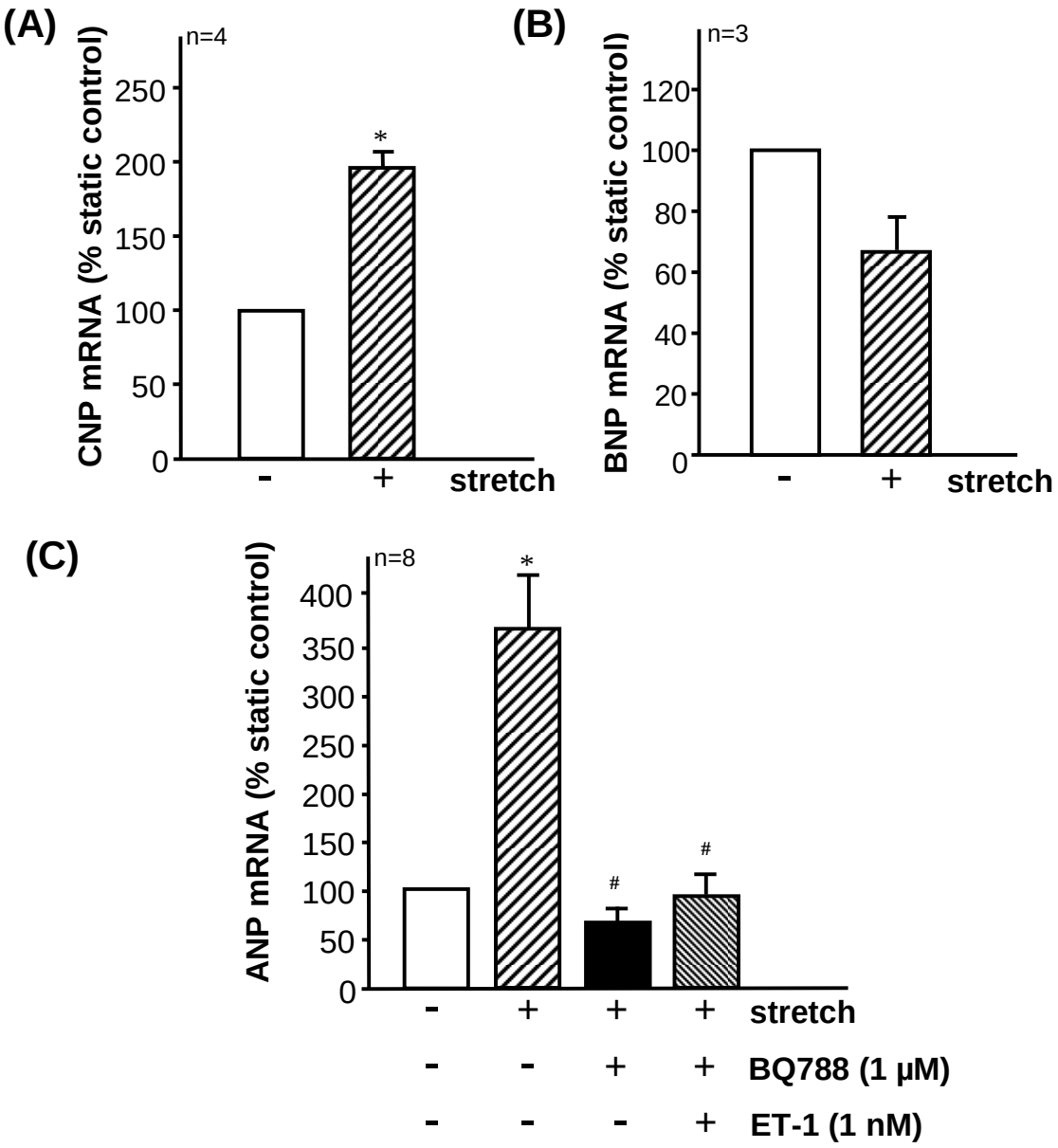

Figure 4.5: Quantitative real-time PCR analysis of CNP (A), BNP (B) and ANP (C) gene expression in HUVEC. (A) CNP mRNA expression is 2-fold increased upon exposure to cyclic stretch, whereas BNP mRNA expression in these cells was not affected (B). (C) ANP mRNA expression is up-regulated upon cyclic stretch in an ET_B-R dependent manner. **P* < 0.02 vs. static control; #*P*<0.05 vs. stretched cells; number of individual experiments as indicated.

4.1.4 Wall tension-induced ANP and ET-1 release

In atria, wall tension-induced release of ANP is mediated by ET-1 secreted by endothelial cells. To analyse whether endothelial cell ANP release is similarly regulated supernatants were collected from cultured HUVEC exposed to cyclic stretch for 0 to 360 minutes an equal volume of fresh media was replaced each time. Concentrations of ET-1 and ANP were measured by ELISA and calculated taking into account the serial dilutions as follows:

$$C_{real} = \frac{2}{(2 - 0.2\ n)} \times C_{measured}$$

Upon static conditions, the cells produced very low amounts of ANP (0.1-0.12 nmol/L). Cyclic stretch rapidly elevated the ANP concentration in supernatant to 3.6 nmol/L after 1 minute and then again after 60 and 360 minutes, although to a much lesser extent (Figure 4.6).

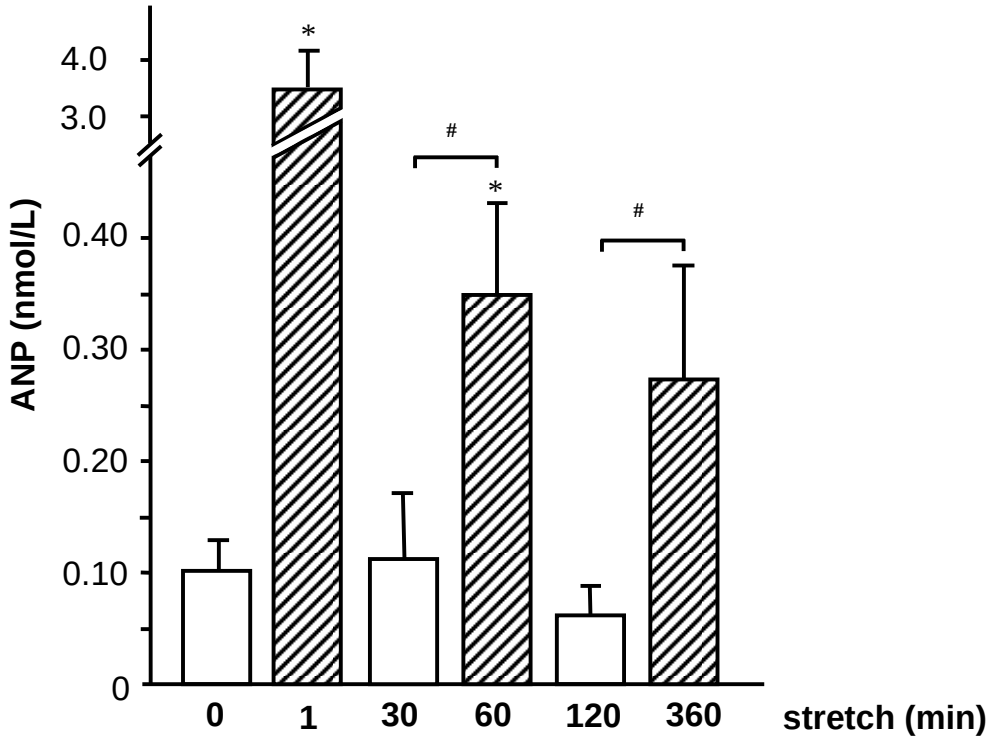

Figure 4.6: Quantitative analysis of ANP concentration in HUVEC supernatants by ELISA. ANP release from endothelial cells upon exposure to cyclic stretch (10% elongation, 0.5 Hz) at different time points. **P*< 0.05 vs. static control; #*P*<0.05 as indicated; n=4.

After 360 minutes, appeared to reach a plateau 2 to 3-fold above the basal level (not shown). In another series of experiments, BQ788 at a final concentration of 1 µmol/L was added to the cells 6 hours before application of cyclic stretch. Under these conditions, cyclic stretch did not lead to an increase in ANP release (Figure 4.7).

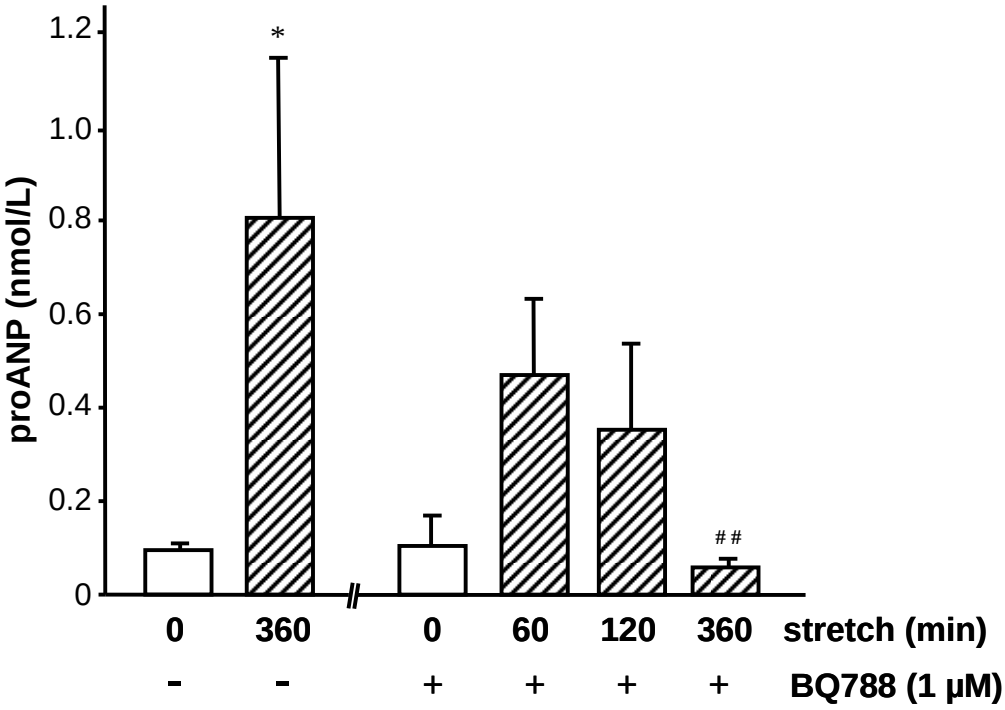

Figure 4.7: Quantitative analysis of ANP concentration in HUVEC supernatants by ELISA. BQ788 was able to completely suppress ANP secretion from these cells after 360 minutes. **P*< 0.05 vs. static control; $^{\#\#}P$<0.01 vs. 360 minutes of stretch; n=4.

Figure 4.8 shows the release of ET-1 upon exposure to cyclic stretch into the conditioned medium of the cultured HUVEC. In this series of experiments, exposure to cyclic stretch for 30 to 360 minutes resulted in an increased ET-1 release, which appeared to reach a plateau beyond 360 minutes (not shown). Like ANP, the kinetics of ET-1 release seems to match those of zyxin translocating to the nucleus.

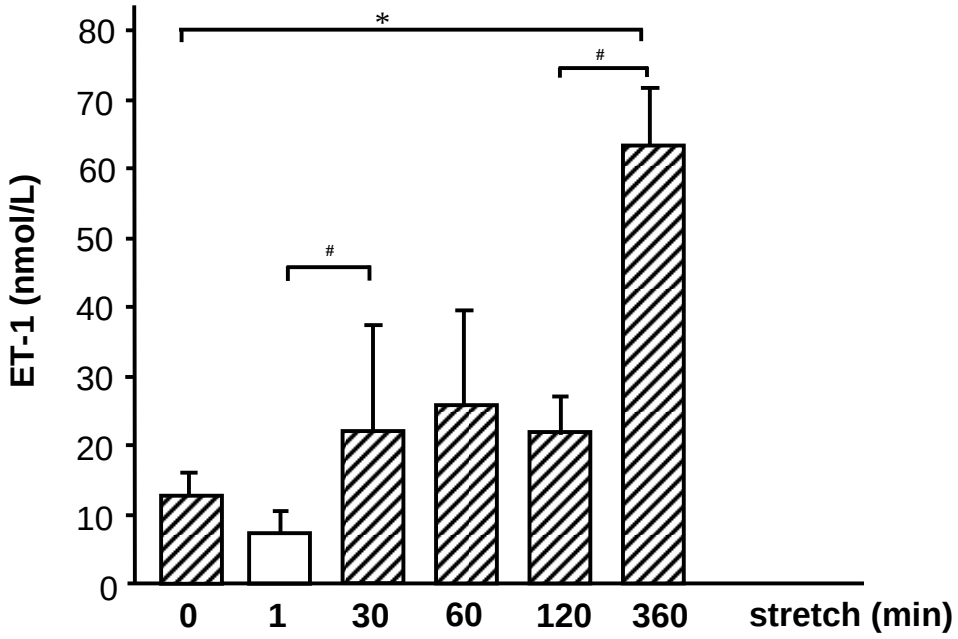

Figure 4.8: Quantitative analysis of endothelin-1 concentration in HUVEC supernatants by ELISA. **P*<0.05 vs. static control; #*P*<0.05 vs. corresponding control; n=4.

Taken together, these data suggest that ET-1 mediates ANP secretion from HUVEC in response to cyclic stretch.

4.1.5 Analysis of natriuretic peptide receptors expression in HUVEC

In endothelial cells, ANP acts via activation of the natriuretic peptide receptor type A, to which it has a high affinity. The C-type receptor, although principally coupled to several trimeric G-proteins, is regarded to be a scavenger receptor, its downstream signalling pathway is not yet known. In respect to these facts, expression of both natriuretic peptide receptors was determined by real-time PCR in cultured HUVEC. These analyses suggest indicated that NPR-A as well as NPR-C is expressed in HUVEC under static conditions, while an increase in cyclic stretch had no effect on the expression level of these receptors (Figure 4.9). Expression of NPR-B, however, was very low (data not shown).

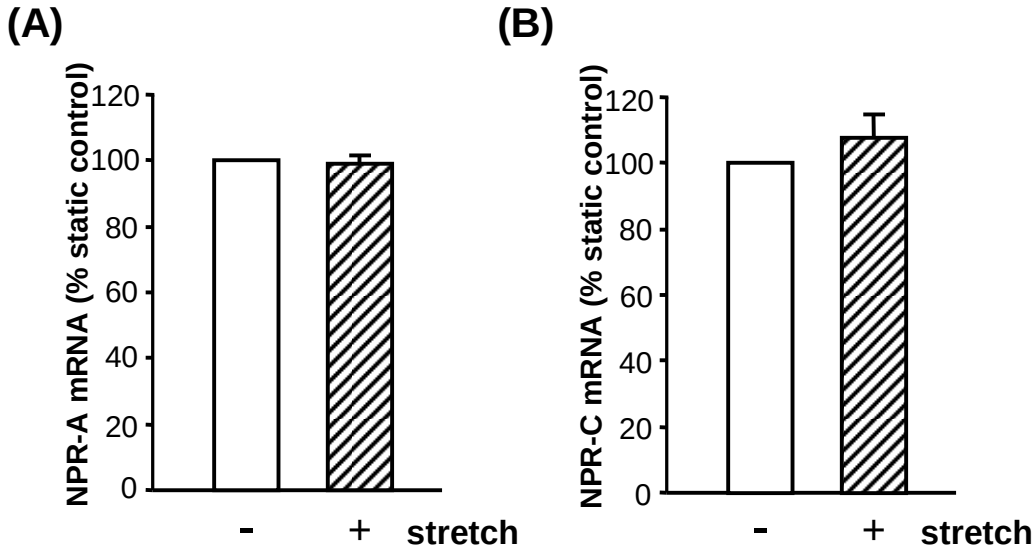

Figure: 4.9: Real-time PCR analysis of NPR-A (A) and NPR-C (B) gene expression in HUVEC. Both ANP-specific natriuretc peptide receptors are expressed in the endothelial cells. Basal mRNA expression, however, does not change in response to 6 hours of cyclic stretch did not alter the expression; n = 4.

To confirm the constitutive expression of both types of receptor, additional immunofluorescence analyses using NPR-A and NPR-C antibodies were preformed. Similar to previous findings, HUVEC stained uniformly positive for either ANP receptor under both static conditions and in response to cyclic stretch (6 hours, 10% elongation, 0.5 Hz) without any apparent changes in expression or localisation (Figure 4.10). Whereas NPR-C seems to be localized mostly in a peri-nuclear vesicular compartment, NPR-A predominantly shows a diffuse staining typical for non-clustered cell surface receptors.

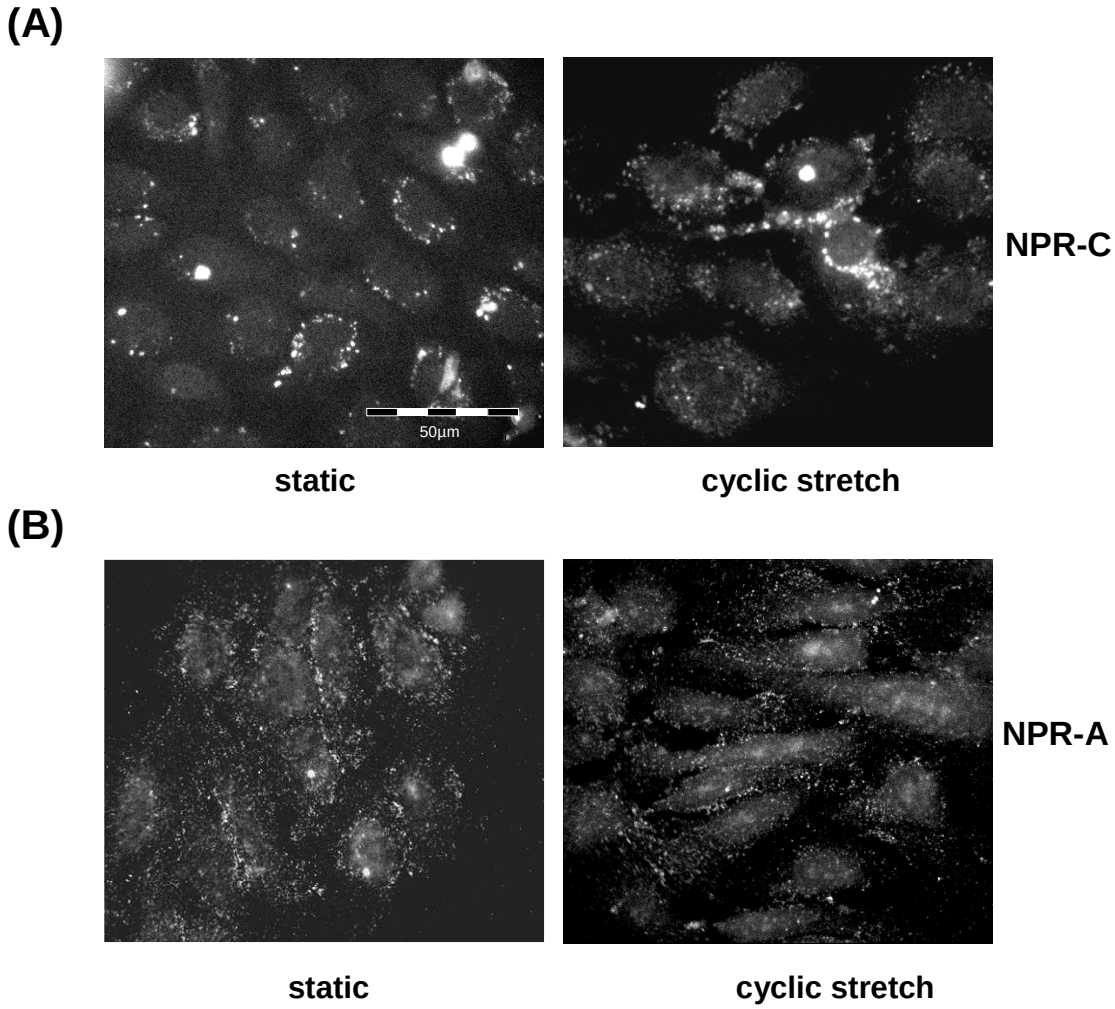

Figure 4.10: Immunofluorescence analysis of NPR-A and NPR-C localization in HUVEC. Both ANP receptors were visualized by immunofluorescence staining using antibodies against NPR-A (panel B) and NPR-C (panel A) counterstained with Alexa green secondary antibodies. Analysis reveals that both natriuretic peptide receptors are equally distributed under both static and stretch conditions.

4.1.6 Determination of the signalling pathway of ANP-mediated zyxin activation

Protein kinase G (PKG), the principal effector kinase activated by cGMP in the cardiovascular system, provides the main signal downstream of ANP. In this context, zyxin localisation in static or stretched HUVEC treated with a potent inhibitor of PKG signalling, Rp8pGPT-cGMPS (100 µM), was investigated next by way of immunofluorescence analysis. As shown in Figure 4.11 panel B, PKG activity in fact seems crucial for the nuclear translocation of zyxin, pointing towards its involvement in stretch-induced zyxin activation.

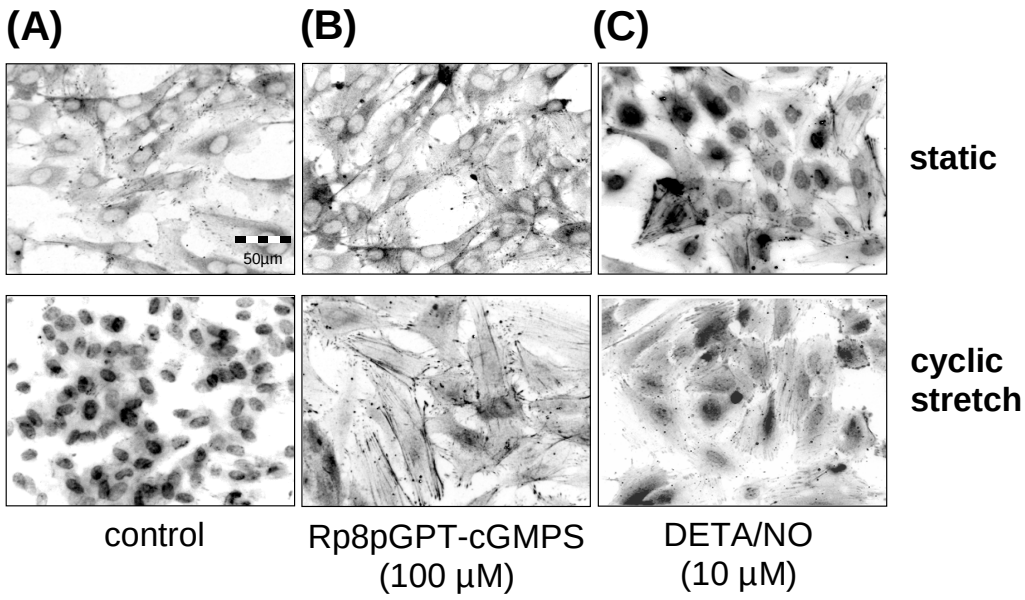

Figure 4.11: Determination of the role of protein kinase G (PKG) signalling in nuclear translocation of zyxin in cultured endothelial cells. HUVEC were stretched (6 hours, 10% elongation, 0.5 Hz). Nuclear translocation of zyxin (A) but not to stress fibers was effectively inhibited by the specific PKG-inhibitor Rp8pGPT-cGMPS (B). In contrast, the NO donor DETA-NONOate elicted nuclear translocation of zyxin already in static cells (C). Representative immunofluorescence analyses.

Endothelial cells produce large amounts of nitric oxide (NO) also leading to high levels of cGMP through activation of soluble guanylate cyclase (sGC; (Denninger 1999; Hamad 2003; Münzel 2003). To analyze whether NO-induced cGMP generation also mediates the extended accumulation of zyxin in the nucleus, DETA-NONOate – a NO donor with slow release kinetics – was added to the cell medium to

simulate continuous production of NO. The NO donor in fact provoked nuclear translocation of zyxin already in static cells, further supporting the pivoral role of PKG therein. However, in stretched endothelial cells accumulation of zyxin in the nucleus appeared to be less prominent (Figure 4.11, panel C).

4.1.7 Analysis of zyxin phosphorylation

To analyse the presumably PKG-mediated phosphorylation of zyxin, 2D-gel electrophoresis followed by Western blot analysis with an antiserum specific for zyxin (B72) was used. For translocation of zyxin the endothelial cells were either subjected to 6 hours of cyclic stretch (10% elongation, 0.5 Hz) or exposed to ANP (1 nM). Either total cell lysates or nuclear extracts were analyzed. As shown in Figure 4.12 two isoforms of zyxin with different pI values (6.76 and 7.0, respectively) could be identified. These changes in pI strongly point towards the formation of a phosphorylated variant of zyxin in response to stretch (Figure 4.12) or ANP (Figure 4.13). To verify that indeed phosphorylation causes this shift in pI the total endothelial protein lysates were pre-incubated with protein phosphatase 1 (PP1) prior to Western blot analysis. This treatment completely eliminated the more acidic protein spot corrobarating that zyxin is in fact phosphorylated in response to cyclic stretch or ANP (Figure 4.14).

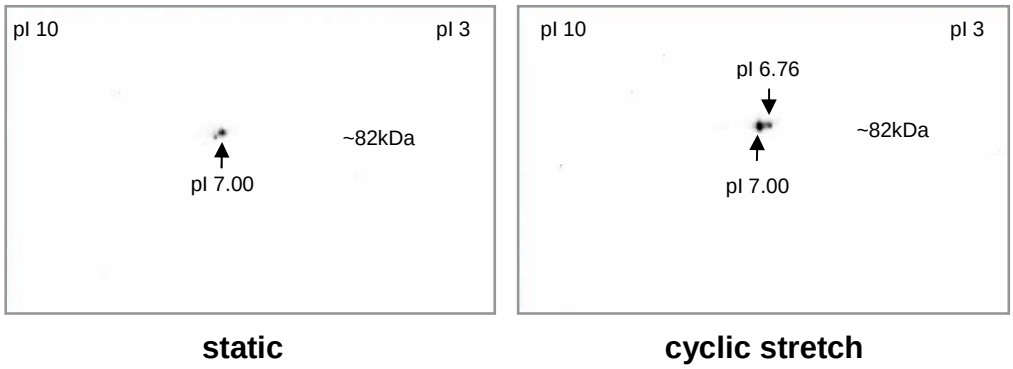

Figure 4.12: Analysis of zyxin phosphorylation in the cultured HUVEC under static conditions and in response to cyclic stretch. Representative Western blot analyses of total protein lysates after 2D-gel electrophoresis. Zyxin was detected by using the B72 antibody.

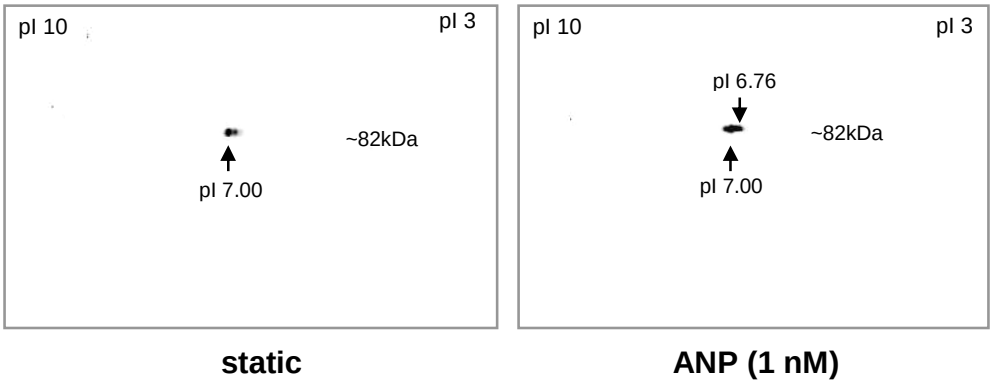

Figure 4.13: Analysis of zyxin phosphorylation in the cultured HUVEC under static conditions and exposed to ANP (1 nM). Representative Western blot analyses of total protein lysates after 2D-gel electrophoresis. Zyxin was detected by using the B72 antibody.

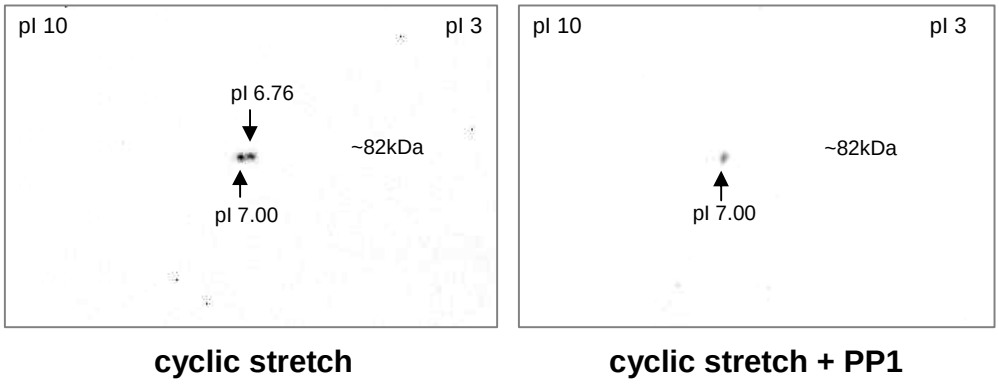

Figure 4.14: Protein phosphatase 1 (PP1)-induced zyxin dephosphorylation. Representative Western blot analyses of total protein lysates after 2D-gel electrophoresis. Lysates obtained from HUVEC exposed to cyclic stretch for 6 hours were either used directly (left panel) or following incubation with PP1 at 30°C for 90 minutes.

To further analyze whether stretch-induced zyxin phosphorylation via ANP correlates with its nuclear accumulation in HUVEC, nuclear protein fractions were prepared and investigated. These data are summarized in Figure 4.15.

Essential differences were observed in all treated samples, as compared to the quiescent controls. Exposure to cyclic stretch and ANP again resulted in the detection of both an acidic and a neutral isoform in the nuclear fraction, which was essentially abolished in the presence of Rp8pGPT-cGMPS (Figure 4.15).

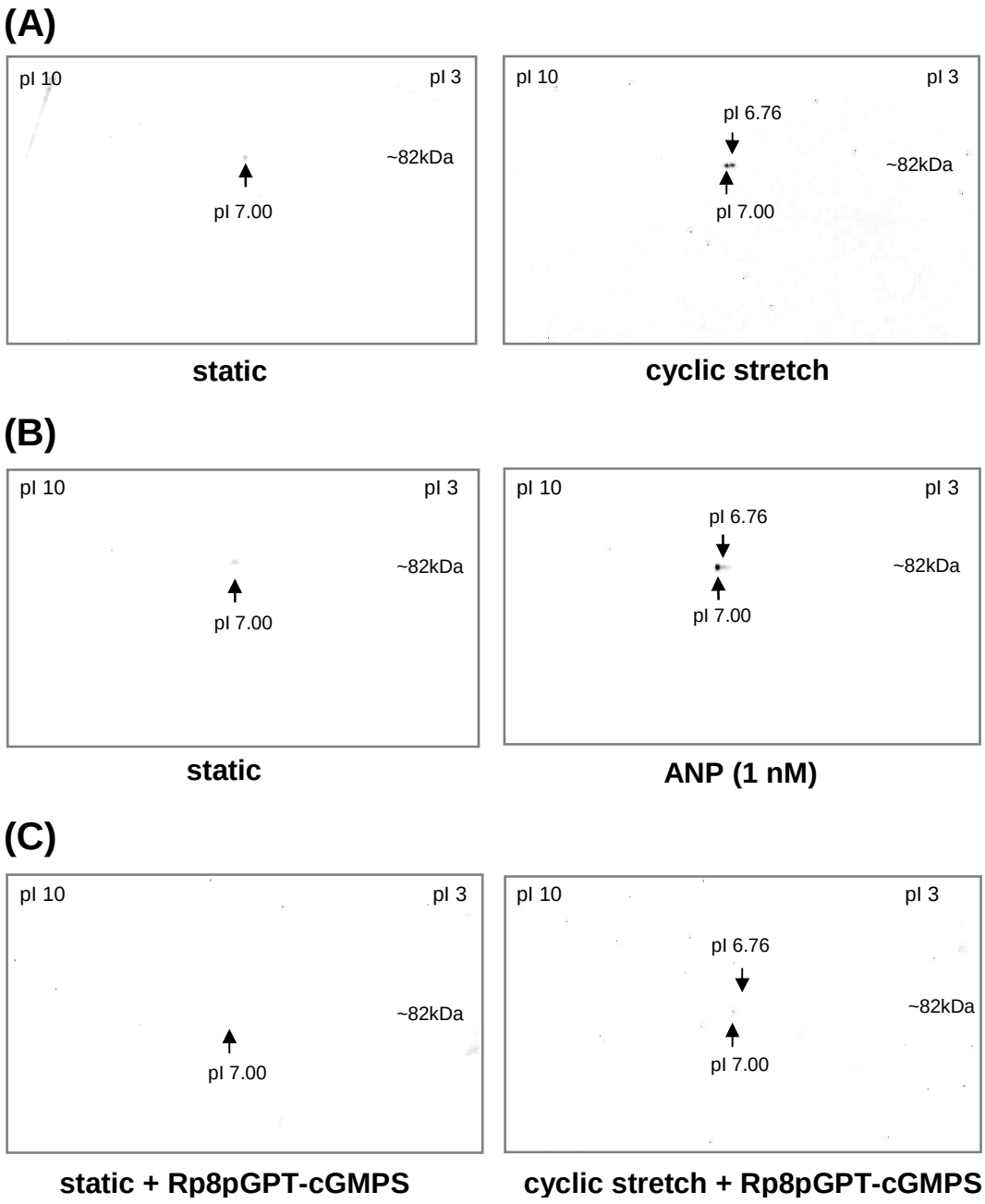

Figure 4.15: 2D-gel electrophoresis. Exposure to cyclic stretch and ANP result in the nuclear accumulation of zyxin. Western blot analysis of nuclear extracts prepared from HUVEC cultured under static conditions (left panels) or exposed to cyclic stretch or ANP (1 nM) for 6 hours with or without Rp8pGPT-cGMPS (100 µM, 6 hours pre-incubation) as indicated (right panels). The Western blots are representative of four individual experiments with essentially the same results.

4.1.8 Optimization of siRNA based silencing of zyxin

To assess the functional role of zyxin in vascular gene expression, a siRNA-based knockdown of zyxin gene expression had to be established. Human primary cultured umbilical vein endothelial cells are rather difficult to transfect with efficiency (≥70%) high enough for gene silencing approaches. As a first approach, metafectene transfection was employed by using antisense oligodeoxynucleotides (ODN) generated against zyxin, however with only low effects on zyxin expression (Figure 4.16). Further, a transfection reagent designed for siRNA, RNAiFect (Qiagen, Hilde, Germany) was evaluated. For this purpose the functionally validated zyxin-specific Hs_Zyx_1HP siRNA (Qiagen) was used. However, also with this approach no optimal results were achieved (Figure 4.16). Finally, a magnetofection approach using the MATra reagent was explored. The results using this approach are summarized in Figure 4.17. With the before mentioned siRNA a sufficient knockdown of zyxin (80±5% of control) was achieved after 72 hours of transfection with pre-stretch. The scrambled control siRNA had no effect. Interestingly, a short pre-stretching protocol further improved the siRNA knock down of zyxin protein, presumably because of a high turn over rate of the protein under conditions of tensil stress (Figure 4.17). Consequently, this effect was exploited in all consecutive experiments.

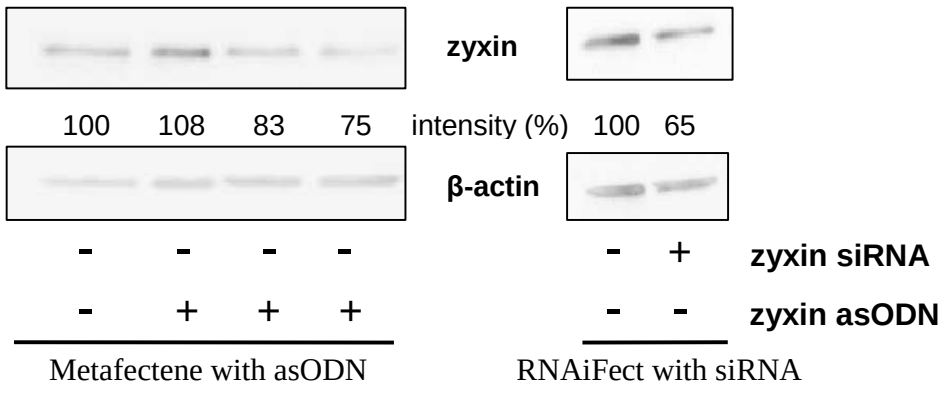

Figure 4.16: Effect of antisense ODN (left panel) and Hs_Zyx_1HP validated siRNA (right panel) on zyxin protein level in HUVEC after transfection with either Metafectene or RNAiFect, respectively. Exemplary Western blot analyses with relative changes in intensity (%) as compared to β-actin band as a loading control.

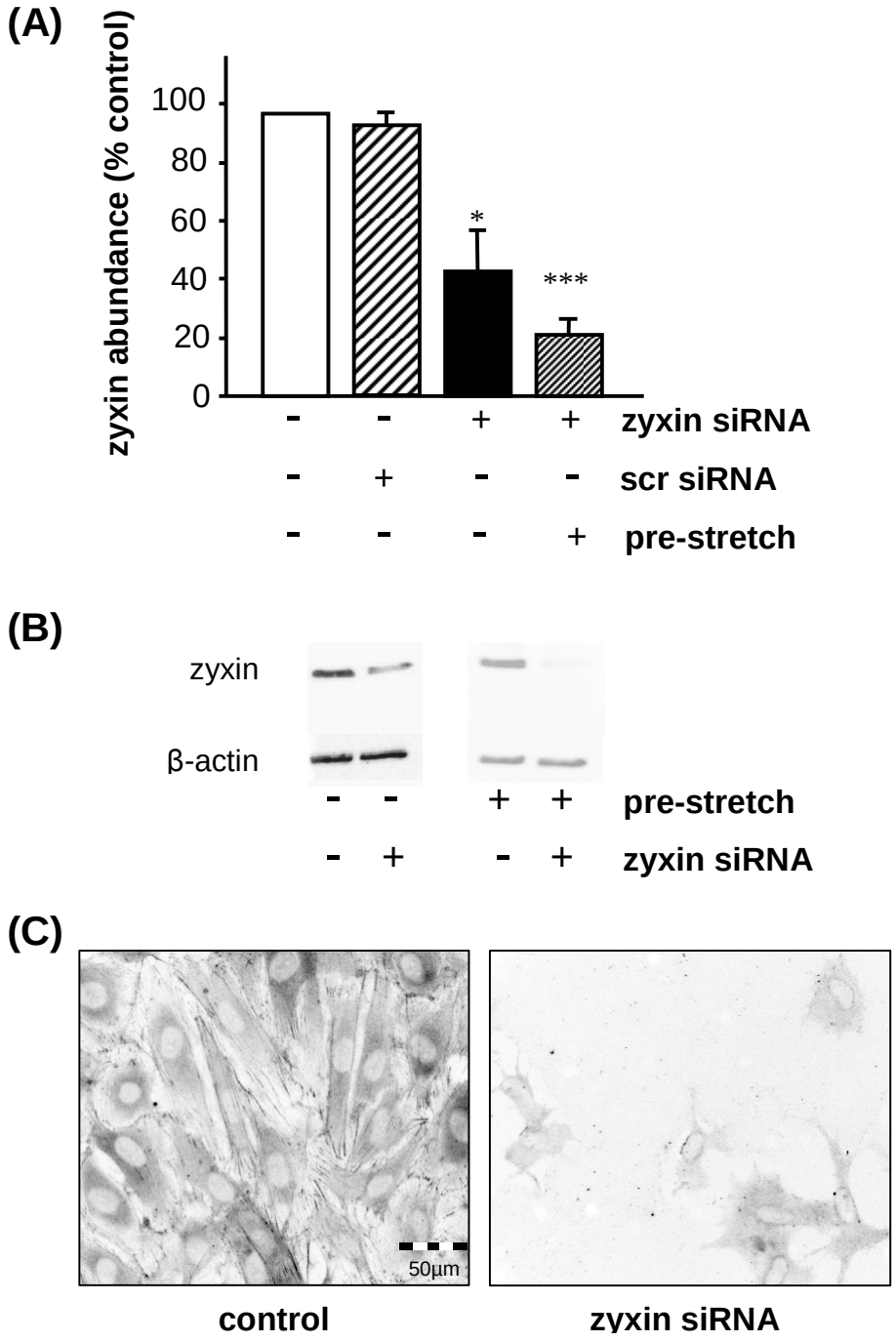

Figure 4.17: Reduction in zyxin protein level after magnetofection. (A) Endothelial cells (HUVEC) were transfected using the MaTra transfection reagent with siRNA directed against zyxin. Seventytwo hours post transfection the protein was extracted and analyzed by Western blot. Zyxin levels in the transfected cells were reduced by 75-85% as compared to the untransfected controls when magnetofection and a short pre-stretch protocol was used. (B) A 30-minute stretch protocol shortly after magnetofection (right panel) increases the efficiency of the siRNA approach. (C) Exemplary immunofluorescence analysis of transfected cells using the B71 antiserum. The results are presented as percentage of the basal zyxin expression. *P<0.05 vs. control, ****P*<0.001 vs. control and scr siRNA control; n=6.

4.1.9 Gene expression profiles in endothelial and smooth muscle cells subjected to cyclic stretch

This part of the thesis concentrates to my knowledge on the first systematic analysis of stretch-induced changes in gene expression in vascular endothelial cells (HUVEC). Using the same approach, the role of zyxin in mechanosensitive gene expression was analysed in two models: HUVEC with or without si-RNA-mediated knock down of zyxin and cultured aortic smooth muscle cells derived from wild type (C57BL6) and strain- and age-matched zyxin-deficient mice. By comparing the mRNA expression profiles of endothelial cells subjected to cyclic stretch with cells cultured under static conditions (static control) in three independent experiments we aimed at a statistically meaningful conclusion. Moreover, knowing of the initial transcriptome changes in the transcriptome of both vascular cell types in response to tensile stress should provide a first insight into the phenotypic changes occurring in these vascular cells at the onset of pressure-induced vascular remodelling (see Chapter 1.1, Figure 1.2). The stretch protocol was programmed exactly as described (see Chapter 3.1.4), i.e. 0.5 Hz, elongation by 10%, for 6 hours.

4.1.9.1 Quality control of microarray chip data

For quality control of the microarray data a correlation analysis of the chip intensity signals in each subgroup was performed (Park 2005; Lee 2007). The correlation of the intensity signals between microarrays in subgroups was calculated and visualized using scatter plots for each microarray chip group, respectively. The ideal outcome of this analysis would be a strength line (r=1.000), whereas zero correlation (r=0.000) would result in a fully random distribution (Tao 2003). Exemplary plot graphs are shown in Figure 4.18 for endothelial cells arrays and Figure 4.19 for smooth muscle cells arrays. The average correlation between samples for the human endothelial cells array was 0.98 (from the highest of 0.9891 in the stretch siRNA group to the lowest of 0.9704 in the static control), and for the mouse smooth muscle cells was 0.977 (from the highest of 0.9927 in the static zyxin-*null* group to the lowest of 0.9621 in the stretch wild type group).

Thus, with correlation coefficients close to 1 both experiments can be considered to be highly reproducible and thus reliable. All plots showed only trace systemic deviations from the line of identity, also indicating a strong correlation between chip data in one in the group and good biological and technical conformity of the chip data as a whole.

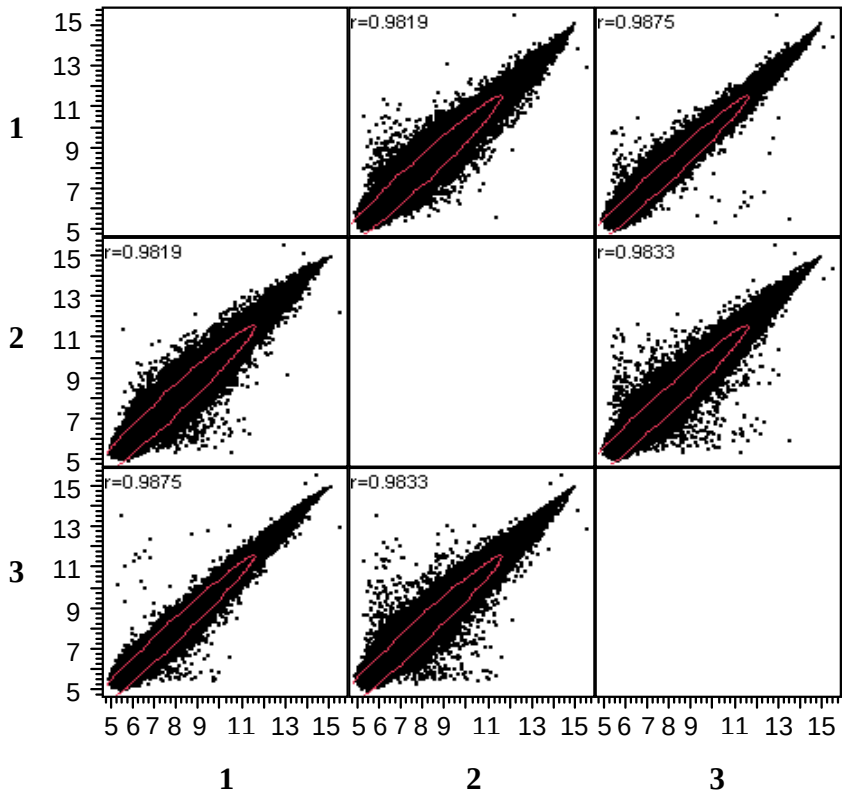

Figure 4.18 Exemplary correlation scatter plots of microarray intensity signals for endothelial cell RNA samples (subgroups 1, 2 and 3 respectively). Each blot compares the expression pattern of one sample with that of another.

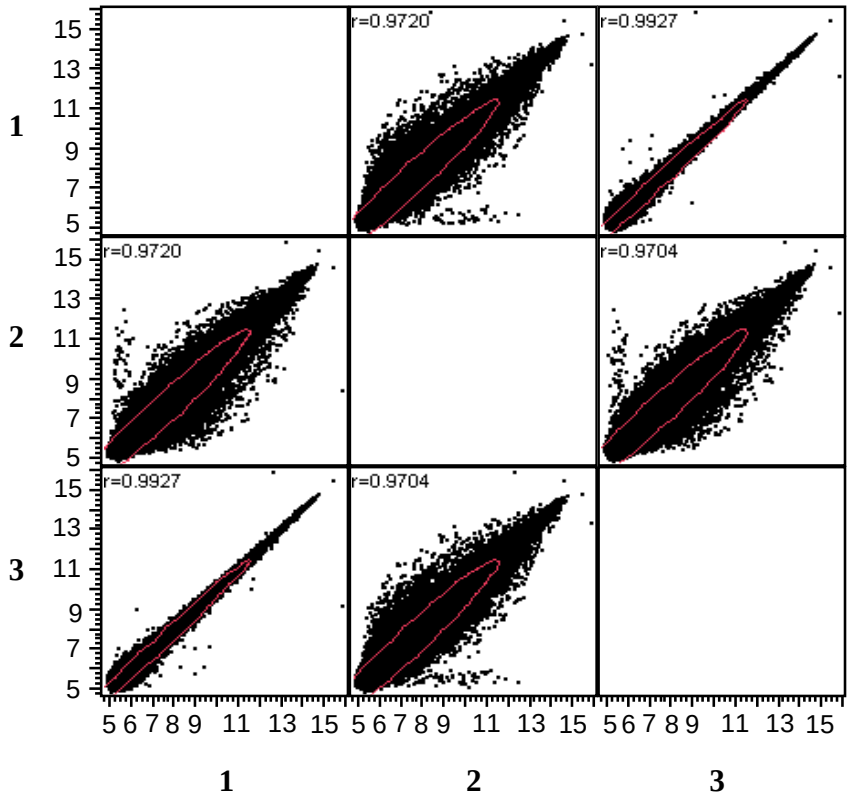

Figure 4.19 Exemplary correlation scatter plots of microarray intensity signals for mouse smooth muscle cell RNA samples (subgroups 1, 2 and 3, respectively). Each blot compares the expression pattern of one sample with that of another.

4.1.9.2 Gene and pathways analysis

As described in detail before (Chapter 3.2.10), besides listing gene products significantly regulated by cyclic stretch in HUVEC or mouse SMC, pathway analysis using the Kyoto Encyclopedia of Genes and Genomes (KEGG) pathway data base, GO annotations, and the module map for cancer compiled were performed. The microarray Gene Set Enrichment Analysis (GSEA, http://www.broad.mit.edu/gsea/) showed significant expression changes in 685 genes by at least 1.5 or 0.67 fold, respectively (Figure 4.20) of 129 pathways (Appendix 1) in endothelial cells, and significant expression changes in 622 genes (Figure 4.22) of 150 pathways (Appendix 2) in the smooth muscle cells. The complex KEGG, GO annotations, and the module map for cancer compiled analyses revealed a number of cellular pathways which have

been associated with stretch-induced vascular remodelling processes before (Table 4.1 for HUVEC and 4.2 for SMC) but also new pathways which shed some new light on the role of zyxin in this process. Zyxin in fact seems to be involved in the differential regulation of numerous pathways and gene products (Tables 4.1 and 4.2, marked with "+")

Table 4.1: Pathways, as defined by KEGG/GSEA with statistically significant differences in the gene expression pattern between groups in the cultured HUVEC. A *P*-value of 0.05 was regarded to be significant for pathway analyses; n=3.

	Pathway EC	*P* value stretch vs. static non affected	*P* value stretch vs. static siRNA zyxin	Zyxin-regulated pathways
1.	Actin pathway (motility)	0.04849	0.24011	+
2.	CD40 pathway	0.46140	0.00382	+
3.	Cell adhesion molecule activity	0.00596	0.12110	+
4.	Cell proliferation	0.02042	0.00038	
5.	Cell signalling	0.00127	0.09292	+
6.	Death pathway	0.19114	0.02236	+
7.	Gα1 pathway (cell differentiation)	0.00625	0.00021	
8.	Gα13 signaling pathway (proliferation)	0.16708	0.00127	+
9.	INFγ pathway	0.04859	0.03636	
10.	LDL pathway (cholesterol transport)	0.04859	0.31314	+
11.	MAPK pathway	0.01679	0.02225	
12.	NFAT pathway (apoptosis, T-cell development)	0.53356	0.00260	+
13.	NFκB induced	0.00048	0.00486	
14.	p38 MAPK pathway	0.00424	0.03516	
15.	PGC (energy metabolism and homeostasis)	0.00616	0.10373	+
16.	Proteasome pathway	0.00055	0.00002	
17.	Ras pathway (apoptosis)	0.52783	0.03140	+
18.	Tgf-β pathway (cell growth, differentiation, apoptosis)	0.00134	0.03474	
19.	TNF and Fas network	0.02487	0.02076	

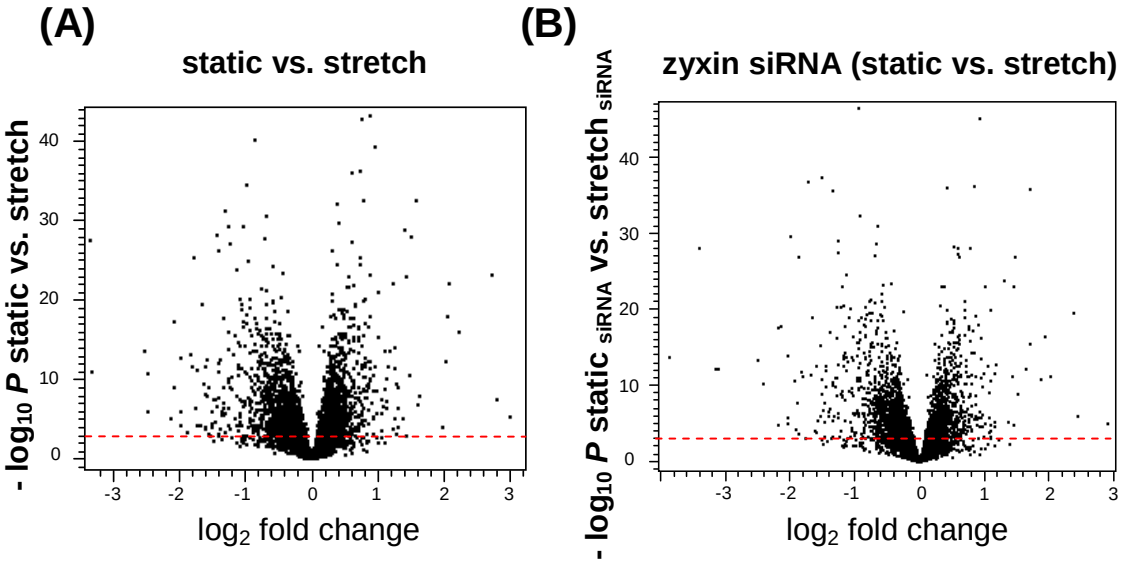

Figure 4.20: Stretch- sensitive gene products in HUVEC. Volcano plots depicting gene products significantly changed in response to cyclic stretch in HUVEC expressing zyxin (A) and after RNAi-mediated zyxin knock-down (B). A *P*-value of 0.001 (dashed line) was regarded to be significant for single gene products.

To evaluate the HUVEC array results, 7 gene products selected for their general interest in vascular biology, i.e. interleukin 8, CXCL1, CXC3L1, VCAM-1, ICAM-1, MCP-1 and ET_B-R were chosen to be analyzed by real time PCR where all gene products proved to be mechanosensitive (Figure 4.21).

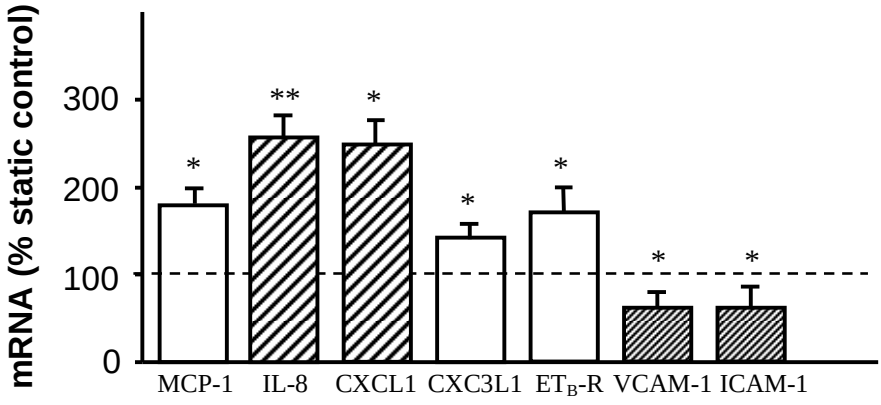

Figure 4.21: Real time PCR analysis of stretch-dependent gene expression in endothelial cells. Cells were exposed to 10% cyclic stretch for 6 hours at 0.5 Hz. Real-time PCR analysis confirmed differential expression of the selected gene products from the microarray analysis. **P*< 0.05; ***P*<0.01 vs. static control; n=4-7.

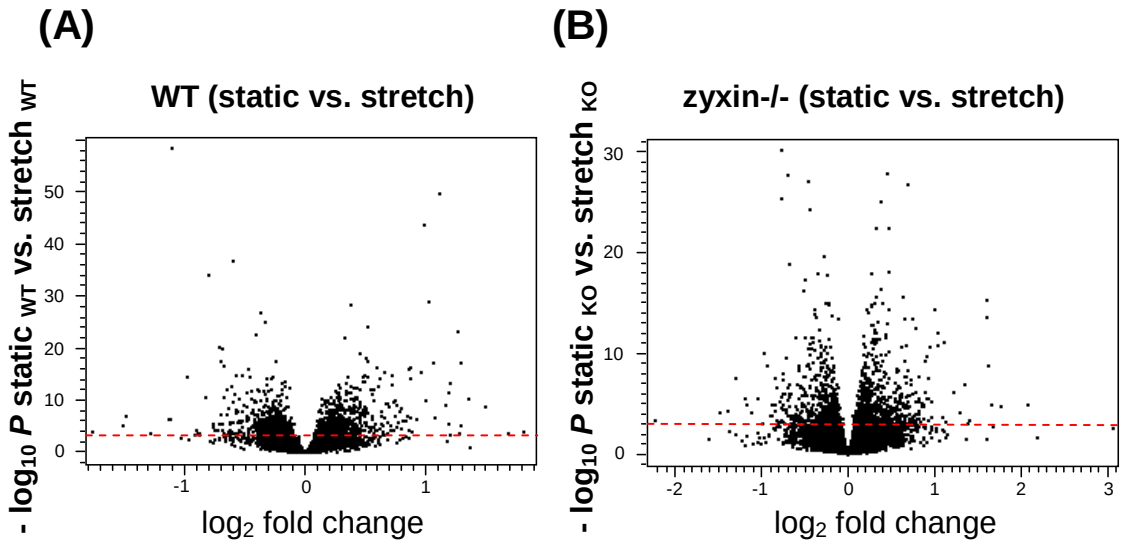

Figure 4.22: Wall tension sensitive gene products in mouse aortic SMC. Volcano plots depicting gene products significantly changed in response to cyclic stretch in SMC expressing zyxin (A) and in zyxin deficient cells (B). A *P*-value of 0.001 (dashed line) was regarded to be significant for single gene products.

Table 4.2: Pathways, as defined by KEGG/GSEA, with statistically significant difference in the gene expression pattern between groups in the cultured mouse SMC. A *P*-value of 0.05 was regarded to be significant for pathway analyses; n=3.

	Pathway maoSMC	*P* value stretch vs. static WT	*P* value stretch vs. static zyxin-/-	Zyxin-regulated pathways
1.	Cell adhesion	0.39092	0.00483	+
2.	Cell cycle regulator	0.02692	0.62950	+
3.	Cell motility	0.28311	0.05545	+
4.	Cell signalling	0.03309	0.00341	
5.	Transcription factors	0.00095	0.26161	+
6.	Death pathway	0.81023	0.00622	+
7.	EphA4 pathway	0.04405	0.49705	+
8.	ROS (oxidative stress)	0.03499	0.01598	
9.	MAPK pathway	0.04874	0.08453	
10.	NFAT pathway (apoptosis, T-cell development)	0.02951	0.03103	
11.	p38 MAPK pathway	0.01623	0.51218	+
12.	PGC (energy metabolism and homeostasis)	0.00772	0.28276	+
13.	Proliferation genes	0.01374	0.17233	+
14.	G1 AND S-PHASES (proliferation)	0.02113	0.08847	+
15.	Jak STAT pathway (proliferation, differentiation and apoptosis)	0.38647	0.04646	+
16.	Phosphoinositide-3-kinase pathway	0.02428	0.27748	+
17.	VEGF pathway	0.06664	0.03189	

To initially determine whether zyxin differentially modulates stretch-induced gene expression in the cultured HUVEC, stretch-induced expression of arbitrarily chosen gene products was analysed following zyxin knock-down by real-time RT-PCR and compared to cells with normal zyxin expression. On the basic of the microarray analysis IL-8, CXCL1, CXC3L1 and MCP-1, the matrix protein versican, the B-type endothelin receptor and the cell adhesion molecules VCAM-1 and ICAM-1 were chosen.

As expected, real-time PCR analysis confirmed the microarray data for all chosen gene products with respect to their stretch sensitivity (Figure 4.21). Moreover, magnetofection of the siRNA directed against zyxin led to a complete inhibition of stretch-induced expression of IL-8 (Figure 4.23) as well as CXC3L1 (Figure 4.24, panel A) stretch-induced CXCL1 mRNA expression was also clearly reduced following zyxin knock-down, however this effect did not gain ststistical significance (Figure 4.24, panel B).

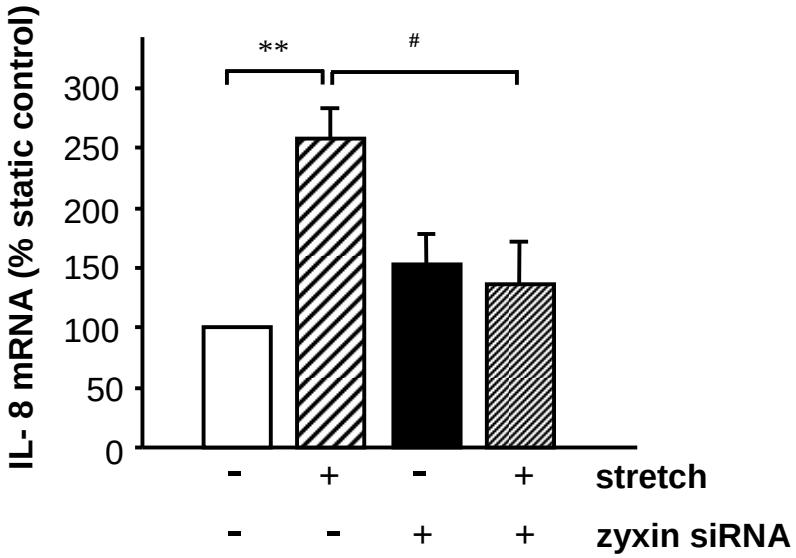

Figure 4.23: Analysis of the role of zyxin in stretch-induced IL-8 expression in endothelial cells. Cells were exposed to cyclic stretch for 6 hours as described (3.1.4). Real-time PCR analysis revealed that zyxin modulates stretch induced IL-8 expression in stretched HUVEC in a zyxin-dependent way. ***P*<0.01 vs. static control; #*P*<0.01 vs. stretch control; n=4.

Interestingly, zyxin knock down did not result in a general alteration of gene expression in response to high levels of stretch. Other tested gene products such as versican, ICAM-1, VCAM-1, ET_B-R and MCP-1 were still stretch inducible also after zyxin knock-down (not shown).

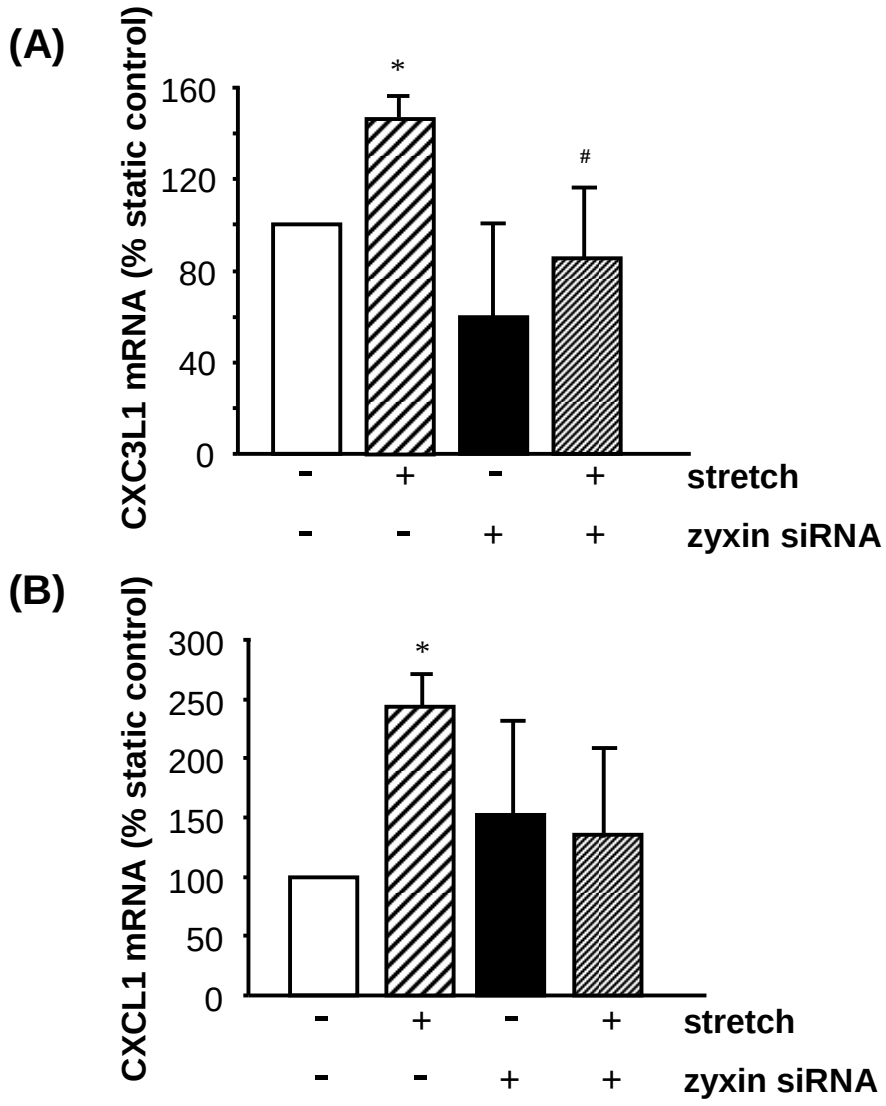

Figure 4.24: Analysis of zyxin-dependent mechanosensitive gene expression in HUVEC. Stretch-dependent expression of (A) CXC3L1 mRNA and (B) CXCL1 mRNA in cells with and without siRNA.based zyxin depletion. $^{*}P<0.05$ vs. static control; $^{\#}P<0.05$ vs. stretch cells; n=7.

4.1.10 Effects of cyclic stretch on IL-8 secretion in HUVEC

To confirm rthat stretch-induced IL-8 mRNA expression is also accompanied by an increased release of this pro-inflammatory chemokine from the endothelial cells, an IL-8 ELISA was used. The results shown in Figure 4.25 demonstrate that together with the transcription of the IL-8 gene, IL-8 concentrations in the supernatant significantly rise in a stretch dependent manner. To confirm that IL-8 secretion also accurs in response to ANP as a surrogate stimulus for cyclic stretch the conditioned medium was also analysed following ANP exposure. As shown in Figure 4.25, ANP also elicted a significant rise in IL-8 protein in the supernatant of the cultured HUVEC.

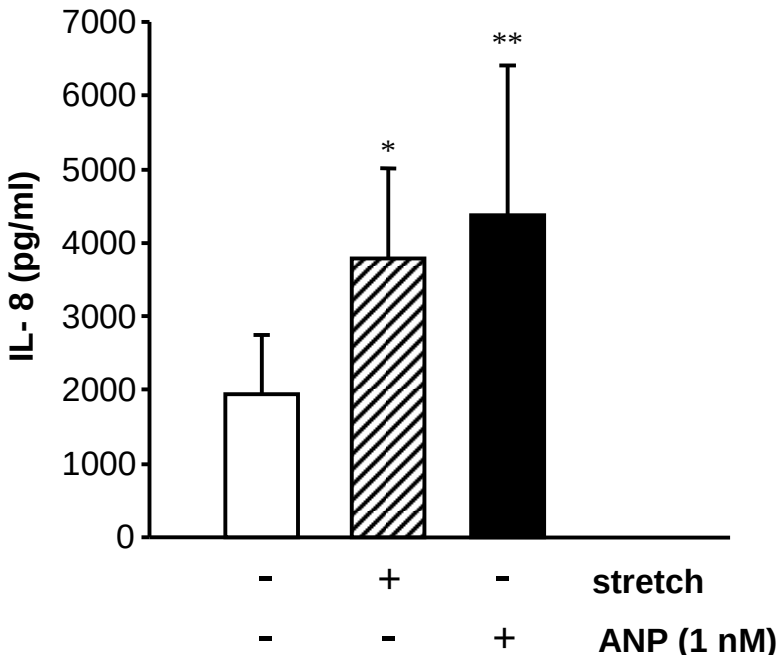

Figure 4.25: Quantification of IL-8 levels in the supernatant of cultured HUVEC. Huvec either kept under static conditions with or without exposure to ANP for 6 hours or exposed to cyclic stretch (10% elongation, 0.5 Hz) for the same period. The IL-8 concentration according the ELISA is expressed as pg protein per ml supernatant. *P<0.05; ** P<0.01 vs. static control; n=7-9.

4.1.11 Analysis of stretch-induced IL-8 expression in HUVEC

As a result of the microarray analyses ~20% of the stretch-sensitive genes in the endothelial cells and ~36% of the stretch-sensitive gene in the smooth muscle cells were found to be modulated by zyxin. To corrobarate the crucial role of ET-1 and ANP release on zyxin-mediated gene expression, HUVEC were incubated with ANP (1 nM) under static conditions with or without the PKG kinase antagonist Rp8pGPT-cGMPS (100 µM) for 6 hours followed by real-time PCR analysis.

As shown in Figure 4.26 ANP to some extent mimics the effect of cyclic stretch on IL-8 mRNA expression in these cells. Its stimulatory effect was mediated through the PKG kinase pathway as evidenced by the inhibitory action of Rp8pGPT-cGMPS (Figure 4.26).

Moreover in the stretched cells exposure to Rp8pGPT-cGMPS resulted in a reduced expression of IL-8 mRNA after 6 hours (Figure 4.27).

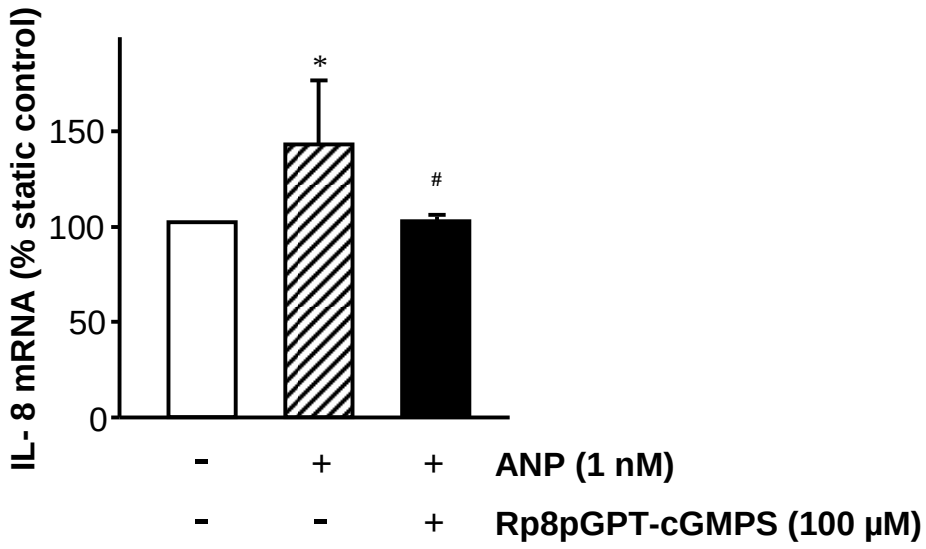

Figure 4.26: Effect of ANP on IL-8 mRNA expression in the cultured HUVEC. HUVEC were incubated under static conditions with 1 nM ANP alone or in combination with Rp8pGPT-cGMPS (100 µM) for 6 hours. Results are expressed as percentage of IL-8/GAPDH ratio in control cells set to 100%. **P*<0.05 vs. control; #*P*<0.05 vs. ANP-treated samples; n=10.

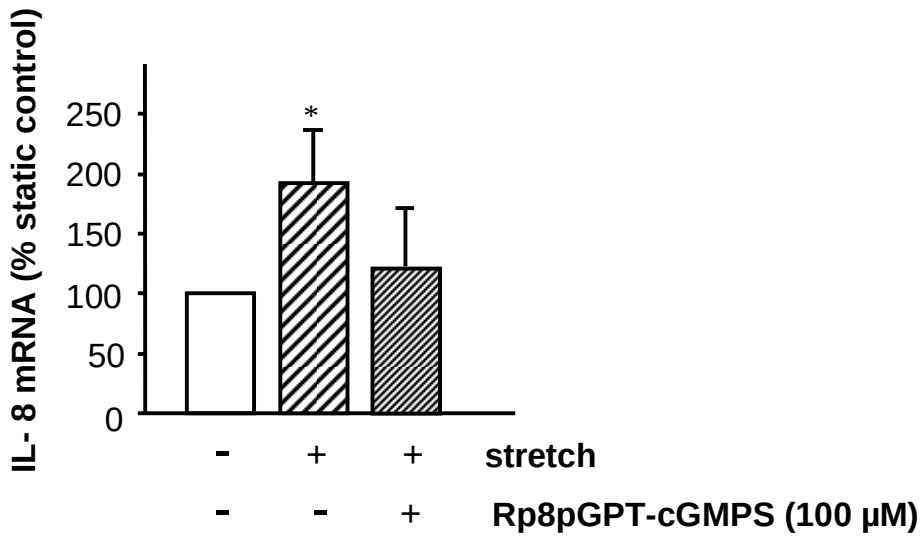

Figure 4.27: Role of PKG in stretch-induced IL-8 mRNA expression. Cells were exposed to cyclic stretch for 6 hours in the cultured HUVEC in the absence or presence of Rp8pGPT-cGMPS (100 µM). Results are expressed as percentage of IL-8/GAPDH ratio in control cells set to 100%. **P*<0.02 vs. static control; n= 4-6.

4.2 Role of zyxin in vascular structure and function

The only way to study the role of zyxin in vascular function was the comparison of wild type vessels with those derived from zyxin-deficient mice. To this end we employed the mice first described by Hoffman et al. (Hoffman 2003) and compared them with matched wild type C57/BL-6 mice.

4.2.1 Phenotype of zyxin-/- mice

As already reported in the orginal paper by Hoffman et al. zyxin-deficient mice do not have an apparent phenotype different form C57BL/6 mice. Comparison of age-mached zyxin-/- and wild type C57BL/6 mice revealed a similar average body weight (approximately 28-32 g) with a slight but not significant tendency of zyxin-deficient mice being smaller (not shown).

Total heart, liver, kidney weight to body weight ratios, were not different between knock out and wild type animals. Also histochemistry of all essential body tissues did not reveal any distinctive features. Interestingly however, age-mached zyxin -/- mice (9 -18 months) had a significantly decreased lung volume as compared to wild type C57BL/6 mice (Figure 4.28).

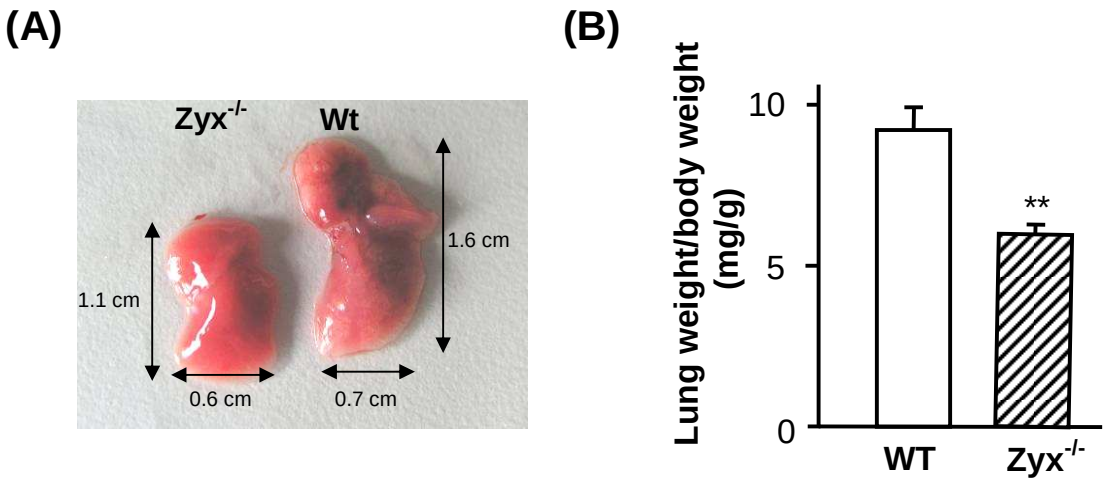

Figure 4.28: Decreased (B) lung weight and (A) size in adult zyxin-/- mice. Data presented in panel A are representative for each of the 12 age-matched (9-18 months) animals. **P*= 0.001; n = 12.

4.2.2 Small vessel perfusion

The set up of a myograph perfusion assay for the measurement of vascular reactivity in response to vasoactive substances (Chapter 3.7) addressed the question whether zyxin has a role in vascular function or not. As a model the femoral artery was chosen because of its diameter and the assistance of relatively few collateral vessels. To verify the anatomical and the functional integrity of the isolated blood vessels, especially that of the endothelial cell layer, after preparation and pressure perfusion, exemplary immuno-fluorescence analyses for the endothelial cell marker proteins NOS-3 and CD31 were performed (Figure 4.29). Moreover at the end of each experiment the constrictor response to phenylephrine followed by a dilator response to acetylcholine was tested.

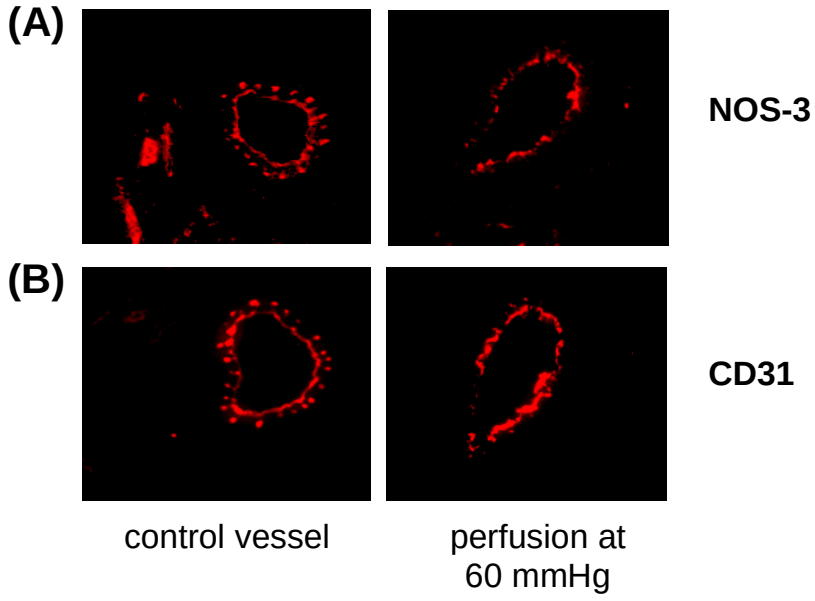

Figure 4.29: Exemplary immunofluorescence verification of the integrity of the endothelium after equilibration followed by pressure perfusion (60 mmHg) of a femoral artery mounted into the pressure myograph. Femoral arteries were either fixed directly post dissection or mounted and exposed to high perfusion pressure for 6 to 12 hours. Stability of the endothelium during the procedure was monitored by the detection of the endothelial markers CD31 (PECAM-1; panel B) and NOS-3 (panel A). As shown on both panels, the endothelium stayed largely intact.

4.2.3 Mechanical overload reveals that zyxin is needed for the structural stability of the vascular wall

To study possible consequences of zyxin deficiency on the structure of the vessel wall, a histological analysis of crossections of perfused vessels from 3, 6, 9 and 18-month old zyxin-deficient mice and age-matched wild type animals was performed. Whereas the orientation of medial SMC in vessels from wild type animals was stably circumferential also after pressure perfusion in all age groups, there was a marked age-dependent reorientation of SMC in zyxin-null mice (Figure 4.30)

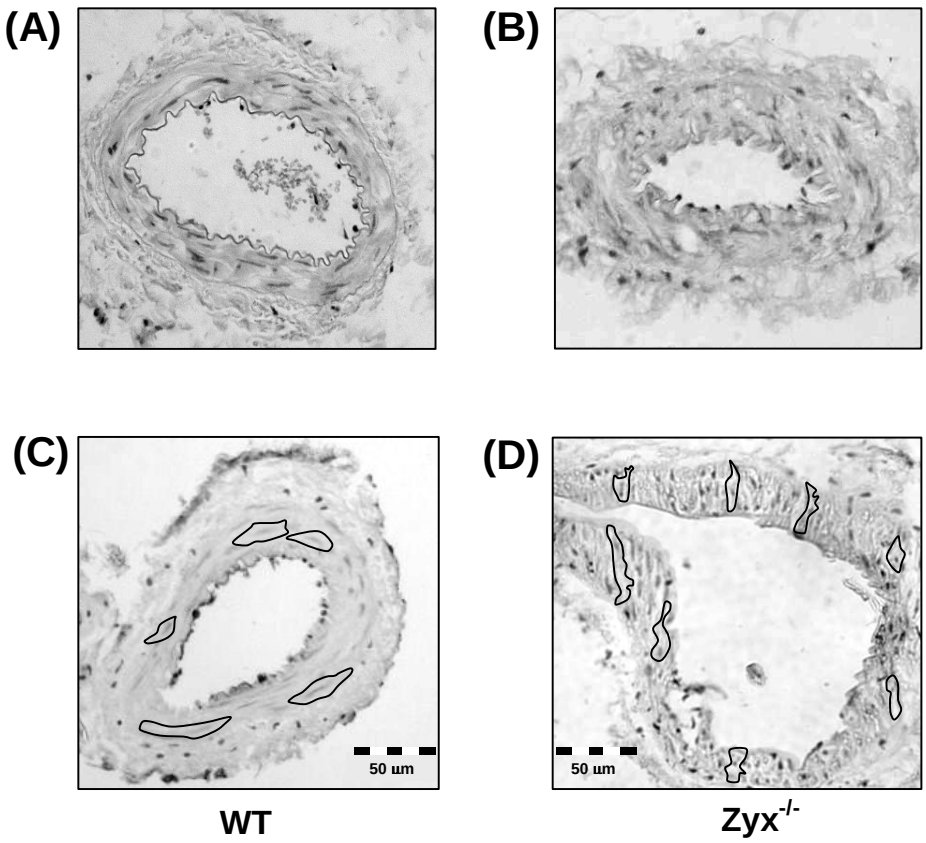

Figure 4.30: **Exemplary cross sections of perfused femoral arteries from zyxin-deficient mice.** Femoral arteries of 9 and 18 months-old mice were isolated, and perfused for 6 hours at an intraluminal pressure of 60 mmHg. Cross sections of zyxin-/- femoral arteries are presented in panel B (9 months) and D (18 months), cross sections of wild type femoral arteries in panel A (9 months) and C (18 months). Endothelal and media smooth muscle cells are normally developed and do not show any pathological alterations in pressure-perfused wild type vessels (A and C) whereas the same segments from zyxin-/- mice (B and D) show a rearrangement of the smooth muscle cell layer after pressure perfusion in an age-dependent manner. Some cells are framed for better visualization of orientation of the cells in the respective sections.

4.2.4 Zyxin-dependent response of femoral arteries to pressure

As a first step in the analysis of zyxin-dependent vascular function, the response of freshly prepared endothelium-intact femoral artery segments to increased pressure was examined. To this end, vessel segments from animals aged from 3 to 18 months were subjected to stepwise increases in perfusion pressure. Comparing the pressure-induced distention of vessels from young animals did not reveal any differences between wild type and zyxin knock-out mice (Figure 4.31 and 4.32).

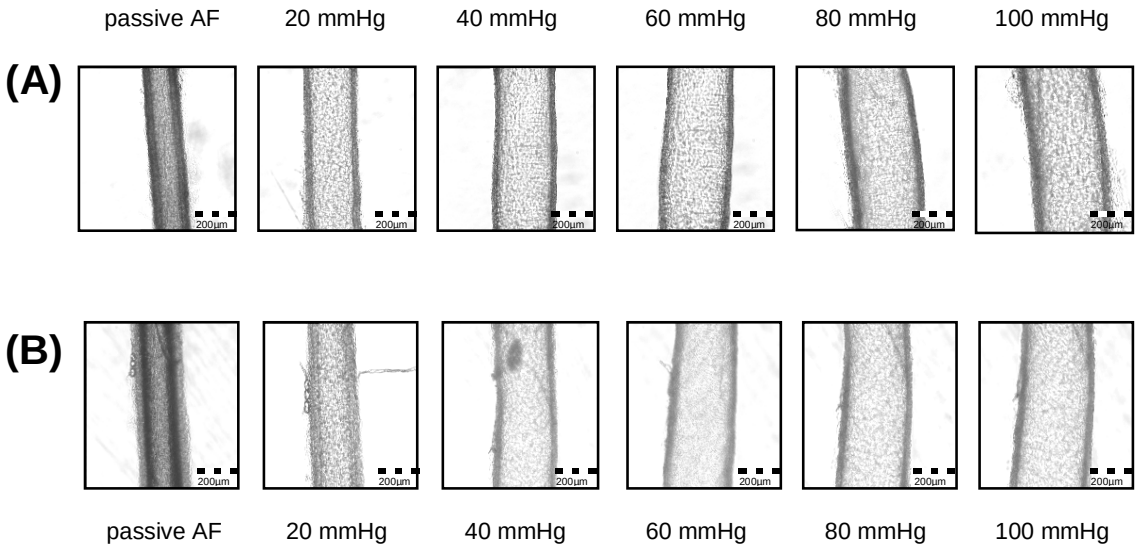

Figure 4.31: Exemplary presentation of the response of zyxin–deficient (A) and wild type (B) femoral arteries (AF, 6 months) to increase in perfusion pressure. Photos where taken after each pressure increase by using a live video imaging system.

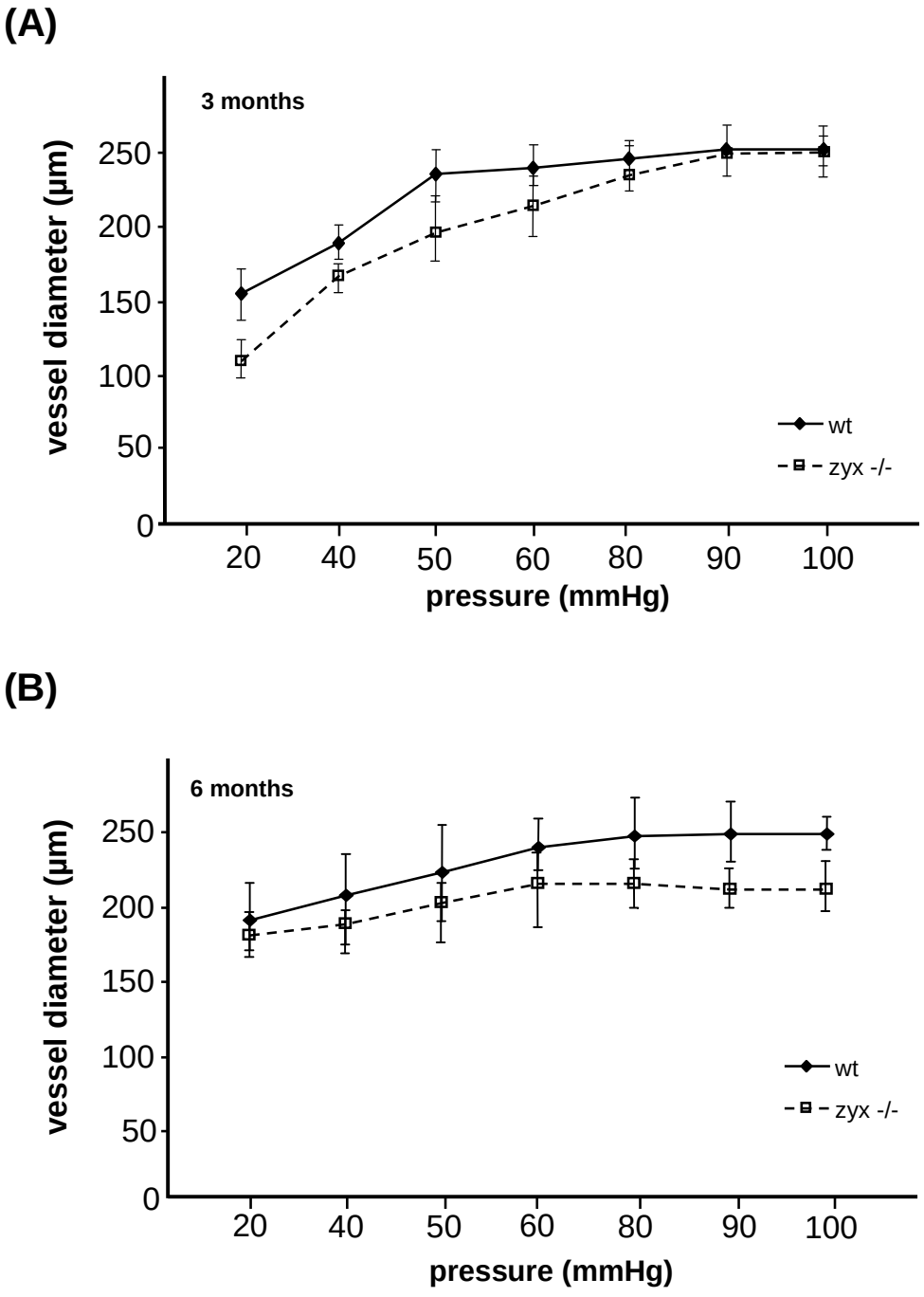

Figure 4.32: Changes in vessel diameter in response to perfusion pressure in femoral arteries isolated from 3 months (A) and 6 months (B) old animals. Femoral artery segments were isolated from wild type and zyxin *null* mice and exposed to intraluminal pressures raising from 20-120 mmHg. Results are shown as absolute changes in outer diameter (µm); n=4-6.

In contrast, a marked decrease in compliance was noted in femoral artery segments derived from 9 and 18 months old zyxin-deficient mice with a maximum distention already at 80 mmHg (Figure 4.35 A and B).

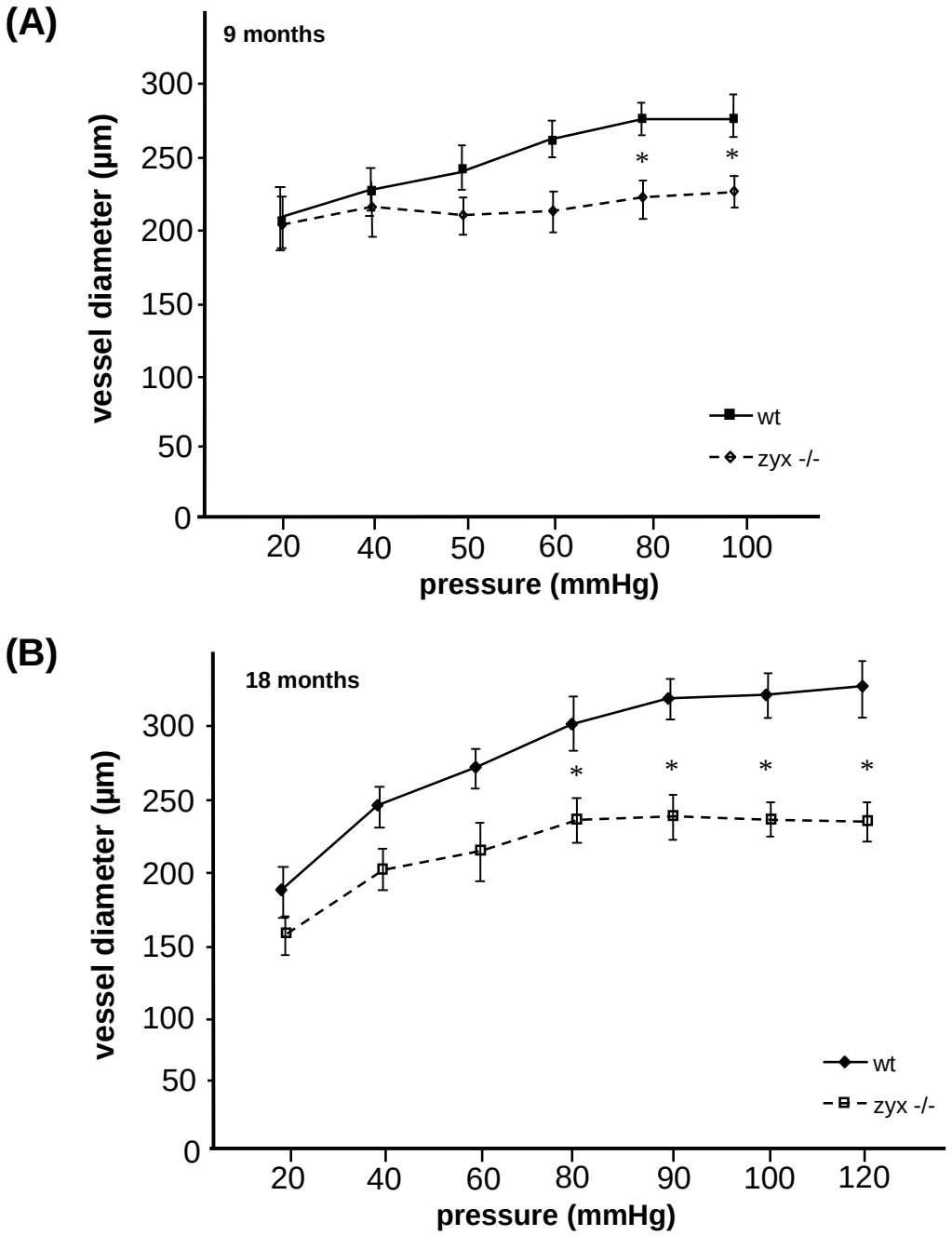

Figure 4.33: Changes in vessel diameter in response to perfusion pressure in femoral arteries isolated from 9 months (A) and 18 months (B) old animals. Femoral artery segments were isolated from wild type and zyxin *null* mice and exposed to intraluminal pressures raising from 20-120 mmHg. Results are shown as absolute changes in outer diameter (µm).*P<0.05; n=3-6.

4.2.5 Differential reactivity of zyxin-/- mouse arteries to vasoactive agents

In another set of experiments, the reactivity of zyxin-deficient arteries to vasoconstrictors such as phenylephrine and ET-1, and to the vasodilator acetylcholine was compared to that of wild type vessels. Control and zyxin-*null* arteries were equilibrated at a pressure of 20 mmHg for a period of 1 hour before starting the experiment. Intraluminal pressure was set to 60 mmHg in order to allow dilator as well as constrictor responses at the vessel segments. Phenylephrine (at 10 nM, 100 nM and 1 µM, respectively), ET-1 (at 10 nM, 100 nM and 1 µM, respectively) and acetylcholine (100 nM and 1 µM) were added extra-luminally consecutively.

The reactivity of zyxin-deficient segments to both vasoconstrictors tended to be weaker in an age-dependent manner. However, there were no significant differences in the response of the vessels from 3 to 6 months old animals to phenylephrine and ET-1 treatment (Figure 4.34).

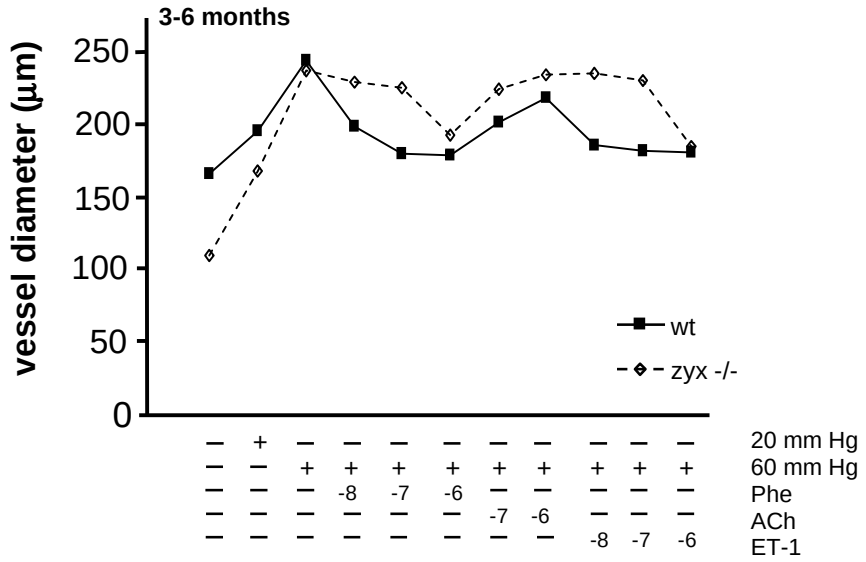

Figure 4.34: Exemplary concentration-dependent response of isolated femoral arteries from 3-6 months old zyxin -/- or wild type mice to different stimuli. After extension of the vessel segments to approximately 250 µm outer diameter, they were constricted with phenylephrine (Phe, decrease in outer diameter) followed by endothelium-dependent dilatation with acetylcholine (ACh, increase in outer diameter) and constriction again with endothelin-1 (ET-1).

Also, in 9 and especially in 18 months old animals the constrictor response of the zyxin-deficient femoral artery segment was readily apparent (Figure 4.35 and 4.36). The dilator response to acetylcholine, on the other hand, was not significantly affected in these segments as compared to those from wild type mice, irrespective of the age. It can be concluded, therefore, that the NO-mediated endothelium-dependent relaxant response to acetylcholine in both types of segments was fully functional, thus confirming the uniform quality of the preparations.

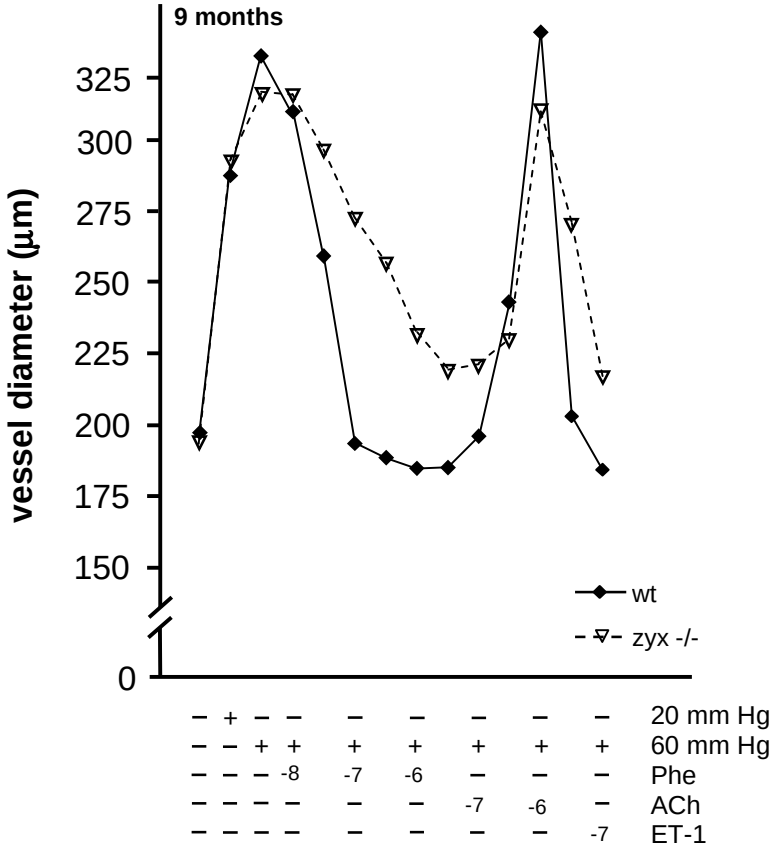

Figure 4.35: Exemplary concentration-dependent response of isolated femoral arteries from 9 months old zyxin -/- or wild type mice to different stimuli. After extension of the vessel segments to approximately 290 µm outer diameter, they were constricted with phenylephrine (Phe, decrease in outer diameter) followed by endothelium-dependent dilatation with acetylcholine (ACh, increase in outer diameter) and constriction again with endothelin-1 (ET-1).

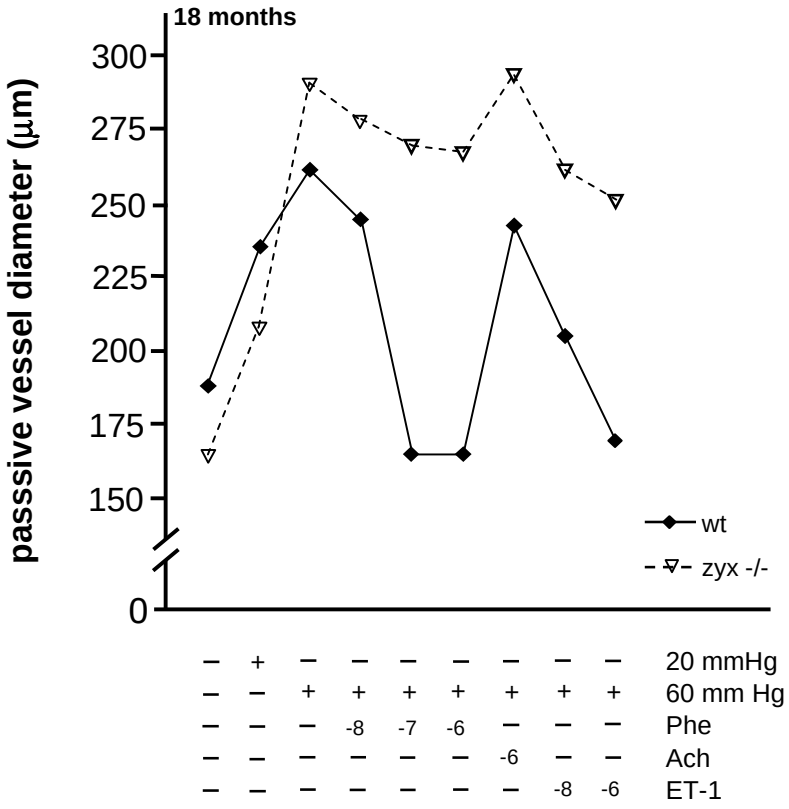

Figure 4.36: Exemplary concentration-dependent response of isolated femoral arteries from 18 months old zyxin -/- or wild type mice to different stimuli. After extension of the vessel segments to approximately 200 µm (WT) and 225 µm (zyxin-/-) outer diameter, they were constricted with phenylephrine (Phe, decrease in outer diameter) followed by endothelium-dependent dilatation with acetylcholine (ACh, increase in outer diameter) and constriction again with endothelin-1 (ET-1).

4.2.6 Effect of zyxin knock-out on pressure induced gene expression *in situ*

In order to find an explanation for the zyxin-dependent differences in vascular reagibility and to evaluate perfusion pressure-induced changes in gene expression in arterial segments from zyxin-/- and wild type mice, real-time PCR analysis was performed to monitor the expression level of the receptors for the main vasoactive agonists, i.e. acetylcholine, noradrenaline, angiotensin II and ET-1 was performed. To this end, age-matched femoral arteries were isolated and perfused for 6 hours with a pressure gradient of 120 to 40 mmHg.

This analysis revealed that expression of the AT-1 receptor for angiotensin II and that of the ET_A-R (Figure 4.37) was up-regulated in response to an increase in perfusion

pressure in femoral arteries from wild type mice. Conversely, this pressure hence stretch-induced AT-1 receptor and ET_A-R expression was blunted in segments from zyxin-deficient animals (Figure 4.37), suggesting that zyxin mediates the biomechanical induction of these genes. In contrast real-time PCR analysis of expression of the AT-2 (angiotensin II), M2 (acetylcholine 2) and the M3 (acetylcholine 3) receptor did not reveal any stretch sensitivity and were also not affected by the loss of zyxin (not shown).

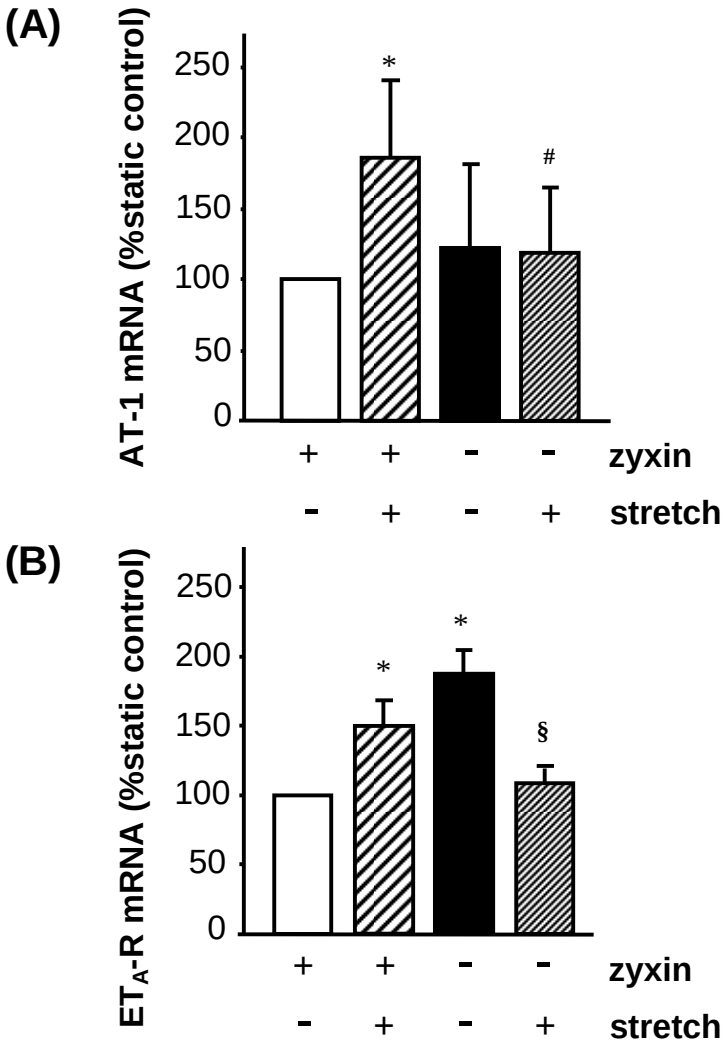

Figure 4.37: Analysis of AT-1 and ET_A-R mRNA expression in isolated pressure-perfused femoral artery segments from wild type and zyxin-/- mice. AT-1 (A) and ET_A-R (B) mRNA expression is up-regulated after exposure to a pressure difference of 80 mmHg for 6 hours in wild type vessel segments. In contrast, zyxin-/- arterial segments increase neither the expression of AT-1 (A) nor that of ET_A-R (B) in response to pressure perfusion. In the case of ET_A-R, the expression level even is diminished upon perfusion as evidenced by PCR. **P*<0.05 vs. WT static control; # *P*<0.05 vs. WT stretchse control; § *P*<0.05 vs. zyxin-/- static control; n=6.

4.2.7 Role of zyxin in regulation of blood pressure

In this preliminary studies, the deoxycorticosterone acetate (DOCA)-salt model has been used as a well-established, clinically relevant model of systemic hypertension. Results are representative only for two experiments, performed on zyxin-/- and wild type mice each, however with very similar pressure characteristics. Therefore could be concidered as distinctive.

Before the administration of DOCA-salt pellet, zyxin-/- and wild type mice exhibited quite comparable systolic arterial pressure (135±28 mmHg; Figure 4.38, panel A), whereas diastolic arterial pressure was markable lower in zyxin-/- animals (84.4±10.2 mmHg) as compared with wild type (106.5±12.5 mmHg) as shown in Figure 4.38, panel B.

After the initiation of DOCA-salt treatment, hypertension was successfully induced in all of wild type animals. As shown in Figure 4.38, the hypertensive response was consistent throughout the 25 days treatment period. In contrast, treatment of zyxin-/- animals with DOCA salt did not provoke the hypertension. Diuring the 25 day period the diastolic pressure did not increase in the DOCA-salt-treated zyxin-/- mice and the effect was not significantly different among two experiments (Figure 4.38, panel A and B). Thus, under basal, unstressed conditions, and after the imposition of DOCA salt, zyxin-/- mice, and at this age, exhibit a anti-hypertensive inclinations.

Heart rates determined in wild-type and zyxin-/- mice before and after the administration of DOCA-salt pellet revealed quite comparable and not significantly different values as shown in table, Figure 4.38.

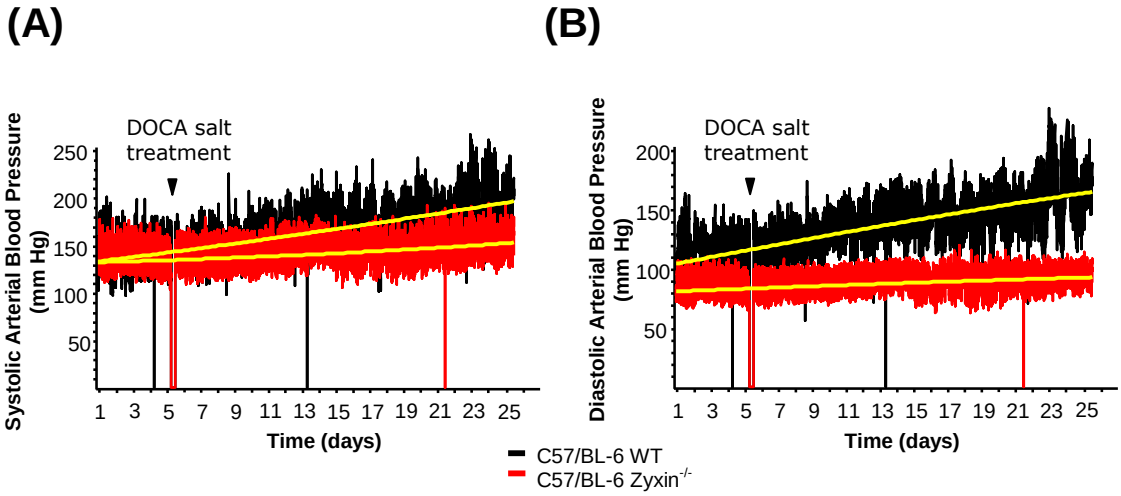

(C)

	heart rate (min^{-1})		blood pressure (mm Hg)		pressure pulse ($\Delta P_{sys-dia}$)	
	WT	$Zyx^{-/-}$	WT	$Zyx^{-/-}$	Wt	$Zyx^{-/-}$
-DOCA	534.8±87.0	564.3±70.3	130.1±16.7 106.5±12.5	124.9±13.6 84.4±10.2	12.9±5.3	40.5±5.2
+DOCA	482.7±81.1	509.7±80.2	157.7±18.4 138.5±16.0	131.3±13.7 89.0±9.6		42.3±6.1

Figure 4.38 Representative real-time blood pressure measurement in the DOCA-salt model of hypertension. (A) Mean systolic arterial blood pressure and (B) mean diastolic blod pressure in age matched zyxin-/- and wild type mice before and three weeks after DOCA salt treatment. Quantitative results are summarized in table, panel C.

5. Discussion

5.1 The vascular response to increased wall tension

It is well established that hypertension and, consecutively, pressure-induced vascular remodelling are responsible for multiple clinical manifestations of cardiovascular disease. Although later phases of these manifestations, such as cardiac insufficiency or coronary artery disease have been described in detail at the molecular level, little is known about the early changes in endothelial and smooth muscle cell phenotype at the onset of the remodelling process. Therefore, we have analyzed which role zyxin (Beckerle 1997), a protein recently characterized to be involved in vascular mechanotransduction (Cattaruzza 2004), plays in the initial response to chronically increased wall tension.

Mechanical forces in the vascular system

As discussed in the introduction (Chapter 1.1, see Figure 1.1), two principally antagonistic mechanical stimuli, fluid shear stress exceeded by the flowing blood and pressure-induced wall tension, modulate the phenotype of endothelial and smooth muscle cells *in vivo*. A balance of these forces is crucial for vascular structure and function. If wall tension rises, the affected cells are preferentially stretched longitudinally. This deformation, if sustained for longer periods, causes the abovementioned phenotype changes of vascular cells resulting in endothelial dysfunction and/or smooth muscle cell hypertrophy and proliferation. This stretch-like deformation, e.g. the smooth muscle cells, is proportional to the magnitude of wall tension which is dependent on both load changes in blood volume hence transmural pressure and the internal diameter or radius of the blood vessel (see Introduction, Figure 1.1). Therefore, the terms ‘stretch’ and ‘wall tension’ may in fact be used synonymously in the context of mechanical overload in the vascular system. However, for the sake of clarity, only the term ‘stretch’ is used throughout this discussion to describe the consequences of an increased wall tension in vascular cells.

High wall tension leads to vascular remodelling

By changing in the degree of stretch to which affected cells are exposed to, blood pressure variations have a major impact on the phenotype of vascular endothelial and smooth muscle cells in conduit or resistant arteries. While a transient increase in blood pressure results in a compensatory increase in vascular tone, as exemplified by the myogenic response (Meininger 1992), chronic pressure overload triggers a profound change in gene expression in these cells that ultimately leads to an adaptive remodelling of the vessel wall (Lehoux 1998; Lehoux 2006). This is characterized by smooth muscle cell hypertrophy, endothelial dysfunction and matrix protein synthesis, resulting in an increase in wall thickness. This structural adaptation, although effectively compensating for the burden of a supra-physiological increase in stretch, essentially fixes the elevated blood pressure (due to the inevitable increase in vascular resistance) and therefore is considered to be a hallmark of manifest hypertension (Heagerty 1993; Lehoux 1998; Prewitt 2002).

5.2 Experimental models

Cyclic stretch as a model to simulate changes in wall tension in vitro

Human primary cultured endothelial cells and mouse cultured aortic smooth muscle cells derived from wild type and zyxin-*null* animals stretched in a Flexercell unit (Flexcell International Corporation, USA) have been used as an *in vitro* model throughout this study. This model has been successfully used as a surrogate stimulus for wall tension in the last years (Shrinsky 1989; Cattaruzza 2004; Kakisis 2004; Lacolley 2004).

As shortly outlined above, an increase in wall tension *in vivo* leads to a longitudinal stretching of the medial smooth muscle cells as well as endothelial cell-to-cell contacts. This stretch mainly depends on the transmural pressure difference and the associated changes in radius of the blood vessel (see Introduction, page 9). However, as it is highly difficult to simulate increases in pressure in cell culture models, the selective use of the radial component of wall tension, i.e., the mechanical stretching of cells, is a well-established model to circumvent this problem. To prevent rapid

adaptation of the cultured cells to this stimulus, they are elongated in a rhythmic fashion, which does not necessarily reflect the pulsatility of regular blood flow, i.e. heart rate. An optimal protocol for cultured endothelial as well as smooth muscle cells was found to be an elongation by 10-15% with a frequency of 0.5 Hz for several hours. Under these conditions on the one hand a strong increase in wall tension was achieved, on the other hand no adverse effects on the viability of the cells was observed as it was the case, e.g., when higher stretch frequencies were chosen.

Besides this merely technical evaluation of the model, also a scientific question arose from using cultured cells: Is this short-term *in vitro* model relevant for the analysis of an long-term *in vivo* process such as vascular remodelling?

Although preserving many characteristics necessary for survival of cultured cells, rapidly lose their ability to regulate many processes compared to the *in vivo* situation (Aird 2007). This loss of “physiological fine tuning” is a major reason for not using cell lines for physiological studies. However, as primary cultures of cells were used throughout this project, the cells were as near to the *in vivo* phenotype as possible. Likewise, many studies show that major determinants of a physiological phenotype in endothelial cells, e.g., the expression of the endothelial isoform of nitric oxide synthase (Johnson 2002; Shi 2004) or sensitivity to vasoactive mediators such as bradykinin(Derhaag 1996; Miura 2002), are well preserved in freshly isolated cells but are lost already in passages as early as p2. Therefore, using freshly isolated endothelial cells and smooth muscle cells in passage 2 to 3 only, the response of these cells to stretch can be regarded as being close to the physiological range. This can also be inferred from the data obtained as discussed below. The careful selection of umbilical cords and maximum uniformity of cell isolation and culture (see 3.1.2, 3.2.10 and 4.1.9) provided some reassurance with regard to the the reproducibility and reliability of the results. This was especially important and evident in case of the microarray analyses.

The other major question regarding the use of cultured cells was that these experiments were performed in the range of hours whereas pressure-induced vascular remodelling in hypertensive patients is a process taking several years if not decades.

However, although taking years and being more complex, for neuro-humoral stimuli as well as leukocytes like monocytes/macrophages play a role in vascular remodeling (Thürmann 1997; Kimura 1998; Martin 2007) – the development of manifest hypertrophy as a result of this process occurs multi-stepwise in rather short intervals. Why is that? Wall tension or cellular stretch typically rises with an increase in blood pressure, which is the consequence of the adaptation of cardiac output to the increased flow resistances in hypertensive patients. Thus, as with hypertension, vascular remodelling is an adaptive process that aims at compensating actual small increases in cellular stretch. Consequently, as a mutual relationship exists between pressure and stretch (see Introduction, Figure 1.2), the whole long-term process must be regarded as a vicious cycle that time and again repeats itself. For studing the onset of such a compensatory phase of the remodelling process, the *in vitro* model of exposing cultured vascular cells to cyclic stretch seems to be ideally suited.

Zyxin knock out mice

The availability of a zyxin-deficient mouse strain (Hoffman 2003) enabled us to directly analyse the role of zyxin in vascular function. Besides these functional analyses using freshly isolated conduit arteries, also an *in vivo* model for hypertension, the DOCA-salt model based on the high increase of volume due to a high salt diet plus the effect of the aldosteron-mimetic DOCA (Mills 2000), was established. Both, the *in situ* analyses of freshly isolated perfused arteries as well as the *in vivo* model will be of fundamental importance to reveal the actual impact of zyxin-induced mechanotransduction for vascular function and stretch-induced remodelling. Unfortunately, although reported to possess no obvious phenotype (Hoffman 2003), zyxin-deficient mice do not mate properly. Therefore, due to insufficient offspring, it was not possible to perform enough experiments for a full functional analysis of zyxin *in vivo*.

5.3 Signalling pathways activated by stretch

Mechanotransduction as a major determinant of pathological signalling in the vascular system has been in the focus of cardiovascular research for many years (Ingber 1991; Davies 1999; Davies 2001; Ingber 2003; Li 2005; Ingber 2006). However, the vast majority of signalling pathways characterized to be involved in mechanically induced signalling had been described before in other conditions of cellular stress, in particular inflammation. This apparent lack of specific "mechanotransduction" pathways has been a matter of debate, especially since the vascular response to mechanical overload, i.e., stretch, is highly specific. The best example for this variance is the particular gene expression pattern induced by stretch in smooth muscle and endothelial cells. Although partially "pro-inflammatory", this response is much more complex when compared to a typical inflammatory response in the vascular system (see below).

Pro-inflammatory pathways activated by stretch

As already outlined in the introduction (Chapter 1.2, page 4), several well-known signalling pathways such as the MAP kinase, Rho-ROCK (Lehoux 1998; Tsuda Y. 2002; Li 2003; Li 2003; Lehoux 2006), and AKT/PI3 kinase pathway as well as many others have been described to be activated and functional in response to stretch in smooth muscle and/or endothelial cells. These pathways definitely are involved in stretch-induced signalling and in gene expression via the activation of several transcription factors such as AP-1, C/EBP (Lauth 2000; Wagner 2000; Cattaruzza 2001; Cattaruzza 2002), NFκB and CREB (Hishikawa 1997; De Martin 2000; Li 2003). However, all these factors seem not to be essential in the setting of mechanotransduction due to the fact that knockdown or inhibition of these pathways never resulted in a true inhibition of stretch-induced signalling, but only in a (mild) modulation of the cellular response (Lauth 2000; Cattaruzza 2002, Hishikawa 1997; De Martin 2000; see also Figure 5.1). Therefore, a specific component of stretch-mechanotransduction pathway in vascular cells has not yet been identified.

5.4 A specific stretch pathway: zyxin as a signalling protein involved in vascular mechanotransduction

Besides stretch-inducible cation channels potentially involved in the sensing of cellular stretch (Lansman 1987; Morris 1990), no signalling pathways particularly specific for stretch in vascular cells have been reported.

The characterization of zyxin as a protein that is down-regulated under pro-inflammatory conditions in vascular smooth muscle cells (Cattaruzza 2002) triggered its analysis as a putative mechanotransducing protein because of its highly suggestive structure (Figure 1.3, page 6). This domain structure possibly facilitating its interaction with both, the stretch sensor, i.e. focal adhesions, and nucleic acids, prompted us to perform preliminary analyses in smooth muscle cells. These experiments in fact revealed an involvement of zyxin in mechanotransduction (Cattaruzza 2004) and lead to the formation of a working hypothesis for stretch-induced signalling in SMC (Figure 5.1). In parallel, another study analysing the function of a homologous protein, the Muscle LIM Protein (MLP), in cardiomyocytes with similar results (Knöll 2002) further substantiated the hypothesis that zyxin might be the long sought specific mechanotransducing protein responsible for the typical response of vascular cells to supra-physiological levels of stretch.

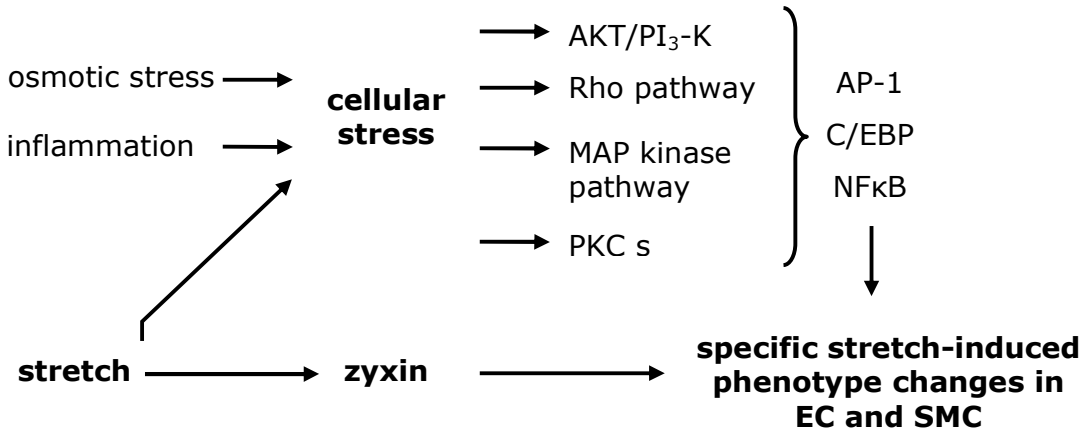

Figure 5.1: Mechanotransduction in SMC. Common and specific stress pathways are activated in response to supra-physiological levels of stretch in vascular smooth muscle cells. Only the combination of both, common stretss pathways and the activation of the specific mechanotransducer zyxin is thought to result in the unique phenotype changes observed in vascular cells during the onset of stretch-induced remodelling of the vessel wall.

Zyxin as a component of focal adhesions

Zyxin is predominantly located in focal adhesions and, in response to stretch, is also recruited to stress fibers. Besides the N-terminal domain, mediating its association to focal adhesions (Beckerle 1997), zyxin has a C-terminal LIM-domain comprising 3 zinc-finger motifs known to mediate protein-protein and/or protein-DNA interactions (Schmeichel 1994). Originally, zyxin was characterized as a protein coordinating the organization of actin filaments at focal adhesions and cell-to-cell contacts in fibroblasts and epithelial cells (Crawford 1991; Crawford 1992; Reinhard 1995; Hoffman 2006). Thus, zyxin is likely to function as a structural protein in endothelial cells, too. Similar to our initial observations, it has been described that zyxin undergoes a major redistribution into newly formed stress fibers also in fibroblasts if exposed to cyclic stretch (Yoshigi 2005). However, these authors could not confirm a nuclear localization of zyxin. Our initial explanation that this might be due to the different cell types analyzed has been further substantiated as fibroblasts generally are insensitive to atrial natriuretic peptide and thus do not possess high activities of protein kinase G, the principal effector kinase of this signalling pathway which is crucial for the nuclear translocation of zyxin (see below).

Zyxin is released from focal adhesions in response to stretch and accumulates in the nucleus

The second function of zyxin, shown in this study, is that of modulating stretch-induced gene expression in endothelial (as well as in vascular smooth muscle) cells. Thus, within minutes zyxin translocates to the nucleus of endothelial cells exposed to cyclic stretch and modulates the expression of mechanosensitive genes.

Zyxin immunofluorence analysis of stretched cultured HUVEC revealed that the protein similar to the situation in rat SMC (Cattaruzza 2004) translocates from focal adhesions to stress fibers and the nucleus. Surprisingly, time course analyse revealed a highly dynamic distribution of zyxin in stretched endothelial cells. Besides the aforementioned fast phase of nuclear accumulation, zyxin was redistributed to its cytoskeletal contacts, i.e., focal adhesions and stress fibers within 120 minutes after the onset of stretch. Extended phases of stretch (>360 minutes), on the other hand,

resulted in a stable localization of the protein in the nucleus with marked changes in the transcriptome that were reminiscent of the phenotype changes typical for the onset of vascular remodelling (Lehoux 1998; Lehoux 2006). Although the mechanism underlying the highly complex shuttling of zyxin into and out of the nucleus could be elucidated to some extent, the teleological background for this highly regulated event remains unclear. So, what may be the reason for this biphasic kinetics of zyxin translocation to the nucleus?

One reason might be that the fulminant initial and fast release of atrial natriuretic peptide, a crucial mediator in zyxin translocation in vascular cells (see below), just causes a pre-mature translocation, which then is "repaired" by a rapid redistribution of zyxin without any functional consequences. Then, in case of prolonged exposure to supra-physiological levels of stretch, the consecutive and constant release of ANP may induce the final and functional translocation of zyxin.

However, as such, an ultimately irreversible initiation of a remodelling process is a complex and potentially serious interference with vascular function, compensatory wall thickening should only take place when the structure of the vessel wall is truly insufficient. To this end, the fast nuclear translocation of zyxin may also serve as a last attempt to retain vascular function by a more transient approach, e.g., by increasing intracellular calcium concentrations and/or energy metabolism. Although speculative, the hypothesis that in a first step zyxin-induced gene expression may aim at increasing the ability of the affected vessel to respond to vasoactive substances such as endothelin-1 and noradrenaline is attractive. An increased expression of the receptors for the aforementioned mediators would in fact lead to a rise in intracellular Ca^{2+} and, consequently, a better capacity for constriction. Further, it may be speculated that, if this response was sufficient, the remodelling program may be shut down at this point with zyxin returning to focal adhesion points. On the other hand, if supra-physiological levels of stretch were still prevalent – as it was the case in the experiments performed in this study – zyxin would again shuttle to the nucleus to ultimately change the gene expression profile, thus irreversibly changing the phenotype of the affected vascular cells. A scheme of this two-step hypothesis can be found in Figure 5.2.

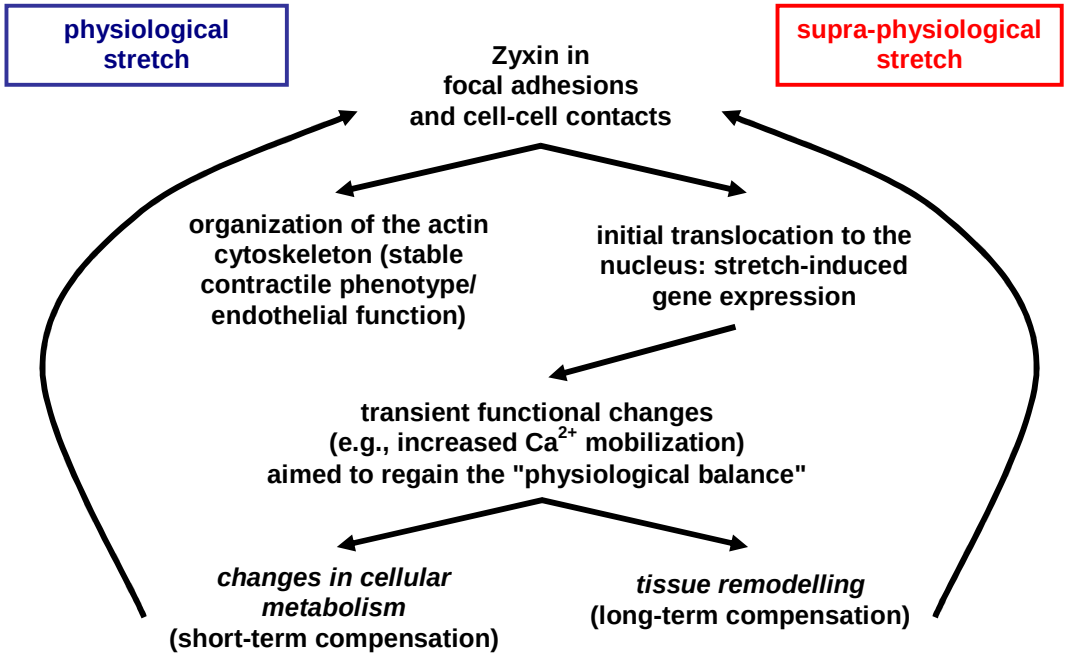

Figure 5.2: Hypothetical two-step model of the vascular response to supraphysiological levels of stretch. Upon exposure to an increased level of stretch, zyxin is released from focal adhesions and accumulates in the nucleus. Here, initial changes in gene expression, along with a rapid redistribution of zyxin, may lead to the retaining of vascular function despite the high level of mechanical strain, and eventually shut down the remodelling process. In the presence of constantly elevated levels of stretch, the second phase of nuclear translocation may be initiated and, as a consequence, changes in the gene expression pattern that are typical for vascular remodelling.

A common mechanism for sensing stretch: Atrial natriuretic peptides in the heart and in arteries

In the course of this study the signalling events leading to the release of zyxin from focal adhesion contacts and its redistribution to stress fibres and to the nucleus could be elucidated. A surprisingly complex chain of events, namely the stretch-induced release of endothelin-1 which in turn induces the expression and release of atrial natriuretic peptide (ANP), was responsible for the complex redistribution of zyxin observed in stretched endothelial cells. ANP, via its receptor(s) NPR-A(B), triggered the activation of the protein kinase G and, finally, the phosphorylation of zyxin. This phosphorylation was necessary (i) to release zyxin from focal adhesions and (ii) to allow the nuclear accumulation of zyxin as shown by PKG inhibition and 2D-

gel/Western blot analysis of total cellular protein and nuclear protein fractions from stretched and ANP-treated endothelial cells. A schematic overview of this signalling pathway can be found in Figure 5.3.

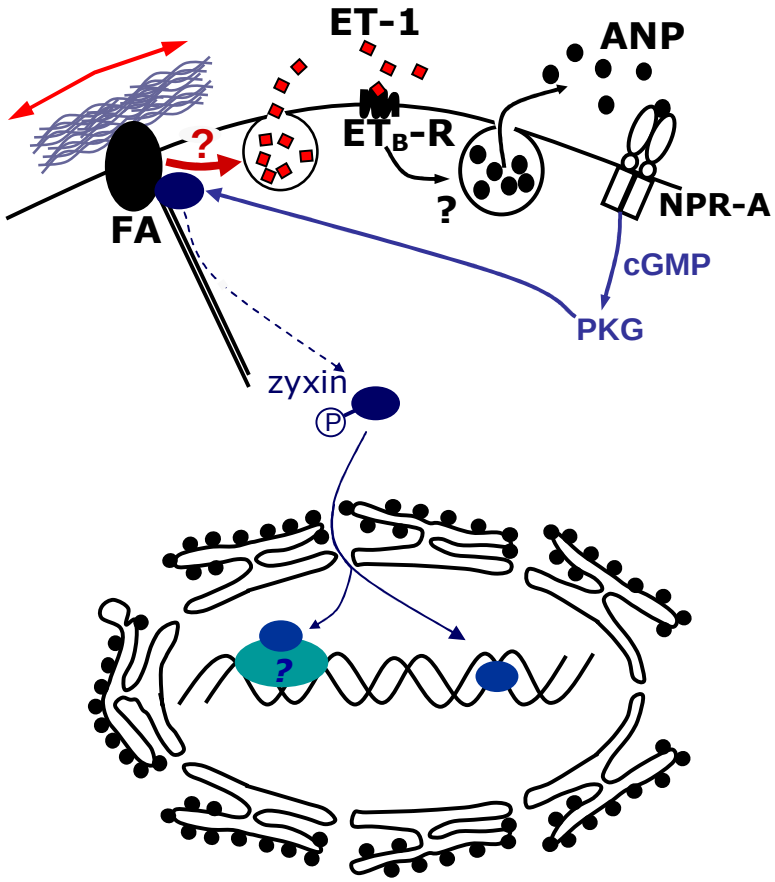

Figure 5.3: Model of stretch-induced release and nuclear translocation of zyxin. The consecutive release of ET-1 and ANP causes activation of the respective receptors (ET_B-R and NPR-A) and a cGMP-mediated activation of protein kinase G (PKG). PKG then phosphorylates zyxin thereby inducing the release from focal adhesions (FA) and its translocation to the nucleus. Here, zyxin modulates gene expression in a complex way (see below), directly, as a transcription factor, or indirectly, by protein-protein interaction.

Again, addressing the suprisingly complex kinetics of zyxin translocation, discussed above, one observation might explain the early translocation of zyxin to the nucleus at a mechanistic level. However, the teleological background remains speculative (see 5.5, page 94). In contrast to endothelin-1, ANP is stored in vesicles similar to von Willebrand factor (vWF) (Weibel 1964; Wagner 1982) in endothelial cells. In contrast

to endothelin-1, ANP is stored in vesicles similar to the typical storage of von Willebrand factor (vWF) (Weibel 1964; Wagner 1982) in endothelial cells. Therefore, an initial stretch-induced increase in intracellular calcium may – similar to that observed for von Willebrand factor in the case of vascular injury (Kermode 2002) – cause a virtually explosive release of ANP. This rapid ANP release could in fact be detected in cell culture supernatants of endothelial cells within 1 minute after starting of the stretch protocol and without any supporting endothelin-1 release (Figures 4.6 and 4.7). This rapid ANP release may be mediated through the activation of stretch-sensitive non-specific cation channels (Lansman 1987; Morris 1990). However, whether this initial zyxin translocation is more like an accident owed to the initial stretch-induced depolarization of endothelial cells without any functional relevance or whether it actively contributes to the two-step process described above (Figure 5.2) remains to be elucidated.

Another point that needs to be clarified is the actual nature of the ANP receptor involved in the aforementioned signal transduction process. Unfortunately, no reliable experimental tools such as NPR-B antibodies, receptor-specific agonists or antagonists are currently available. As the cGMP-induced activation of PKG is fundamental for downstream signalling, only the membrane-bound guanylate cyclases NPR-A and NPR-B can be involved therein (see the Introduction 1.5, page 9). Although both natriuretic peptide receptors are expressed in endothelial cells, mRNA levels of NPR-B are rather low. Moreover, the cellular distribution of NPR-A, for which antibodies are aviable, was clearly altered in response to stretch. As in quiescent endothelial cells, most of the receptors seem to be localized in a vesicular compartment, while stretch leads to an equal distribution to the cell membrane. Therefore, without definitive proof for this assumption, NPR-A most probably is the receptor responsible for stretch-induced ANP-mediated signalling in human endothelial cells.

Local ANP and systemic ANP: variations on one theme

Why is the endothelial cell signalling in response to cyclic stretch so complicated? It is well-known for sometime that the release of ANP from atrial monocytes into the blood is regulated in a very similar way (Ruskoaho 1886; Lang 1985; Kinnunen 1993; Dietz 2005). As described in the introduction, ANP is released from the atria in response to high filling during diastole, i.e. in response to volume hence pressure-induced stretching of the atrial wall. The cells actually sensing this stretch are the atrial endothelial cells, which in turn release endothelin-1. Endothelin-1 – similarly as described here for endothelial cells – then induces the release of ANP through activation of the ET_A-R from the atrial myocytes. ANP circulating in the blood acts both on blood vessels to decrease pheripherial resistance and the kidnes to enhance sodium and water secretion and thus lower blood volume and pressure. In the context of systemic volume control, this complex multi-cell pathway makes perfect sense: whereas one cell type (endothelial cells) senses and transduces the actual stimulus for the release of ANP, the next (atrial myocytes) is responsible for propagation of the signal through ANP synthesis and discharge. Finally, effector cells in the vasculature and the kidney receive the signal and execute the program, i.e. they effectively reduce the circulating blood volume thereby closing the control circuit through elimination of the activating stimulus, i.e. atrial wall stretch. Interestingly, together with the release of ANP zyxin may be localized in the nucleus of cardiomyocytes (Smolenski 2000; Kato 2005). Thus, all building blocks of the vascular stretch sensor characterized for the first time in this study seem to be preformed, “available” and active in multiple cells throughout the organism and must be reassembled in just one cell type, the endothelial cell (and to some extent the vascular smooth muscle cell), for designing an autocrine stretch sensor and effector system. Therefore, the initial amazement regarding the highly complicated endothelial signalling pathway for “just” releasing zyxin from focal adhesions, may be replaced by an admiring the effective use of pre-existing signaling building blocks for a different task.

Thus, the effector pathways for relieving systemic and local vascular wall tension seem to be quite different while the actual stimulus, stretching of cells is the same.

This way, highly efficient and sensitive sensor and signalling pathways can be preserved.

Zyxin in the nucleus: stretch-induced gene expression in vascular cells

The basis for the phenotype changes of vascular cells observed in pressure-induced vascular remodelling is a complex alteration of gene expression that specifically promotes this process. Up to now only a very limited number of preliminary reports describing the effects of stretch on vascular smooth muscle or endothelial cells at this molecular level have been published (Resnick 1995; Obuwole 1997). In particular, no complex and statistically valid screening of the endothelial or smooth muscle cell transcriptome in response to stretch has been described.

In this study, the first systematic analysis of stretch-induced changes in endothelial as well as smooth muscle cell gene expression has been performed based on statistical significance. In the literature, a vast number of microarray analyses can be found comparing tissues or primary cells. However, although such an approach from a physiological point of view is correct, many of these studies suffer from the considerable variability of the samples used for analysis (Park 2005; Lee 2007). To really achieve statistical significance with only three independent microarray analyses, we aimed at using cells as comparable as possible by taking care of absolutely uniform conditions from isolating the cells to harvesting the RNA samples for all experiments (for details see 3.2.10). The optimal uniformity, thus quality, of our microarray experiments was retro-spectively checked by analyzing several known stretch-inducible gene products. As verified by microarray signal intensity analysis (Tao 2003; see also page 57), the series of experiments analyzed was in fact highly comparable and reproducible. To evaluate and confirm the microarray data, real-time PCR analysis of several randomly chosen gene products was performed. All gene products re-tested were stretch-sensitive, thus corroborating the reliability of the microarray analyses.

The pathway analysis (Manoli 2006) performed with the computational tool *gene set enrichment analysis* (GSEA) not only allowed to determine the transcriptional profile (Mootha 2003; Subramanian 2005), but also facilitated the understanding of the

complex changes in gene expression by grouping differentially expressed gene products into functional pathways. It thus provided a physiologically highly significant and meaningful interpretation aid for the large amount of data generated by microarray analyses. Thus, this analysis tool provides far more than just a list of single gene products.

Besides a substantial amount of new data, several pathways, reported to be involved in stretch-induced vascular remodelling in one or the other way, could be confirmed to be in fact stretch-inducible both in endothelial and smooth muscle cells. Among these pathways, cell proliferation (Lee 1995), migration (Dajnowiec 2007), differentiation (Haga 2007) and apoptosis (Cho 1995; Hamet 1996; Cattaruzza 2000) were most prominent. Moreover, also biochemical pathways such as energy consumption (Deedwania 2004), cytoskeletal remodelling and oxidative stress (Cai 2000; Touyz 2001; Touyz 2004; Fortuño 2005) were confirmed to be affected. Most interesting, however, was the exact characterization of several signalling cascades such as the MAP kinase pathways as well as the activation of transcription factors such as AP-1, C/EBP or NFAT, which all have been implicated in vascular remodelling as well as cardiac hypertrophy (Agrotis 1996; Lauth 2000; Cattaruzza 2001; Intengan 2001; Luft 2001).

The second major question addressed by this analysis was, if and in which way zyxin is involved in the stretch-induced reprogramming of the endothelial and smooth muscle cells transcriptome. The careful and effective knockdown of zyxin using a specific siRNA (see page 55) and in parallel the comparison of aortic cultured smooth muscle cells derived from wild type and zyxin-deficient mice confirmed the fundamental influence of this protein on stretch-induced gene expression. According to these analyses, zyxin is involved in the regulation of ~20% (EC) and ~36% (SMC) of all stretch-sensitive gene products. Most of these gene products can be arranged in pathways which are of special importance for pressure-induced vascular remodelling. In particular, zyxin is important for the expression of gene products involved in cell migration and proliferation, protection from apoptosis and high energy consumption (see Results, page 60 and 63, Tables 4.1 and 4.2). Moreover, uptake as well as synthesis of cholesterol depends on zyxin signalling in endothelial cells.

Does zyxin-induced gene expression reflect early phases of remodelling and endothelial dysfunction?

All zyxin-dependent pathways defined above tend to promote vascular remodelling in endothelial as well as smooth muscle cells. These processes are specific for endothelial dysfunction and hypertrophic and/or hyperplastic growth of the vessel wall. Therefore, the hypothesis that zyxin is critically important for stretch-induced vascular remodelling is highly suggestive when considering the aforementioned microarray data.

Another aspect of zyxin-mediated gene expression in endothelial cells is the possible involvement of the protein in the development of atherosclerosis. Hypertension, hence chronic exposure to supra-physiological levels of stretch constitutes an important risk factor for the development of this disease. Interestingly, also cholesterol metabolism is influenced by zyxin in stretched endothelial cells. As this molecule, especially in connection with the high levels of oxidative stress observed under conditions of mechanical overload, plays a central role in the early development and maintenance of atherosclerosis, zyxin-mediated uptake and synthesis of cholesterol might well play a role in the early sub-endothelial accumulation of oxidized cholesterol (Witztum 1991; Pillarisetti 1997; Skålén 2002; Birukov 2007). Moreover, several chemokines such as IL-8, which seem to be essential for the recruitment of leukocytes to the early atherosclerotic lesion are expressed under the control of zyxin. IL-8 is a well known chemoattractant for neutrophils (Detmers 1990; Rollins 1997; Zlotnik 2000; Patterson 2002), T-lymphocytes (Larsen 1989) and monocytes (Mukaida 1998; Gerszten 1999). The levels of zyxin-dependent endothelial IL-8 secretion in response to stretch at least match those of activated peripheral blood monocyte/macrophages (20±6 ng/mg as cellular protein measured by ELISA from Figure 4.25 vs. 25±5 ng/mg cellular protein for macrophages; Persson 2006). Thus, the stretch-induced release of IL-8 from endothelial cells alone may be sufficient for monocyte recruitment in the early stages of atherosclerosis (Mukaida 1998; Gerszten 1999). Together with the imbalance in cholesterol metabolism discussed above, stretch-induced and zyxin-mediated endothelial gene expression might be an important factor strongly facilitating and

promoting the formation of early atherosclerotic plaques (Chobanin 1996; Lehoux 2006).

5.5 Zyxin and vascular function

Zyxin-deficiency and vascular function – a matter of gene expression?

Besides its signalling properties, zyxin is thought to be important for the organisation of the actin-myosin system and its connection to the extracellular matrix via focal adhesions and stress fibres. Therefore, a second aim of this study was to characterize whether zyxin indeed modulates vascular structure and tone. To this end, an *in situ* perfusion model with defined flow conditions was chosen and adapted for isolated mouse femoral arteries. With the access to zyxin-deficient mice, the role of zyxin in vascular function could be ideally addressed in this model.

Interestingly, the first description of zyxin knockout mice available to us neither revealed any functional phenotype nor was able to demonstrate any morphological changes as a result of zyxin deficiency (Hoffman 2003). However, in this study only relatively young mice (>6 months) were analysed. While herein always gender and age-matched (from 3 to 18 month old) animals were investigated side by side with a major focus on the vasculature. This way we could demonstrate fundamental differences in both structure and function of freshly isolated perfused femoral arteries derived from wild type and knockout mice. By inspection, the vessels from wild type mice appeared to be mechanically more stable than those from zyxin knockout animals. Consequently, preparation of the femoral artery from wild type mice was easy and the mounting unproblematic, whereas vessels obtained from zyxin-deficient mice were brittle and easily disrupted pointing to a major difference in structure and matrix composition.

While distension in response to different levels of pressure was similar in all arteries, the comparative analysis of the response to vasoconstrictor substances such as phenylephrine and endothelin-1 revealed an impaired ability of zyxin-deficient vessels to constrict. Most surprisingly, in vessels from older animals a complete rearrangement of smooth muscle cells in response to pressure perfusion could be

observed. The new perpendicular orientation of the cells, on the one hand, helped to explain the weak constrictor response since even a good contractility of cells oriented longitudinally could not result in efficient (concentric) constriction (see Figure 4.30, page 70). On the other hand, the reason for this complete rearrangement of the somooth muscle cells in the media remains to be determined and thus far is unparalleled in the literature. One starting point for approaching this amazing finding would be a thorough analysis of the composition of the extracellular matrix. Due to insufficient numbers of mice, however this analysis could not be done yet.

The few *in vivo* experiments possible revealed another fascinating aspect of vascular function in zyxin-deficient mice. These mice responded with a surprisingly low increase to DOCA-salt treatment when compared to wild type animals. Moreover, monitoring of blood pressure revealed a rather low diastolic pressure and a large pressure pulse in zyxin-deficient animals. These data point to a low resistance *and* a low (i.e. bad) compliance of the arterial system in these animals. At first sight, especially in view of the perfusion data, this seems to be contradictory, even paradoxical, since physiologically a high compliance together with a relatively low resistance are regarded as “healthy” and, *vice versa*, in most pathological conditions low compliance is accompanied by high resistance. However, at second sight, these findings may become interpretable.

Zyxin-deficient arteries: weak resistance and low compliance - paradox behavior due to altered gene expression?

Zyxin is an important regulator of vascular gene expression. Besides the expression of receptors for vasoconstrictors as analyzed in the vessel segments after pressure perfusion (see Results, page 76 and 77), the protein also strongly modulates the expression of matrix proteins. Reanalysis of the smooth muscle cell microarray data on the single gene level revealed a striking imbalance in the expression of several collagen isoforms and the matrix proteins fibronectin and tenascin-C. Whereas wild type cells respond to stretch with the expression of the stabilizing matrix protein fibronectin (Ohashi 1999) and collagen isoforms responsible for stabilization and maintenance of the cellular phenotype (Leung 1976; Li 1998), zyxin-deficient cells

predominantly express the proliferation-associated matrix protein tenascin-C (Mackie 1997; Feng 1999; Jones 2000; Cattaruzza 2004) as well as collagen isoforms characteristic for other tissues.

Overall, zyxin deficiency implies a completely altered matrix composition. How may this explain the finding that both compliance resistance are lower than expected? A short consideration of the situation in the venous system may be helpful. Generally, the compliance of veins is considered very high, as they can "store" rather large volumes without a major increase in pressure. This is mostly due to the phenomenon that these vessels are rarely fully extended by the blood filling them. In fact, if a vein under high-pressure conditions is completely filled with blood, its compliance tends to be even lower than that of comparable arteries (see any physiology textbook). Keeping in mind the low mechanical stability of zyxin-deficient vessels, the impaired receptor expression and matrix production and their easily disturbed smooth muscle cell-matrix interactions, as demonstrated by the rearrangement of smooth muscle cells in response to pressure perfusion, a vein-like behavior of these arteries does not seem too far-fetched.

In the arterial system, blood filling is always high (due to the high pressure) and in this case, the compliance might be low. On the other hand, if the caliber of the vessel is normal but its capacity to constrict is weak, the resistance may be also low. This seemingly paradox mixture of vascular (dys-)function due to zyxin-deficiency may be explained by an imbalanced gene expression in affected animals.

In light of the above, it is quite surprising that the vascular phenotype of zyxin-deficient mice is relatively mild and only becomes apparent in the second year of their life. Two principal reasons may account for this. First, wild type mice naturally never develope hypertension. Thus, without a challenge resulting in high levels of mechanical strain, vascular dysfunction due to a loss of zyxin-induced gene expression may never become apparent. Secondally, these animals are much less active than their age-matched counterparts. They show less interest in social contacts, playing and mating, thereby potentially avoiding any cardiovascular stress that could jeorpadize their cardiovascular function. This may be part of a compensatory mechanism that zyxin-deficient mice employ in order to survive despite an impaired

vascular function. Such compensatory phenomena are well characterized in other knockout mice. In cardiovascular physiology, the most prominent example is that of endothelial nitric oxide synthase-deficient mice. These animals were expected to suffer from severe hypertension. However, as other vasodilator molecules partially substitute for the loss of nitric oxide, the phenotype is relatively mild (Huang 1995; Shesely 1996; Liu 2008).

5.6 Perspective

The present study provides an almoust conclusive description of the mechanisms underlying the stretch-induced release of zyxin from focal adhesions and its accumulation in the nucleus. Moreover, the systematic analysis of zyxin-dependent endothelial and smooth muscle cell gene expression provided multiple insights into stretch-induced vascular remodelling and the potential role of zyxin therein. Finally, a first exploration of the role of zyxin in vascular function under physiological conditions was presented.

Based on these findings, several interesting and fundamental questions arise that will be addressed in the future:

1) What is the actual mechanism of zyxin-induced gene expression? Is zyxin a transcription factor or does the protein act at a more global level? In this context, we could characterize a stretch-responsive promoter element, the pyrimidine-purine box, in the most zyxin-dependent genes. It is not clear yet, however, whether zyxin binds directly or indirectly to this motif.

2) In light of the new and detailed information regarding stretch-induced gene expression, early changes in endothelial and smooth muscle cell phenotype should be approached on a functional level. Such analyses could encompass the role and mechanism of apoptosis, proliferation and different signalling pathways *in vitro* and *in vivo*. In this regard, the generation of a cell-specific conditional zyxin-*knockout* mouse, which is currently under way, will be of great help.

3) With a better supply of zyxin-deficient mice, two central questions may be addressed in more detail. First, does the lack of zyxin-induced gene expression account for the weak vascular structure and function in zyxin-deficient mice? To this end, zyxin-dependent gene and protein expression will be analyzed in situ and in vivo. A special focus will be on the expression of matrix proteins. Secondly and maybe most interesting: Is zyxin a promising target to interfere with stretch-induced vascular remodelling? By employing a hypertension model with wild type and zyxin-deficient mice it should be possible to analyze whether zyxin is in fact a critical determinant of stretch-induced vascular remodelling. Further, if zyxin is indeed responsible for this process, one could design strategies to interfere with it *in vivo*, e.g. by the use of decoy oligonucleotides (Morishita 1996; Tomita 1997; Wagner 2000) possessing the sequence of the pyrimidine-purine box and, therefore able to selectively inhibit the zyxin-dependent gene expression.

These projects will lead not only to a better understanding of the principles of mechanotransduction in vascular cells, but may also help to define a new therapeutic approach to prevent an exaggerated stretch or pressure-induced remodelling process, as e.g. in arterial hypertension.

6. Summary

Hypertrophy in conduit and hyperplasia in resistance-sized arteries is the clinically visible outcome of a supra-physiological pressure-induced stretching of endothelial and smooth muscle cells, e.g. in arterial hypertension. This adaptive remodelling of the vessel wall in response to mechanical overload results in the fixation of vascular resistance at devoted levels and, therefore, is a major contributor to coronary heart disease, dilated cardiomyopathy and stroke. Although phenomenologically characterized in detail, the signal transduction pathways underlying the stretch-induced shift in vascular gene expression and, consecutively, long-term phenotype changes of endothelial as well as smooth muscle cells are still poorly understood.

In this thesis, the first specifically mechanotransducing protein in endothelial cells could be defined with the focal adhesion protein zyxin. Moreover, it could be shown that zyxin after nuclear translocation orchestrates stretch-induced gene expression in a highly complex way. By comparing isolated perfused arteries from wild type and zyxin-deficient mice, it could be further demonstrated that zyxin plays a decesive role in maintaining vascular structure and function under conditions of high perfusion pressure.

Supra-physiological levels of stretch caused a dissociation of zyxin from focal adhesions in endothelial cells. This event was mediated by the consecutive stretch-induced release and coordinated action of endothelin-1 (ET-1) and atrial natriuretic peptide (ANP). The ET-1-mediated release of ANP resulted in a presumably A-type natriuretic peptide receptor-mediated, cGMP-induced activation of protein kinase G, which in turn phosphorylated zyxin, thereby facilitating its dissociation from the focal adhesions and accumulation in the nucleus. This complex stretch-induced signalling cascade described herein for the first time for endothelial cells, closely resembles the multi-cellular events preceding the cardiac release of ANP. Thus, endothelial cells are not only able to sense stretch, but also specifically transduce and respond to mechanical overload by activating the newly characterized mechanotransducer zyxin.

Moreover, the first systematic genome-wide microarray analysis of human endothelial and mouse vascular smooth muscle cells revealed a highly complex – albeit similar – response of these cells to mechanical overload. Against the background of the long

known effects of chronic stretch in the arterial system, namely hypertension, the microarray results obtained are highly suggestive. In both cell types, more than 600 gene products were differentially expressed in response to cyclic stretch. These could be grouped into in several well-defined cellular pathways that are known to be crucial for the development of hypertrophy and/or hyperplasia in the course of vascular remodelling. Most interesting, a parallel microarray analysis comparing zyxin-deficient stretched endothelial and smooth muscle cells with their zyxin-expressing counterparts revealed that zyxin is fundamental for the changes in gene expression preceding stretch-induced vascular remodelling processes. Zyxin suppression would thus result in the inhibition of pro-hypertrophic pathways, e.g. by a shift towards pro-apoptotic gene expression, but also may affect signalling pathways involved in normal vascular function.

Finally, by using freshly isolated perfused segments of the mouse femoral artery from wild type and zyxin-deficient mice, it could be demonstrated that vascular function depends on the presence of zyxin. Although the phenotype of zyxin-deficient mice is mild in young animals, vascular function and structure is strongly impaired in aged mice. Vasoconstriction and, thus, the ability for the regulation of flow resistance, is strongly diminished in zyxin-deficient animals. This effect most probably occurs due to missing zyxin-induced expression. The crucial function of zyxin in vascular physiology could be further substantiated by initial experiments employing the DOCA-salt hypertension model in wild type and zyxin-deficient mice.

In conclusion, besides thoroughly analyzing stretch-induced zyxin signalling and gene expression in vascular cells, this thesis provides some interesting insights into the pathophysiological relevance of this molecule, which in the future may be decisive to develop novel therapeutic strategies against hypertension-induced alterations in vascular structure and function.

Agrotis, A., Bobik A. (1996). "Vascular remodelling and molecular biology: new concepts and therapeutic possibilities." Clin Exp Pharmacol Physiol. **23**: 363-368.

Aird, W. C. (2007). "Phenotypic Heterogeneity of the Endothelium." Circ Res. **100**: 158-173.

Beckerle, M. C. (1997). "Zyxin: zinc fingers at sites of cell adhesion." Bioessays **19**: 949-957.

Birukov, K. G. (2007). "The two faces of vascular inflammation." Current Atherosclerosis Reports **8**: 223-231.

Bradford, M. M. (1976). "A rapid and sensitive method for the quantitation of microgram quantities of protein utilizing the principle of protein-dye binding." Anal. Biochem. **72** 248-254

Burridge, K., Fath K., Kelly T., Nuckolls G., Turner C. (1988). "Focal adhesions: transmembrane junctions between the extracellular matrix and the cytoskeleton." Annu. Rev. Cell Biol. **4**: 487-525.

Cai, H., Harrison D.G. (2000). "Endothelial dysfunction in cardiovascular diseases: the role of oxidant stress. ." Circ Res. **87**: 840-844.

Cai, W., Bodin P, Sexton A, Loesch A, Burnstock G (1993). "Localization of neuropeptide Y and atrial natriuretic peptide in the endothelial cells of human umbilical blood vessels." Cell Tissue Res. **272**: 175-181.

Cattaruzza, M., Berger M.M., Ochs M., Fayyazi A., Hecker M. (2002). "Deformation-induced endothelin B receptor-mediated smooth muscle cell apoptosis is matrix-dependent." Cell Death Differ **9**: 219-226.

Cattaruzza, M., Dimigen, C., Ehrenreich, H., Hecker, M. (2000). "Stretch-induced endothelin receptor-mediated apoptosis in vascular smooth muscle cells." The FASEB Journal **14**: 991-998.

Cattaruzza, M., Eberhardt I., Hecker M. (2001). "Mechanosensitive transcription factors involved in endothelin B receptor expression." J. Biol. Chem. **276**: 36999-37003.

Cattaruzza, M., Lattrich C., Hecker M. (2004). "Focal adhesion protein zyxin is a mechanosensitive modulator of gene expression in vascular smooth muscle cells." Hypertension **43**: 726-730.

Cattaruzza, M., Schafer K., Hecker M. (2002). "Cytokine-induced down-regulation of zfm1/splicing factor-1 promotes smooth muscle cell proliferation." J. Biol. Chem. **277**(February 22): 6582-6589.

Cho, A., Cantman D.W., Langille B.L. (1995). "Apoptosis (programmed cell death) in arteries of the neonatal lamb. ." Circ Res. **76**: 168-175.

Chobanin, A. V., Alexander R.W. (1996). "Exacerbation of atherosclerosis by hypertension. Potential mechnism and clinical implications." Arch Intern Med. **156**: 1952-1956.

Cohen, R. A., Vanhoutte P.M. (1995). "Endothelium-dependent hyperpolarization. Beyond nitric oxide and cyclic GMP." Circulation **92**: 3337-3349.

Collins, R., Peto R., MacMahon S., Hebert P., Fiebach N.H., Eberlein K.A., Godwin J., Qizilbash N., Taylor J.O., Hennekens C.H. (1990). "Blood pressure, stroke, and coronary heart disease. Part 2, Short-term reductions in blood pressure: overview of randomised drug trials in their epidemiological context." Lancet. **335**: 827-838.

Consortium, T. G. O. (2000). "Gene Ontology: tool for the unification of biology." Nature Genet. **25**: 25-29.

Crawford, A. W., Beckerle M.C. (1991). "Purification and characterization of zyxin, an 82,000-dalton component of adherens junctions." J. Biol. Chem **266**(March 25): 5847-5853.

Crawford, A. W., Michelsen J.W., Beckerle M.C. (1992). "An interaction between zyxin and alpha-actinin." J Cell Biol. **116**: 1381-1393.

Dajnowiec, D., Sabatini P.J.B., Van Rossum T.C., Lam J.T.K., Zhang M., Kapus A., Langille B. L. (2007). "Force-Induced Polarized Mitosis of Endothelial and Smooth Muscle Cells in Arterial Remodeling. ." Hypertension. **50**: 255-260.

Davies, M. J., Wu X., Nurkiewicz T.R., Kawasaki J., Davis G.E., Hill M.A., Meininger G.A. (2001). "Integrins and mechanotransduction of the vascular myogenic response." Am. J. Physiol. **280**: H1427-H1433.

Davies, P. F., Polacek D.C., Handen J.S., Helmke B.P., DePaola N. (1999). "A spatial approach to transcriptional profiling: mechanotransduction and the focal origin of atherosclerosis." Trends Biotechnol. **17**(9): 347-351.

Davis, M., Hill MA. (1999). "Signaling mechanisms underlying the vascular myogenic response." Physiol. Rev. **79**: 387-423.

Day, R., Lariviere R., Schiffrin E.L. (1995). "In situ hybridization shows increased endothelin-1 mRNA levels in endothelial cells of blood vessels of deoxycorticosterone acetate-salt hypertensive rats." Am. J. Hypert. **8**: 294-300.

De Martin, R., Hoeth M., Hofer-Warbinek R., Schmid J.A. (2000). "The transcription factor NF- B and the regulation of vascular cell function. ." Arterioscler Thromb Vasc Biol. **20**: E83–E88. .

Deedwania, P. C. (2004). "Metabolic Syndrome and Vascular Disease. Is Nature or Nurture Leading the New Epidemic of Cardiovascular Disease? ." Circulation **109**: 2-4.

Denninger, J., Marletta MA. (1999). "Guanylate cyclase and the .NO/cGMP signaling pathway." Biochim Biophys Acta. **1411**: 334-350.

Derhaag, J. G., Duijvestijn A.M., Emeis J.J., Engels W., van Breda Vriesman P.J. (1996). "Production and characterization of spontaneous rat heart endothelial cell lines. ." Lab. Invest. **74**(2): 437-451.

Detmers, P. A., Lo S.K., Olsen E.E., Walz A., Baggiolini M., Cohn Z.A. (1990). "Neutrophil-activating protein 1/interleukin-8 stimulates the binding activity of the leukocytes adhesion receptor CD11b/CD18 on human neutrophils." J. Exp. Med. **171**: 1155-1162.

Dietz, J. R. (2005). "Mechanisms of atrial natriuretic peptide secretion from the atrium." Cardiovasc. Res. **68**: 8-17.

Feng, Y., Yang J.H., Huang H. (1999). "Transcrptional profile of mechanically induced genes in human vascular smooth muscle cells." Circ. Res **85**: 1118-1123.

Folkow, B., Hallbäck M., Lundgren Y., Sivertsson R., Weiss L. (1973). "Importance of adaptive changes in vascular design for establishment of primary hypertension, studied in man and in spontaneously hypertensive rats." Circ. Res **32:Suppl 1**: 2-16.

Fortuño, A., San José G., Moreno MU, Díez J, Zalba G. (2005). "Oxidative stress and vascular remodelling. ." Exp Physiol. **90**: 457-462. .

Frye, S. R., Yee A., Eskin S.G., Guerra R., Cong X., McIntire L.V. (2005). "cDNA microarray analysis of endothelial cells subjected to cyclic mechanical strain: importance of motion control." Physol Genomics. **21**: 124-130.

Garbers, D. L. (1991). "Guanyl cyclase-linked receptors." Pharmacol. Ther. **50**: 337-345.

Garbers, D. L., Lowe D.G. (1994). "Guanyl cyclase receptors." J. Biol. Chem. **269**: 30741-30744.

Gerszten, R. E., E. A. Garcia-Zepeda, Y. C. Lim, M. Yoshida, H. A. Ding, M. A. Gimbrone, Jr., A. D. Luster, F. W. Luscinskas, Rosenzweig A. (1999). "MCP-1 and IL-8 trigger firm adhesion of monocytes to vascular endothelium under flow conditions." Nature **398**: 718-723.

Gertler, F. B., Niebuhr K., Reinhard M., Wehland J., Soriano P. (1996). "Mena, a relative of VASP and Drosophila Enabled, is implicated in the control of microfilament dynamics." Cell **87**: 227-239.

Gimbrone, M. J., Cybulsky MI, Kume N, Collins T, Resnick N. (1995). "Vascular endothelium. An integrator of pathophysiological stimuli in atherogenesis." Ann N Y Acad Sci. **748**: 122-131.

Glagov, S., Vito R., Giddens D.P., Zarins C.K. (1992). "Micro-architecture and composition of artery walls: relationship to location, diameter and the distribution of mechanical stress." J Hypertens Suppl **10**: S101-104.

Haga, J. H., Li Y-S.J., Chien S. (2007). "Molecular basis of the effects of mechanical stretch on vascular smooth muscle cells." J Biomechanics **40**: 947-960.

Hamad, A., Clayton A, Islam B, Knox AJ. (2003). "Guanylyl cyclases, nitric oxide, natriuretic peptides, and airway smooth muscle function." Am J Physiol Lung Cell Mol Physiol. **285**: L973-L983.

Hamet, P., deBlois D., Dam T.V., Richard L., Teiger E., Tea B.S., Orlov S.N., Tremblay J. (1996). "Apoptosis and vascular wall remodeling in hypertension." Can J Physiol Pharmacol. **74**: 850-861.

Harrison, V. J., Barnes K., Turner A.J., Wood E., Corder R., Vane J.R. (1995). "Identification of endothelin1 and big endothelin 1 in secretory vesicles isolated from bovine aortic endothelial cells." PNAS **92**: 6344-6348.

Heagerty, A. M., Aalkjaer C., Bund S.J., Korsgaard N., Mulvany M.J. (1993). "Small artery structure in hypertension. Dual processes of remodeling and growth." Hypertension **21**: 391-397.

Hishikawa, K., Oemar B.S., Yang Z., Luscher T.F. (1997). "Pulsatile stretch stimulates superoxide production and activates nuclear factor-{kappa}B in human coronary smooth muscle." Circ Res. **81**: 797–803.

Hoffman, L., Nix D.A., Benson B., Beckerle M.C. (2003). "Target disruption of the murine zyxin gene." Mol. Cell. Biol. **23**: 70-79.

Hoffman, L. M., Jensen C.C., Kloeker S., Wang C.L., Yoshigi M., Beckerle M.C. (2006). "Genetic ablation of zyxin causes Mena/VASP mislocalization, increased motility, and deficits in actin remodeling." J Cell Biol. **172**: 771-782.

Huang, P. L., Huang Z., Mashimo H., Bloch K.D., Moskowitz M.A., Bevan J.A. (1995). "Hypertension in mice lacking the gene for endothelial nitric oxide synthase. ." Nature **377**: 239–242.

Ingber, D. (1991). "Integrins as mechanochemical transducers." Curr. Opin. Cell Biol. **3**: 841-848.

Ingber, D. E. (2002). "Mechanical signaling and the cellular response to extracellular matrix in angiogenesis and cardiovascular physiologie." Circ. Res. **91**: 877-887.

Ingber, D. E. (2003). "Mechanobiology and diseases of mechanotransduction." Ann Med. **35**(8): 564-577.

Ingber, D. E. (2006). "Cellular mechanotransduction: putting all the pieces together again." FASEB J. **20**: 811-827.

Intengan, H. D., Schiffrin E.L. (2001). "Vascular Remodeling in Hypertension. Roles of Apoptosis, Inflammation, and Fibrosis " Hypertension **38**: 581.

Johnson, E. K., Schelling M.E., Quitadamo I.J., Andrew S., Johnson E.C. (2002). "Cultivation and characterization of coronary microvascular endothelial cells: a novel porcine model using micropigs. ." Microvasc Res. **64**(2): 278-288.

Jones, F. S., Jones P.L. (2000). "The tenascin family of ECM glycoproteins: structure, function, and regulation during embryonic development and tissue remodeling." Dev Dyn. **218**: 235-259.

Kakisis, J. D., Liapis Ch.D., Sumpio B.E. (2004). "Effects of cyclic strain on vascular cells." Endothelium **11**: 17-28.

Kato, T., Muraski J., Chen Y. (2005). "Atrial natriuretic peptide promotes cardiomyocyte survival by cGMP-dependent nuclear accumulation of zyxin and Akt." J. Clin. Invest. **115**: 2716-2730.

Kimura, H., Kasahara Y., Kurosu K., Sugito K., Takiguchi Y., Terai M., Mikata A., Natsume M., Mukaida N., Matsushima K., Kuriyama T. (1998). "Alleviation of monocrotaline-induced pulmonary hypertension by antibodies to a monocyte chemotactic and activating factor/monocyte chemoattractant protein-1." Lab. Invest. **78**: 571-581.

Kinnunen, P., Vuolteenaho O., Ruskoaho H. (1993). "Mechanisms of atrial and brain natriuretic peptide release from rat ventricular myocardium: effect of stretching." Endocrinology **132**: 1961-1970.

Knöll, R., Hoshijima M., Hoffman H.M., Person V., Lorenzen-Schmidt I., Bang M.L., Hayashi T., Shiga N., Yasukawa H., Schaper W., McKenna W., Yokoyama M., Schork N.J., Omens J.H., McCulloch A.D., Kimura A., Gregorio C.C., Poller W., Schaper J., Schultheiss H.P., Chien R.K. (2002). "The cardiac mechanical stretch sensor machinery involves a Z disc complex that is defective in a subset of human dilated cardiomyopathy." Cell **111**(7): 943-955.

Kojda, G., Harrison D. (1999). "Interactions between NO and reactive oxygen species: pathophysiological importance in atherosclerosis, hypertension, diabetes and heart failure." Cardiovasc. Res. **43**: 562-571.

Koller, K. J., Goeddel D.V. (1992). "Molecular biology of the natriuretic peptides and their receptors." Circulation **86**: 1081-1088.

Komuro, I., Yazaki Y. (1993). "Control of cardiac gene expression by mechanical stress." Ann. Rev. Physiol. **55**: 55-75.

Lacolley, P. (2004). "Mechanical influence of cyclic stretch on vascular endothelial cells." Cardiovascular Res. **63**: 577-579.

Laemmli, U. K. (1970). "Cleavage of structural proteins during the assembly of the head of bacteriophage T4." Nature **227**: 680-685.

Lang, R., Tho¨lken H, Ganten D, Luft FC, Ruskoaho H, Unger T (1985). "Atrial natriuretic factor–a circulating hormone stimulated by volume loading." Nature **314**: 264-266.

Lansman, J. B., Hallam T.J., Rink T.J. (1987). "Single stretch-activated ion channels in vascular endothelial cells as mechanotransducers." Nature **325**: 811-813.

Larsen, C. G., Anderson A.O., Appella E., Oppenheim J.J., Matsushima K. (1989). "The neutrophil-activating protein (NAP-1) is also chemotactic for T lymphocytes." Science. **243**: 1464-1466.

Lauth, M., Wagner A.H., Orzechowski H.D., Paul M., Cattaruzza M., Hecker M. (2000). "Transcriptional control of deformation-induced preproendothelin-1 gene expression." J. Mol. Med. **78**: 441-450.

Lee, E. K., Park T. (2007). "Exploratory methods for checking quality of microarray data." Bioinformatics **1**(10): 423-428.

Lee, R. M. K. W., Owens G.K., Scott-Burden T., Head R.J., Mulvany M.J., Schiffrin E.L. (1995). "Pathophysiology of smooth muscle in hypertension. ." Can J Physiol Pharmacol. **73**: 574-584.

Lehoux, S., Castier Y., Tedgui A. (2006). "Molecular mechanisms of vascular responses to heamodynamic forces." J Int Med **259**: 381-392.

Lehoux, S., Tedgui A. (1998). "Signal transduction of mechanical stresses in the vascular wall." Hypertension **32**: 338-345.

Leung, D. Y., Glagow S., Mathews M.B. (1976). "Cyclic stretching stimulates synthesis of matrix components by arterial smooth muscle cells in vitro." Science. **191**: 475-477.

Li, G., Qian H. (2003). "Sensitivity and specificity amplification in signal transduction." Cell Biochem Biophys. **39**: 45-59.

Li, Q., Muragaki Y., Hatamura I., Ueno H., Ooshima A. (1998). "Stretch-Induced Collagen Synthesis in Cultured Smooth Muscle Cells from Rabbit Aortic Media and a Possible Involvement of Angiotensin II and Transforming Growth Factor-β. ." J Vasc Res. **35**: 93-103.

Li, S., Huang N.F., Hsu S. (2005). "Mechanotransduction in endothelial cells." J. Cell. Bioch. **96**: 1110-1126.

Li, S., Moon J.J., Miao H., Jin G., Chen B.P., Yuan S., Hu Y., Usami S., Chien S. (2003). "Signal transduction in matrix contraction and the migration of vascular smooth muscle cells in three-dimensional matrix." J Vasc Res **40**: 378-388.

Lienenlüke, B., Germann T., Kroczek R.A., Hecker M. (2000). "CD154 stimulation of interleukin-12 synthesis in human endothelial cells. ." Eur J Immunol. **30**: 2864-2870.

Liu, V. W. T., Huang P.L. (2008). "Cardiovascular roles of nitric oxide: A review of insights from nitric oxide synthase gene disrupted mice. ." Cardiovasc. Res. **77**(1): 19-29.

Luft, F. C. (2001). "Angiotensin, inflammation, hypertension, and cardiovascular disease." Curr Hypertens Rep. **3**: 61-67.

Lüscher, T. F., Vanhoutte P.M. (1986). "Endothelium-dependent contractions to acetylcholine in the aorta of the spontaneously hypertensive rat." Hypertension **8**: 344-348.

Lüscher, T. F., Vanhoutte P.M. (1986). "Endothelium-dependent responses to platelets and serotonin in spontaneously hypertensive rats." Hypertension **8**: II55-60.

Mackie, E. J. (1997). "Moceckules in focus:tenascin-C." Int J Biochem Cell Biol. **29**: 1133-1137.

MacMahon, S., Peto R., Cutler J., Collins R., Sorlie P., Neaton J., Abbott R., Godwin J., Dyer A., Stamler J. (1990). "Blood pressure, stroke, and coronary heart disease. Part 1, Prolonged differences in blood pressure: prospective observational studies corrected for the regression dilution bias." Lancet. **335**: 765-774.

Manoli, T., Gretz N., Grne H.J., Kenzelmann M., Eils R., Brors B. (2006). "Group testing for pathway analysis improves comparability of different microarray datasets." Bioinformatics **22**(20): 2500-2506.

Mäntymaa, P., Leppaluoto J., Ruskoaho H. (1990). "Endothelin stimulates basal and stretch-induced atrial natriuretic peptide secretion from the perfused rat heart." Endocrinology **126**: 587-595.

Martin, J., Collot-Teixeira S., McGregor L., McGregor J.L. (2007). "The dialogue between endothelial cells and monocytes/macrophages in vascular syndromes." Curr Pharm Des. **13**: 1751-1751.

McIntyre, M., Bohr D.F., Dominiczak A.F. (1999). "Endothelial function in hypertension: the role of superoxide anion." Hypertension **34**: 539-545.

Meininger, G., Davis MJ. (1992). "Cellular mechanisms involved in the vascular myogenic response." Am. J. Physiol. **263**: H647-659.

Mills, P. A., Huetteman D.A., Brockway B.P., Zwiers L.M., Gelsema A.J., Schwartz R.S., Kramer K. (2000). "A new method for measurement of blood pressure, heart rate, and activity in the mouse by radiotelemetry." J. Appl. Physiol. **88**: 1537-1544.

Miura, S., Fujino M., Tanigawa H., Matsuo Y., Saku K. (2002). "Transactivation of the vascular endothelial growth factor receptor KDR/Flk-1 by the bradykinin B2 receptor induces an angiogenic phenotype in human cultured coronary endothelial cells. ." Nippon Yakurigaku Zasshi. **120**(2): 104P-1005P.

Moncada, S., Higgs E.A. (1991). "Endogenous nitric oxide: physiology, pathology and clinical relevance." Eur J Clin Invest. **21**: 361-374.

Mootha, V., Lindgren CM, Eriksson KF, Subramanian A, Sihag S, Lehar J, Puigserver P, Carlsson E, Ridderstråle M, Laurila E, Houstis N, Daly MJ, Patterson N, Mesirov JP, Golub TR, Tamayo P, Spiegelman B, Lander ES, Hirschhorn JN, Altshuler D, Groop LC. (2003). "PGC-1alpha-responsive genes involved in oxidative phosphorylation are coordinately downregulated in human diabetes." Nat. Genet. **34**: 267-273.

Morawietz, H., Ma Y.H., Vives F., Wilson E., Sukhatme V.P., Holtz J., Ives H.E. (1999). "Rapid induction and translocation of Egr-1 in response to mechanical strain in vascular smooth muscle cells." Circ. Res **84**: 678-687.

Morishita, R., Ogihara T. (1996). "Application of decoy strategy." Nippon Rinsho. **54**(9): 2583-2590.

Morris, C. E. (1990). "Mechanosensitive ion channels." J Membr Biol. **113**: 93-107.

Mukaida, N., Harada A., Matsushima K. (1998). "Interleukin-8 (IL-8) and monocyte chemotactic and activating factor (MCAF/MCP-1), chemokines essentially involved in inflammatory and immune reactions." Cytokine Growth Factor Rev. **9**: 9-23.

Mullis. K.B., F. F. A. (1987). "Specific synthesis of DNA in vitro via a polymerase-catalyzed chain reaction. ." Methods Enzymol. **155**: 335-350.

Münzel, T., Feil R, Mülsch A, Lohmann SM, Hofmann F, Walter U. (2003). "Physiology and pathophysiology of vascular signaling controlled by guanosine 3',5'-cyclic monophosphate-dependent protein kinase [corrected]." Circulation **108**: 2172-2183.

Nix, D. A., Beckerle M. (1997). "Nuclear-cytoplasmatic shuttling of the focal contact protein, zyxin: a potential mechanism for comunication between sites of cell adhesion and the nucleus." J. Cell. Biol. **138**(5): 1139-1147.

O'Farrell, P. H. (1975). "High resolution two-dimensional electrophoresis of proteins." J. Biol. Chem. **250**: 4007-4021.

Obuwole, B. O., Du W., Mills I., Sumpio B.E. (1997). "Gene regulation by mechanical forces." Endothelium **5**: 85-93.

Ohashi, T., Kiehart P.D., Erickson H.P. (1999). "Dynamics and elasticity of the fibronectin matrix in living cell culture visualized by fibronectin–green fluorescent protein." PNAS. **96**(5): 2153-2158.

Park, T., Yi S.G., Lee S., Lee K.J. (2005). "Diagnostic plots for detecting outlying slides in a cDNA microarray experiment." Biotechniques. **38**(3): 463-471.

Pasterkamp, G., de Kleijn D.P., Borst C. (2000). "Arterial remodeling in atherosclerosis, restenosis and after alteration of blood flow: potential mechanisms and clinical implications. ." Cardiovasc. Res. **45**: 843-852.

Patterson, A. M., Schmutz C., Davis S., Gardner L., Ashton B.A., Middleton J. (2002). "Differential binding of cheokines to macrophages and neutrophils in the human inflament synovium." Athrritis Res. **4**: 209-214.

Perry, H. M. J., Miller J.P., Fornoff J.R., Baty J.D., Sambhi M.P., Rutan G., Moskowitz D.W., Carmody S.E. (1995). "Early predictors of 15-year end-stage renal disease in hypertensive patients." Hypertension **25**: 587-594.

Persson, J., Nilsson J., Lindholm M.W. (2006). "Cytokine response to lipoprotein lipid loading in human monocyte-derived macrophages. ." Lipids Health Dis. **5**: 17-.

Pillarisetti, S., Paka L., Obunike J.C., Berglund L., Goldberg I.J. (1997). "Subendothelial Retention of Lipoprotein (a). Evidence That Reduced Heparan Sulfate Promotes Lipoprotein Binding to Subendothelial Matrix." J Clin Invest. **100**: 867-874.

Prewitt, R. L., Rice D.C., Dobrian A.D. (2002). "Adaptation of resistance arteries to increases in pressure." Microcirculation **9**: 295-304.

Reinhard, M., Jouvenal K., Tripier D., Walter U. (1995). "Identification, purification and characterization of zyxin-related protein that binds the focal adhesion and microfilament protein VASP." Proc. Natl. Acad. Sci. USA. **92**: 7956-7960.

Resnick, N., Gimbrone M.A. (1995). "Hemodynamic forces are complex regulators of endothelial gene expression." FASEB J. **9**: 874-882.

Rollins, B. J. (1997). "Chemokines." Blood **90**: 909-928.

Ruskoaho, H., Tho¨lken H, Lang RE (1886). "Increase in atrial pressure releases atrial natriuretic peptide from isolated perfused rat hearts." Pfluegers. Arch. **407**: 170-174.

Ruskohao, H. (1992). "Atrial natriuretic peptide: synthesis, release, and metabolism." Pharmacol. Rev. **44**: 481-602.

Sadler, I., Crawford A.W., Michelsen J.W., Beckerle M.C. (1992). "Zyxin and cCRP: two interactive LIM domain proteins associated with the cytoskeleton." J Cell Biol. **119**: 1573-1587.

Saiki, R. K., Gelfand D.H., Stoffel S., Scharf S.J., Higuchi R., Horn G.T., Mullis K.B., Erlich H.A. (1988). "Primer-directed enzymatic amplification of DNA with a thermostable DNA polymerase." Science **239**: 487-491.

Schiffrin, E. L. (1999). "State-of-the -Art lecture. Role of the endothelin-1 in hypertension." Hypertension **34**: 876-881.

Schmeichel, K. L., Beckerle M.C. (1994). "The LIM domain is a modular protein-binding interface." Cell **79**: 211-219.

Shesely, E. G., Maeda N., Kim H.S., Desai K.M., Krege J.H., Laubach V.E. (1996). "Elevated blood pressures in mice lacking endothelial nitric oxide synthase. ." Proc Natl Acad Sci U S A. **93**(23): 13176-13181.

Shi, Q., Aida K., Vandeberg J.L., Wang X.L. (2004). "Passage-dependent changes in baboon endothelial cells--relevance to in vitro aging. ." DNA Cell Biol. **23**(8): 502-509.

Shirakami, G., Magaribuchi T., Shingu K., Suga S., Tamai S., Nakao K., Mori K. (1993). "Positive end-expiratory pressure ventilation decreases plasma atrial and brain natriuretic peptide levels in humans." Anesth Analg **77**: 1116-1121.

Shrinsky, V. P., Antonov A.S., Birukov K.G., Sobolevsky A.V., Romanov Y.A., Kabeva N.V., Antonova G.N., Smirnov V.N. (1989). "Mechano-chemical control of human endothelium orientation and size." J Cell Biol. **109**: 331-339.

Shyy, J., Chien S. (2002). "Role of integrins in endothelial mechanosensing of shear stress." Circ. Res **91**: 769-775.

Skålén, K., Gustafsson M., Knutsen-Rydberg E., Hultén L.M., Wiklund O., Innerarity T.L., Borén J. (2002). " Subendothelial retention of atherogenic lipoproteins in early atherosclerosis." Nature **417**: 750-754.

Smolenski, A., Poller W., Walter U., Lohmann S.M. (2000). "Regulation of human endothelial cell focal adhesion sites and migration by cGMP-dependent Protein Kinase I." J. Biol. Chem. **275**(August 18): 25723-25732.

Subramanian, A., Tamayo P., Mootha V.K., Mukherjee S., Ebert B.L., Gillette M.A,. Paulovich A., Pomeroy S.L., Golub T.R., Lander E.S., Mesirov J.P. (2005). "Gene set enrichment analysis: a knowledge-based approach for interpreting genome-wide expression profiles." Proc Natl Acad Sci U S A. **102**(43): 15278-152789.

Suga, S., Itoh H., Komatsu Y., Ogawa Y., Hama N., Yoshimasa T., Nakao K. (1993). "Cytokine-induced C-type natriuretic peptide (CNP) secretion from vascular endothelial cells – evidence for CNP as a novel autocrine/paracrine regulator from endothelial cells." Endocrinology **133**: 3038-3041.

Sumpio, B. E., Wildmann M.D. (1990). "Enhanced production of endothelium-derived contracting factor by endothelial cells subjected to pulsatile stretch." Surgery **108**: 277-282.

Thürmann, P. A. (1997). "Left ventricular and microvascular hypertrophy in essential hypertension: clinical relevance and prognostic implications." Int J Clin Pharmacol Ther. **35**(5): 181-187.

Tomita, N., Morishita R., Higaki J., Ogihara T. (1997). "A novel strategy for gene therapy and gene regulation analysis using transcription factor decoy oligonucleotides. Exp Nephrol. ." Exp Nephrol. **5**(5): 429-434.

Touyz, R. M., Schiffrin E.L. (2001). "Increased generation of superoxide by angiotensin II in smooth muscle cells from resistance arteries of hypertensive patients: role of phospholipase D-dependent NAD(P)H oxidase-sensitive pathways. ." J Hypertens. **7**: 1245–1254.

Touyz, R. M., Schiffrin E.L. (2004). "Reactive oxygen species in vascular biology: implications in hypertension. ." Histochem Cell Biol. **122**: 339–352.

Tsuda Y., O. M., Uezono Y., Osajima A., Kato H., Okuda H., Oishi Y., Yashiro A., Nakashima Y.. (2002). "Activation of extracellular signal-regulated kinases is essential for pressure-induced proliferation of vascular smooth muscle cells." Eur J Pharmacol. **446**: 15-24.

van Wamel, A., Ruwhof C, van der Valk-Kokshoom LE, Schrier PI, van der Laarse A. (2001). "The role of angiotensin II, endothelin-1 and transforming growth factor-beta as autocrine/paracrine mediators of stretch-induced cardiomyocyte hypertrophy." Mol Cell Biochem **218**: 113-124.

Wagner, A. H., Gebauer M., Güldenzoph B., Hecker M. (2002). "3-Hydroxy-3-methylglutaryl coenzyme A reductase-independent inhibition of CD40 expression by atorvastatin in human endothelial cells." Arterioscler Tromb Vasc Biol. **22**: 1784-1789.

Wagner, A. H., Krzesz R., Gao D., Schroader C., Cattaruzza M., Hecker M. (2000). "Decoy oligodeoxynucleotide characterization of transcription factors controlling endothelin-B receptor expression in vascular smooth muscle cells." Mol. Pharmacol **58**: 1333-1340.

Wagner, D. D., Olmsted J.B., Marder V.J. (1982). "Immunolocalization of von Willebrand protein in Weibel-Palade bodies of human endothelial cells." J. Cell Biol. **95**(1): 355–60.

Weibel, E. R., Palade G.E. (1964). " New cytoplasmic components in arterial endothelia. ." J Cell Biol. **23**(1): 101–112.

Wilson, E., Vives F., Collins T., Ives H.E. (1998). "Strain-responsive regions in the platelet-derived growth factor-A gene promoter." Hypertension **31**: 170-175.

Witztum, J. L., Steinberg D. (1991). " Role of oxidized low density lipoprotein in atherogenesis. ." J Clin Invest. **88**: 1785-1792.

Yandle, T. (1994). "Biochemistry of natriuretic peptides." J. Intern. Med. **235**: 561-576.

Yoshigi, M., Hoffman L.M., Jensen Ch.C., Beckerle M.C. (2005). "Mechanical force mobilizes zyxin from focal adhesion to actin filaments and regulates cytoskeletal reinforcement." J. Cell. Biol. **171**(October 24): 209-215.

Zlotnik, A., Yoshire O. (2000). "Chemokines: a new classification system and their role in immunity." Immunity. **12**: 121-127.

Appendix 1:

	Pathway EC	*P* value stretch vs. static non affected	*P* value stretch vs. static siRNA zyxin	Zyxin-dependent pathways
1.	Actin y pathway	0,04849	0,24011	+
2.	Agpcr pathway	0,46141	0,04038	+
3.	Akap 96 pathway	0,01029	0,16243	+
4.	Akap 13 pathway	0,46141	0,04038	+
5.	Akt pathway	0,31388	0,00554	+
6.	Androgen up genes	0,00000	0,00007	
7.	Arap pathway	0,04368	0,05357	+
8.	Arginine C pathway	0,22713	0,03980	+
9.	B lymphocyte pathway	0,02209	0,03448	
10.	Bad pathway	0,05592	0,00343	
11.	Breast cancer estrogen signalling	0,00195	0,02972	
12.	Ca nf at signalling	0,25428	0,03386	+
13.	Cardiac egf pathway	0,25033	0,02368	+
14.	Carm1 pathway	0,31389	0,02635	+
15.	Ccr5 pathway	0,21545	0,00390	+
16.	CD40 pathway	0,46141	0,00382	+
17.	Cell adhesion molecule activity	0,00596	0,12110	+
18.	Cell cycle	0,00353	0,00405	
19.	Cell cycle arrest	0,01876	0,04840	
20.	Cell proliferation	0,02042	0,00038	
21.	Chrebp pathway	0,35843	0,00834	+
22.	CAM	0,00001	0,00007	
23.	Cell cycle	0,00576	0,07400	+
24.	Death	0,03593	0,09764	+
25.	DNA met and mod	0,03859	0,13494	+
26.	Signalling	0,00127	0,09292	+
27.	Creb pathway	0,32589	0,01489	+
28.	Death pathway	0,19114	0,02236	+
29.	Downregulated by hoxa9	0,00159	0,09764	+
30.	Drug resistance and metabolism	0,13717	0,02506	+
31.	Electron transport chain	0,92179	0,03116	
32.	Electron transporter activity	0,02333	0,26126	
33.	EMT down	0,03095	0,02220	
34.	EMT up	0,00009	0,00012	
35.	Erbb3 pathway	0,02735	0,02220	
36.	Erythrocyte pathway	0,01208	0,07748	+
37.	Fcer1 pathway	0,20173	0,02829	+
38.	Fetal liver hs enriched TF jp	0,00006	0,00139	
39.	Fmlp pathway	0,48516	0,01868	+
40.	Frasor er down	0,00094	0,00123	
41.	G1 pathway	0,00625	0,00021	
42.	G13 signaling pathway	0,16708	0,00127	+
43.	G2 pathway	0,02303	0,01697	
44.	Gata3 pathway	0,35843	0,00540	+
45.	Gcr pathway	0,26946	0,01829	+

46.	**Glucose down**	**0,02384**	**0,13890**	**+**
47.	**Glucose up**	**0,05102**	**0,03448**	
48.	**Glutation down**	**1,97555 E-08**	**9,42137 E-08**	
49.	**Glutation up**	**0,00057**	**0,00004**	
50.	**GO Ros**	**0,01204**	**0,04954**	
51.	**Gpcr pathway**	**0,85403**	**0,01868**	**+**
52.	**Hdac pathway**	**0,69933**	**0,03376**	**+**
53.	**Hemo tf list jp**	**0,00033**	**0,00004**	
54.	**Hoxa9 down**	**0,00059**	**0,00123**	
55.	**Htert down**	**0,00006**	**0,00026**	
56.	**Htert up**	**4,65167 E-08**	**0,00001**	
57.	**Human CD34 enriched tf jp**	**0,00170**	**0,01360**	
58.	**Ifng pathway**	**0,04859**	**0,03636**	
59.	**Il 10 pathway**	**0,03549**	**0,02719**	
60.	**Il 17 pathway**	**0,03549**	**0,09764**	**+**
61.	**Insulin 2f down**	**0,00107**	**0,00039**	
62.	**Kras top100 control**	**0,04394**	**0,18741**	**+**
63.	**Kras top100 knockdown**	**0,000001**	**0.000002**	
64.	**Lair pathway**	**0,00008**	**0,00038**	
65.	**LDL pathway**	**0,04859**	**0,31314**	**+**
66.	**Leu down**	**1,88119 E-13**	**1,26000 E-08**	
67.	**Leu up**	**0,00002**	**0,00002**	
68.	**Lymphocyte pathway**	**0,00005**	**0,00419**	
69.	**Map00100 sterol biosynthesis**	**0,00007**	**0,00954**	
70.	**Map00240 pyrimidine metabolism**	**0,09689**	**0,02795**	**+**
71.	**Map00251 glutamate metabolism**	**0,01244**	**0,03636**	
72.	**Map00260 glycine serine and thre**	**0,01717**	**0,15300**	**+**
73.	**Map00330 arginine and proline me**	**0,05102**	**0,03448**	
74.	**Map00450 selenoamino acid metabo**	**0,02735**	**0,01777**	
75.	**Map00480 glutathione metabolism**	**0,00009**	**0,00038**	
76.	**Map00620 pyruvate metabolism**	**0,01466**	**0,09740**	**+**
77.	**Map00640 propanoate metabolism**	**0,03327**	**0,53098**	**+**
78.	**Map00670 one carbon pool by fola**	**0,03506**	**0,04844**	
79.	**Map00970 aminoacyl tRNA biosynth**	**0,08183**	**0,00382**	**+**
80.	**Mapk pathway**	**0,01679**	**0,02225**	
81.	**Mapkkk cascade**	**0,00587**	**0,00246**	
82.	**Mef2d pathway**	**0,21545**	**0,01759**	**+**
83.	**Methionine pathway**	**0,02735**	**0,01829**	
84.	**Monocyte pathway**	**0,00001**	**0,00096**	
85.	**Mrna processing**	**0,00226**	**0,00069**	
86.	**Mrna splicing**	**0,037736**	**0,07873**	**+**
87.	**Myc mut**	**0,02296**	**0,04577**	
88.	**Neutrophil pathway**	**0,00007**	**0,00954**	
89.	**NFAT pathway**	**0,53356**	**0,00260**	**+**
90.	**NFκB induced**	**0,00048**	**0,00486**	
91.	**Nkt pathway**	**0,29413**	**0,04206**	**+**
92.	**Nos1 pathway**	**0,35976**	**0,00267**	**+**
93.	**p38 mapk pathway**	**0,00424**	**0,03516**	
94.	**p53 hypoxia pathway**	**0,01759**	**0,06084**	**+**
95.	**p53 pathway**	**0,03549**	**0,02719**	

96.	**p53 signalling**	**0,00509**	**0,13494**	**+**
97.	**Parkin pathway**	**0,03506**	**0,43487**	**+**
98.	**Pentose phosphate pathway**	**0,04859**	**0,03980**	
99.	**PGC**	**0,00616**	**0,10373**	**+**
100.	**Pitx2 pathway**	**0,00790**	**0,05132**	**+**
101.	**Ppara pathway**	**0,01645**	**0,16911**	**+**
102.	**Proliferation genes**	**0,01085**	**8,69721 E-05**	
103.	**Proteasome degradation**	**0,01204**	**0,02662**	
104.	**Proteasome pathway**	**0,00055**	**0,00002**	
105.	**Raccycd pathway**	**0,39657**	**0,00742**	**+**
106.	**Radiation sensitivity**	**0,00881**	**0,09764**	**+**
107.	**Rap down**	**0,000004**	**0,00021**	
108.	**Ras pathway**	**0,52782**	**0,03140**	**+**
109.	**Reck pathway**	**0,28772**	**0,00834**	**+**
110.	**Reelin pathway**	**0,02735**	**0,02220**	
111.	**Set pathway**	**0,18377**	**0,04038**	**+**
112.	**Shh lisa**	**0,01759**	**0,00267**	
113.	**Bcr signaling pathway**	**0,55225**	**0,00954**	
114.	**CD40 pathway map**	**0,11990**	**0,00267**	**+**
115.	**Pip3 sigin cardiac myoctes**	**0,44721**	**0,04073**	**+**
116.	**Sig pip3 signalling in B lymphocytes**	**0,68685**	**0,01868**	**+**
117.	**Slrp2 pathway**	**0,01233**	**0,00765**	
118.	**Erk1 erk2 mapk pathway**	**0,26992**	**0,01580**	**+**
119.	**Jnk mapk pathway**	**0,03598**	**0,02635**	
120.	**p38 mapk pathway**	**0,00059**	**2,27987E-05**	
121.	**Tel pathway**	**0,04850**	**0,05758**	**+**
122.	**TGF- β signaling pathway**	**0,01663**	**0,01031**	
123.	**TGF-β pathway**	**0,00134**	**0,03474**	
124.	**TNF and fas network**	**0,02488**	**0,02076**	
125.	**Upreg by hoxa9**	**0,01606**	**0,00824**	
126.	**Urea cycle pathway**	**0,22713**	**0,03980**	**+**
127.	**Vip pathway**	**0,50376**	**0,00087**	**+**
128.	**Voxphos**	**0,87114**	**0,02942**	**+**
129.	**Wnt pathway**	**0,00627**	**0,00373**	

Appendix 2

pathway maoSMC	*P* value stretch vs. static WT	*P* value stretch vs. static zyxin -/-	
1. Adult liver vs fetal liver GNF2	0,26066	0,01440	
2. Agpcr pathway	0,05868	0,03212	
3. Akap96 pathway	0,02113	0,08847	
4. Akap centrosome pathway	0,13273	0,00084	+
5. Androgen up genes	0,14135	0,02004	+
6. AP00120 bile acid biosynthesis	1,00000	0,01598	
7. Arenrf2 pathway	0,01444	0,04180	
8. Atm pathway	0,05868	0,03212	
9. Bad pathway	0,05485	0,02585	
10. Bcl2 family and regulatory network	0,03499	0,65676	+
11. Bcr pathway	0,00498	0,09519	
12. Biopeptides pathway	0,00999	0,31876	+
13. BRCA down	0,00384	0,00159	
14. Breast cancer estrogen signalling	0,01389	0,09561	+
15. Calcineurin pathway	0,04430	0,30316	+
16. Carm1 pathway	0,05868	0,03212	
17. Ccr5 pathway	0,02009	0,21899	+
18. Cdmac pathway	0,04405	0,13771	+
19. Cell adhesion	0,39092	0,00483	+
20. Cell cycle checkpoint	0,04430	0,30316	+
21. Cell cycle regulator	0,02692	0,62950	+
22. Cell motility	0,28311	0,05545	+
23. Cftr pathway	0,23715	0,00424	+
24. Chemical pathway	0,05485	0,10822	+
25. Cilia proteins	0,00175	0,01680	
26. Ck1pathway	0,07528	0,00629	+
27. CAM	0,09004	0,00102	+
28. Cell cycle	0,01292	0,05082	
29. Hormonal functions	0,05868	0,16411	+
30. Repair	0,05485	1,00000	+
31. Signalling	0,03309	0,00341	
32. Transcription factors	0,00095	0,26161	+
33. Transport	0,07155	0,04646	
34. Creb pathway	0,00053	0,00415	
35. Death pathway	0,81023	0,00622	+
36. DNA damage signalling	0,03486	0,06538	+
37. Downreg by HOXA9	0,28371	0,00245	+
38. Dream pathway	0,04405	0,00020	
39. Egf pathway	0,03993	0,06364	+
40. Eif4 pathway	0,07962	0,03869	+
41. Electron_transporter_activity	0,21636	0,00504	+
42. EMT down	0,04072	0,01440	

43. EMT up	**0,00923**	**0,00892**	
44. Epha4 pathway	**0,04405**	**0,49705**	**+**
45. Epon f kb pathway	**0,01296**	**0,36752**	**+**
46. Erbb4 pathway	**0,00696**	**1,00000**	**+**
47. Erk pathway	**0,00289**	**0,07345**	**+**
48. Fas pathway	**0,53918**	**0,04625**	**+**
49. Free pathway	**0,32349**	**0,02929**	**+**
50. Gata3 pathway	**0,03499**	**0,00242**	
51. Gleevec pathway	**6,1E-05**	**0,12458**	**+**
52. Glucose up	**0,04785**	**0,00415**	
53. Glutation down	**0,00390**	**0,08825**	**+**
54. Glutation up	**7,9E-05**	**0,00005**	
55. GO ROS	**0,03499**	**0,01598**	
56. HEMO TF list jp	**0,00631**	**0,42432**	**+**
57. Hif pathway	**0,03150**	**0,45712**	**+**
58. HOXA9 down	**0,16047**	**0,00528**	**+**
59. HTERT down	**0,0004**	**0,05687**	
60. Human CD34 enriched TF JP	**0,00104**	**0,15889**	**+**
61. Human mito db62002	**0,00089**	**0,12195**	**+**
62. IGFL pathway	**0,30901**	**0,05277**	**+**
63. Il10 pathway	**0,05868**	**0,16411**	**+**
64. Il1 r pathway	**0,07962**	**0,00810**	**+**
65. Il22 bp pathway	**0,04405**	**0,49705**	**+**
66. Il6 pathway	**0,00061**	**0,24700**	**+**
67. INS	**0,00109**	**0,76579**	**+**
68. Insulin 2f up	**0,07626**	**0,03694**	**+**
69. Keratinocyte pathway	**0,01491**	**0,00421**	
70. KRAS TOP100 control	**0,23960**	**0,00051**	**+**
71. KRAS TOP100 knockdown	**0,00049**	**0,00977**	
72. Krebs TCA cycle	**0,05485**	**0,70541**	**+**
73. LEU up	**0,00031**	**0,00044**	
74. MAP kinase kinase activity	**0,38647**	**0,04646**	**+**
75. Malatex pathway	**0,00080**	**0,20469**	**+**
76. MAP00030 pentose phosphate pathway	**0,00384**	**0,45712**	**+**
77. MAP00051 fructose and mannose metabolism	**0,03499**	**0,65676**	**+**
78. MAP00062 fatty acid biosynthesis	**0,04571**	**0,26315**	**+**
79. MAP00240 pyrimidine metabolism	**0,03993**	**0,19731**	**+**
80. MAP00251 glutamate metabolism	**0,00677**	**0,07833**	
81. MAP00252 alanine and aspartate metabolism	**0,04430**	**0,02055**	
82. MAP00280 valine leucine and isoleucine	**0,00601**	**0,15967**	**+**
83. MAP00310 lysine degradation	**0,02009**	**0,6000**	**+**
84. MAP00330 arginine and proline metabolism	**0,04785**	**1,00000**	**+**
85. MAP00350 tyrosine metabolism	**0,03286**	**0,05457**	
86. MAP00380 tryptophan metabolism	**0,01024**	**0,19731**	**+**
87. MAP00480 glutathione metabolism	**0,05868**	**0,00424**	**+**
88. MAP00632 benzoate degradation	**0,04571**	**1,00000**	**+**
89. MAP00640 propanoate metabolism	**0,05485**	**0,70541**	**+**

90. MAP00860 porphyrin and chlorophy	**0,02113**	**0,08847**	
91. MAP00970 aminoacyl tRNA biosynth	**0,01444**	**0,00067**	
92. MAPK cascade	**0,05277**	**0,30901**	**+**
93. Mapk pathway	**0,04874**	**0,08453**	**+**
94. Mitochondr	**0,00089**	**0,03333**	
95. mRNA processing	**0,01299**	**0,81380**	**+**
96. mRNA splicing	**0,00383**	**1,00000**	**+**
97. Mtor pathway	**0,18166**	**0,02585**	**+**
98. NFAT pathway	**0,02951**	**0,03103**	
99. NGF pathway	**0,09367**	**0,05277**	**+**
100. No1 pathway	**0,04785**	**0,21687**	**+**
101. Nos1 pathway	**0,11370**	**0,01211**	**+**
102. Notch pathway	**0,00696**	**1,00000**	**+**
103. Nthi pathway	**0,09367**	**0,05277**	
104. p38 mapk pathway	**0,01623**	**0,51218**	**+**
105. p53 UP	**0,00018**	**0,02790**	
106. p53 hypoxiapathway	**0,00036**	**0,21899**	**+**
107. p53 pathway	**0,01444**	**0,00629**	
108. PDGF pathway	**0,00792**	**0,01297**	
109. PGC	**0,00772**	**0,28276**	**+**
110. Plce pathway	**0,20146**	**0,02375**	
111. Ppara pathway	**0,00197**	**0,00176**	
112. Proliferation GENES	**0,01374**	**0,17233**	**+**
113. Ptdins pathway	**0,00322**	**0,12458**	**+**
114. Pyk2 pathway	**0,04785**	**0,21687**	**+**
115. PYR	**0,03150**	**0,45712**	**+**
116. Rac1 pathway	**0,05485**	**0,02585**	
117. Rac cycd pathway	**0,09367**	**0,05277**	**+**
118. Radiation sensitivity	**0,04430**	**0,09278**	
119. RAP DOWN	**0,00206**	**0,00771**	
120. RAP UP	**0,00859**	**0,47674**	**+**
121. RAR UP	**0,05664**	**0,00528**	
122. B-cell receptor complexes	**0,00601**	**0,04625**	
123. Bone morphogenetic	**1,00000**	**0,00539**	
124. G1 and s phases	**0,02113**	**0,08847**	**+**
125. Pten pathway	**0,02009**	**1,00000**	**+**
126. Trka receptor	**0,02692**	**0,24700**	**+**
127. SHH pathway	**0,30901**	**0,05277**	**+**
128. BCR signalling pathway	**0,00827**	**0,32148**	**+**
129. Insulin receptor pathway in card	**0,00473**	**0,49936**	**+**
130. PIP3 signalling in B-lymphocythes	**0,00186**	**0,29808**	**+**
131. PIP3 siginalling in cardiac myoctes	**0,01576**	**0,20618**	**+**
132. Regulation of the actin cytoskeleton	**0,00498**	**0,09519**	**+**
133. Slrp2 pathway	**0,02435**	**1,00000**	**+**
134. Differentiation pathway in PC	**0,51471**	**0,05773**	**+**
135. G protein independ 7 trans rec	**0,32349**	**0,02929**	**+**
136. Ga13 pathway	**0,00803**	**1,00000**	**+**

137. Gaq pathway	**0,03286**	**1,00000**	**+**
138. Jak STAT pathway	**0,38647**	**0,04646**	**+**
139. Phosphoinositide 3 Kinase pathway	**0,02428**	**0,27748**	**+**
140. Stress pathway	**0,02692**	**0,01211**	
141. Tall 1 pathway	**0,38647**	**0,04646**	**+**
142. Tel pathway	**0,00036**	**0,60007**	**+**
143. Tid pathway	**0,01444**	**0,56832**	
144. Toll pathway	**0,31012**	**0,01602**	**+**
145. Tpo pathway	**0,00446**	**0,03869**	
146. Trna synthetases	**0,01444**	**0,00067**	
147. Tumor supressor	**0,01263**	**0,70541**	**+**
148. VEGF pathway	**0,06664**	**0,03189**	
149. Vip pathway	**0,01263**	**0,00065**	
150. Wnt signalling	**0,00433**	**0,01035**	

I would like to express my sincere gratitude to Prof. Dr. Markus Hecker for giving me a great chance to make PhD study in the Department of Cardiovascular Physiology at University of Heidelberg. Participating in one of the scientific projects at the Department of Physiology was certainly great experience. I stoutly appreciate his support, encouragement and valuable scientific discussions.

I wish to express my deepest appreciation to my supervisor and mentor PD Dr. Marco Cattaruzza for his permanent enormous help during the whole time of my studies. I certainly value expertis he shared with me. His insightful observation, as well as interesting discussions and constructive scientific meetings on the project had enormous impact on my development. Besides, I am grateful for friendly relationship we had throughout my whole PhD time, which was certainly highly supportive.

I sincerely thank Prof. Dr. Felix Wieland to be my formal supervisor and also co-referee of this thesis. I also extend my sincere thanks to Prof. Dr. Stephan Frings and Prof. Dr. Thomas Rausch for accepting to be my examiners.

I would like to acknowledge Prof. Dr. Mary Beckerle from Huntsman Cancer Research Centre, University of Utah, Salt Lake City, who kindly provided us with the zyxin-deficient mice and zyxin specific antisera.

I specially would like to express thankfulness to four of my lab colleagues, best friends and supporters: Elena Demicheva, Nicole Nogoy, Christina Duhig and Robert Krzesz for their loyalty, patience and encouragement. Also would like to express my deepest appreciations to two other very important persons that I had pleasure to work with: Danijela Heide and Renate Cattaruzza, not only for their excellent technical assistance but also true friendship and care. I would also acknowledge Violetta Powajbo for her essential support and kindness. I will always memorize all great moments we all could share together. I also want to admit all of the other former and current members of institute for friendly atmosphere.

Finally, I want to express my deepest gratitude to my family. It is their constant support, faith and love that helped me follow my ambitions. Specially, my mum Ewa for encouraging me to pursue that challenge, strongly believing, that this goal one day will become true. I extend here my appreciations also to two of my best friends: Antonina Mazur and Andres Miguel Miguéles, whose presence in my life is of special importance.

CURRICULUM VITAE

Name: Agnieszka Maria Wójtowicz

Date of birth: December, 5th, 1979

Place of birth: Wrocław, Poland

Nationality/ Citizenship: Polish

EDUCATION

2004 – current Ph.D. in Biology at University of Heidelberg.
Graduating in July, 2008.
Institute of Physiology and Pathophysiology, Medical Faculty, University of Heidelberg, Heidelberg, Germany.

Ph.D. thesis: "The focal adhesion protein zyxin mediates wall tension–induced signalling in vascular endothelial cells."

2001 - 2003 Diploma (equivalent to Master's degree) in Biotechnology, specialization Molecular Biology.
Institute of Molecular Biology, Department of Cell Pathology, Faculty of Biotechnology,
University of Wrocław, Wrocław, Poland.

Diploma thesis: "Actin and function of human polinuclear neutrophils in children with reccurent respiratory tract infections."

1998-2001 Diploma (equivalent to Bachelor's degree) in Biotechnology.
Institute of Molecular Biology, Department of Cell Pathology, Faculty of Biotechnology,
University of Wrocław, Wrocław, Poland.

Diploma thesis: "Molecular basics of Cardiomyopathy."

1993 - 1998 Secondary school. Certificate with extensive knowledge in biology and chemistry.
Wrocław, Poland.